

Mineralogical and geochemical characterization of the Boom Clay in the Netherlands

OPERA-PU-TNO521-1

Radioactive substances and ionizing radiation are used in medicine, industry, agriculture, research, education and electricity production. This generates radioactive waste. In the Netherlands, this waste is collected, treated and stored by COVRA (Centrale Organisatie Voor Radioactief Afval). After interim storage for a period of at least 100 years radioactive waste is intended for disposal. There is a world-wide scientific and technical consensus that geological disposal represents the safest long-term option for radioactive waste.

Geological disposal is emplacement of radioactive waste in deep underground formations. The goal of geological disposal is long-term isolation of radioactive waste from our living environment in order to avoid exposure of future generations to ionising radiation from the waste. OPERA (OnderzoeksProgramma Eindberging Radioactief Afval) is the Dutch research programme on geological disposal of radioactive waste.

Within OPERA, researchers of different organisations in different areas of expertise will cooperate on the initial, conditional Safety Cases for the host rocks Boom Clay and Zechstein rock salt. As the radioactive waste disposal process in the Netherlands is at an early, conceptual phase and the previous research programme has ended more than a decade ago, in OPERA a first preliminary or initial safety case will be developed to structure the research necessary for the eventual development of a repository in the Netherlands. The safety case is conditional since only the long-term safety of a generic repository will be assessed. OPERA is financed by the Dutch Ministry of Economic Affairs and the public limited liability company Electriciteits-Produktiemaatschappij Zuid-Nederland (EPZ) and coordinated by COVRA. Further details on OPERA and its outcomes can be accessed at www.covra.nl.

This report concerns a study conducted in the framework of OPERA. The conclusions and viewpoints presented in the report are those of the author(s). COVRA may draw modified conclusions, based on additional literature sources and expert opinions. A .pdf version of this document can be downloaded from www.covra.nl

OPERA-PU-TNO521-1

Title: Mineralogical and geochemical characterization of the Boom Clay in the Netherlands

Authors: M. Koenen & J. Griffioen

Date of publication: November 2014

Keywords: sediment, analysis, geochemistry, mineralogy, composition



Contents

Summary	5
Samenvatting	5
1. Introduction	7
1.1. Background	7
1.2. Objectives.....	7
1.3. Realization	7
1.4. Explanation of contents.....	7
2. Sample selection and preparation	9
3. Methodology.....	11
3.1. Geochemical analyses	11
3.1.1. XRF and ICP-MS	11
3.1.2. X-Ray Diffraction (XRD).....	11
3.1.3. Interpretation.....	12
3.2. Grain size analyses.....	12
3.3. Statistical analyses	12
3.3.1. Percentile plots.....	12
3.3.2. Factor analysis	12
3.3.3. Cluster analysis	12
3.4. Depth profiles	13
4. Results chemical analyses.....	15
4.1. Chemical composition of Boom clay	15
4.1.1. Data check.....	15
4.1.2. Carbon, sulfur and oxide concentrations.....	15
4.1.3. Trace elements	17
4.2. Boom clay mineralogy	18
4.3. Mineralogy and geochemistry	19
4.4. Grain size distribution.....	21
4.5. Depth profiles	22
5. Statistical analyses.....	23
5.1. Geochemical data correlation	23
5.2. Cluster analysis.....	23
5.3. Factor analysis	25
5.4. Mineralogy	28
5.5. Mineralogy and geochemistry	29
6. Discussion and conclusions	31
6.1. Characterization	31
6.2. Implications for geological radioactive waste disposal.....	36
6.3. Limitations and considerations	38
References.....	39
Appendix A.....	41
Appendix B.....	44
Appendix C.....	70
Appendix D.....	73
Appendix E.....	79
Appendix F.....	93
Appendix G	97
Appendix H	101
Appendix I	104
Appendix J	105

Summary

The Boom Clay (or Rupel Clay according to the Dutch geological stratigraphy) is selected as potential host rock for geological disposal of radioactive waste in the Netherlands and Belgium because of the isolating potential of low permeable, clay-rich rocks. The lateral and depth-related heterogeneity of the Boom Clay in the Netherlands is studied in this task and compared to the results from Belgian Boom Clay. For this purpose, 152 Boom Clay samples were selected from 17 cores spread over the Netherlands. Subsequently, geochemical and grain size analyses were performed and (statistically) analysed.

The results show that the samples have quite some variability, mainly in their clay, quartz, carbonate and pyrite contents. The main part of the heavy and trace elements can be associated with the clay mineralogy. Strontium and uranium are linked to calcite and organic carbon respectively.

Geographically, three statistically different groups are recognized. The Boom Clay in the southern part of the Netherlands has coarser, silty upper and lower parts. The central part is finer grained and more clay-rich with occasional silty layers. This is consistent with the cyclic alternation of clay- and silt-rich layers found in the Belgian Boom Clay. In the Southeast of the Netherlands, the Boom Clay has a higher carbonate content than in the Southwest. The Boom Clay in the north of the Netherlands is significantly different from the Southeast and Southwest. The Boom Clay is fine grained and clay- and carbonate-rich over the total depth interval. Both the pyrite and organic carbon content are important parameters due to their reactivity and potential impact on the safety function ‘delay and attenuation of releases’. The pyrite and organic carbon contents vary among the samples but they do not show geographic or depth-related variations.

Samenvatting

De Boom klei (of Rupel klei volgens de Nederlandse geologische stratigrafie) is geselecteerd als potentieel gast gesteente voor de geologische eindberging van radioactief afval in Nederland en België vanwege de isolerende capaciteit van impermeabele, kleirijke gesteentes. In deze task is de laterale en diepte-gerelateerde heterogeniteit van de Boom klei in Nederland bestudeerd en vergeleken met de resultaten van de Boom klei in België. Voor dit doel zijn 152 Boom klei samples van 17 kernen verspreid over Nederland geselecteerd. Vervolgens zijn geochemische en korrelgrootte analyses gedaan en (statistisch) geanalyseerd.

De resultaten laten behoorlijk wat variatie zien tussen de samples, vooral in de klei, kwarts, carbonaat en pyriet content. De meeste zware en spoorelementen zijn geassocieerd met de kleimineralen. Strontium en uranium zijn gelinkt aan respectievelijk calciet en organisch koolstof.

Geografisch gezien zijn drie statistisch verschillende groepen herkend. De Boom klei in het zuiden van Nederland is grover en meer silt-rijk boven- en onderin de unit. Het centrale gedeelte is fijnkorreliger en bevat meer klei met lokaal meer silt-rijke lagen ertussen. Deze stratigrafie is consistent met de cyclische afwisseling van klei- en silt-rijke lagen zoals die gevonden zijn in de Belgische Boom klei. In het zuidoosten van Nederland is de carbonaat concentratie in de Boom klei hoger dan in het zuidwesten. De Boom klei in het noorden van Nederland is significant anders dan in het zuidoosten en zuidwesten. Het is fijnkorrelig en rijk aan klei en carbonaat over het totale diepte-interval. Zowel de pyriet als de organische koolstof concentratie zijn belangrijke parameters vanwege hun reactiviteit en mogelijke impact op de veiligheidsfunctie ‘delay and attenuation of releases’. De concentratie van beide varieert tussen de samples maar geografische of diepte gerelateerde variaties zijn niet geobserveerd.

1. Introduction

1.1. Background

Clayrocks (fine-grained, low permeable material with a significant amount of clay minerals) are investigated as potential host rock for the geological disposal of radioactive waste in several European countries. These rock types generally have properties which are advantageous for the retention of radionuclides, once they escape the repository. These properties are mainly due to the high amount of clay minerals. The Boom Clay in the Netherlands (or Rupel Clay according to Dutch geological stratigraphy) is assigned as a potential formation for future geological disposal of radioactive waste. Within OPERA the feasibility and long-term safety of a repository in this formation is investigated. The main function of the Boom Clay upon disposal would be the isolation of radionuclides, and other potentially released matter, from the biosphere. The clay should be able to prevent significant and fast migration of the radionuclides from the waste itself, as well as any gases or liquids produced by the waste and its potential interaction with the engineered containment, for geological times. Furthermore, any changes in the geochemical properties of the clay upon interaction with the waste should not be as such that heavy metals or other harmful substances present in the (clay) minerals become mobile and cause potential risk for groundwater quality or (subsurface) organisms.

In Belgium the Boom Clay has been studied for the purpose of geological disposal of radioactive waste for decades. The Boom Clay in the investigated area in Mol is located at a depth of approximately 200 - 300 m. In the Netherlands the Boom Clay reaches much greater depth in the eastern and northern part of the country..

1.2. Objectives

The central objective of this study is to characterise the mineralogical and geochemical properties of the Boom Clay in the Netherlands with their geographical and depth-related variations. Because of their importance with regard to radionuclide retention, the focus will be on the clay minerals. The results will indicate whether the characteristics of the Boom Clay vary significantly with location and/or depth within the Netherlands, and whether they are different from those in Belgium.

1.3. Realization

This study is performed within task 5-2-1 of the OPERA programme, which focal point is “geochemical properties and long-term evolution of the Boom Clay”. Furthermore, the resulting geochemical characteristics will be used as input in several tasks under WP 6 and WP 7, which will investigate reactive transport of radionuclides. The data is also relevant for WP3 and WP 5, which consider physico-chemical properties and geomechanical aspects, respectively.

Sample selection and preparation was performed by TNO supported by Utrecht University. Analysis of the samples was performed by ACME and Qmineral. The data interpretation, statistical analyses and literature study were performed by TNO.

1.4. Explanation of contents

In chapter 2 the sample selection and preparation are discussed. Chapter 3 gives an overview of the different kinds of analyses performed on the selected samples as well as the subsequent statistical analysis on the results. The results of the mineralogical, geochemical and grain size analyses are reported in chapter 4, the results of the statistical analysis in chapter 5. Chapter 6 presents the discussion and the conclusions.

2. Sample selection and preparation

For this task 132 Boom Clay samples were collected from 15 different cores which are stored at the TNO core house in Zeist, the Netherlands (Figure 1 and Figure 2). The cores were selected based on geographical spreading and depth. For the purpose of this project, samples from locations where the Boom Clay is deeper than 400 meter and thicker than 100 meter were preferred for comparison with the shallower Boom Clay in Belgium. Since limited cores are available and core material is not always sufficient, shallower core material was also sampled. Note that, due to preservation regulations at the core house and the availability of limited sample material, each sample often represents several tens of decimeters, and in rare cases up to many meters of core material. In general, the core material was dried out and moldy, and some cores contained some fungi. Six samples were taken from a core provided by COVRA. Another 14 fresh Boom Clay samples were taken during the drilling of a new well. The location of this well cannot be provided due to confidentiality reasons. The locations of the other drillings are shown in Figure 3. An overview of the cores and samples is given in Appendix A. Table 7 shows an overview of the samples per core and their average depth. In Table 8 the core length represented by each sample is given. The samples from core XIV and XV represent very large core sections, and one sample of core XI and one of core XVII represent large sections.

The total of 152 samples were analyzed by XRF, ICP after acid destruction and CS elemental analyzer at ACME, Canada. Grain size distributions were measured by Qmineral in Leuven, Belgium. Of the 152 samples 30 were selected for XRD analysis by Qmineral.



Figure 1. Photographs of the TNO core house with lower left drillings cuttings preserved in plastic bags.



Figure 2. A piece of Boom Clay from several hundreds of meters depth. The circular spots could be secondary gypsum after pyrite oxidation.



Figure 3. Map with locations of the sampled cores. The location of the recent drilling is confidential.

3. Methodology

3.1. Geochemical analyses

3.1.1. XRF and ICP-MS

The samples were air dried ($<40^{\circ}\text{C}$) and pulverized to a 100 mesh (149 μm) according to the ASTM standard in a mild-steel pulverizer. The samples were subsequently analyzed by ICP-emission spectrometry for the major oxides and by ICP-mass spectrometry for the total set of rare earth and refractory elements as well as the precious and base metals. The major oxides and rare earth and refractory elements were analyzed following a lithium metaborate/tetraborate fusion and dilute nitric digestion. The precious and base metals were analyzed following digestion in Aqua Regia.

Additionally, XRF analysis was performed for the major oxides and some rare earth and refractory elements. In both ICP and XRF analysis the loss on ignition (LOI) is calculated, which is the weight difference after ignition at 1000°C .

Total carbon, organic carbon and total sulfur were measured by Leco combustion elemental analysis. The inorganic C content was subsequently calculated by subtracting the organic C from the total C content.

3.1.2. X-Ray Diffraction (XRD)

Thirty samples were selected for XRD analysis. The selection was based on geographical spreading and depth. Deeper samples were preferred for comparison with the shallower Boom Clay in Belgium. In order to obtain depth profiles, the samples were chosen from 7 out of 17 cores (Appendix A, Table 7).

XRD analysis was performed by Qmineral in Leuven, Belgium. Each sample was pulverized in a porcelain mortar and 2.7 gram of material was sampled. 0.3 gram of an internal standard (ZnO - Zincite) was added. The mixture was pulverized in ethanol using Korund elements and subsequently homogenized using a McCrone micronizing mill for 5 minutes. The samples were loaded in the XRD sample holders via ‘sideloading’. The measurements were performed with a Siemens D5000 in Bragg-Brentano configuration, equipped with a $\text{CuK}\alpha$ X-ray source and a graphite monochromator.

For the mineral identification the program Eva, developed by Bruker Corporation, and available databases (Crystallography Open Database) were used. The crystalline phases are quantified via the Rietveld methodology. This methodology ‘calculates’ an XRD pattern based on structure models of the identified minerals the way they are present in the literature and the databases. The pattern is fitted as good as possible with the measured pattern by refinement of the structure parameters. Since this methodology is not well applicable to all clay minerals due to ‘stacking disorder’ the clay minerals are quantified via the PONKCS method (Partial Or No Known Crystal Structures). For this method several standards for the 2:1 clays were selected:

- Fe-poor illite-rich illite/smectite ‘mixed layer’
- Fe-poor 2M_1 muscovite
- Smectite with average Fe-content
- Glauconite ($d_{060} = 1.512\text{\AA}$)
- Glauconite ($d_{060} = 1.515\text{\AA}$)

The clay fraction was measured by oriented clay slides. For this purpose, 5 gram of sample material was decalcified using a pH-buffering Na-acetate solution. Next, the organic material was removed via oxidation with H_2O_2 and the Fe-oxides/hydroxides using a Na-hypochlorite solution.

Subsequently, the separation of the clay fraction ($< 2 \mu\text{m}$) was accomplished by centrifuge. Finally, the clays with exchangeable cations are converted to Ca-containing clays using a saturated CaCl_2 -solution. The Cl ions were removed by dialysis. Dried material was mixed with water and applied on a sedimentation plate and measured by XRD, both air dried and saturated in ethylene glycol.

3.1.3. Interpretation

XRD analyses were performed on a subset of the samples and the (absence of) correlation between mineralogical content and oxide/trace element concentration might provide proxies for mineralogy of the remaining samples. Also, the (absence of) correlation between mineralogical content and oxide/trace element concentration might give additional insight in the composition of the complex clay mineralogy in the Boom Clay.

3.2. Grain size analyses

The samples were prepared for grain size analysis by removal of carbonate cements, Fe-oxides/hydroxides and organic compounds to liberate the individual grains. This was done by addition of 1.5 N HCl, reduction of Fe(III) using oxalic acid and an Al-plate, and H_2O_2 , respectively. The samples were shaken for one night using an agitator and treated with ultrasonics for one minute. The treated samples were split in 5 representative quantities using a ‘Rotary Cone Sample Divider’.

- One fifth was used for grain size analysis via laser diffraction using a ‘Malvern Mastersizer S Long Bed’;
- Three fifth was used for grain size analysis via Sedigraph (X-ray sedimentation technique) using a Micromeritics Sedigraph 5100 on the fraction $< 250\mu\text{m}$;
- One fifth was used to determine the fractions $< 250\mu\text{m}$ and $> 250\mu\text{m}$ by sieving.

3.3. Statistical analyses

3.3.1. Percentile plots

Percentile plots were made in excel for a selection of oxides and trace elements and for organic and inorganic carbon. These plots give insight in the frequency distribution of the geochemical parameter over the set of samples. On the x-axis the percentiles and the z-scores are shown. The latter is defined as $(x - \text{mean}) / (\text{standard deviation})$ and gives the number of standard deviations from the mean (z-score at the mean is zero). The percentile plots aid in the distinction between normal and lognormal distribution required for the factor and cluster analysis.

3.3.2. Factor analysis

The factor analysis, performed with the statistical software program SPSS Statistics version 20, calculates which of the variables (parameters) can explain the largest part of the original variance between the samples. It can assess which variables correlate highly with a group of other variables, but correlate badly with variables outside of the group. The variables with high intercorrelations might represent one underlying variable, which is called a factor. Furthermore, it gives insight in the association between the elements.

To select parameters for the factor analysis, correlations between the variables were checked using the correlate procedure in SPSS. Variables that do not correlate with any other variable or that correlate highly with other variables (with $R > 0.9$ or $R^2 > 0.81$) were eliminated from the dataset. Variables with many analyses below the detection limit were also eliminated.

3.3.3. Cluster analysis

A cluster analysis is performed with the statistical software program SPSS Statistics version 20. Cluster analysis enables the identification of groups of relatively similar geochemical

characteristics. The results will be used to assess whether geographical or depth-related differences can be observed. The clustering is based on the ‘distance’ between selected variables of the different samples. The distance is a measure for how far apart the variables are. Clustering can be done in various ways. The most common method is the k-means clustering. In this approach the number of clusters needs to be assigned a priori. Initial cluster means are randomly chosen and samples are assigned to the clusters to which they are nearest. Then, the cluster means are re-calculated based on the assigned samples. Subsequently, the samples are re-assigned to the clusters based on their new cluster means, and the cluster means are re-calculated again. This process is iterated until the cluster means are stable or the maximum number of iterations is reached. The k-means method uses the simple Euclidean measure for calculation of the distance between two samples:

$$d_{x,y} = \sqrt{\sum_{j=1}^J (x_j - y_j)^2}$$

Where x and y represent two values from the two different samples for the same variable, and j = 1 J represent all the variables included in the analysis.

For the k-means cluster analysis a selection of variables will be made. For each selected variable, the percentile plot is used to assess whether its distribution can be better described as lognormal instead of normal. Next, the (log)values of all selected variables are standardized by the following equation:

Standardized value = (original value - mean) / standard deviation

Standardization is necessary to correct for different scales of the different variables. Otherwise, the variable with the highest values, which probably will also have the largest (absolute) spread, will dominate the clustering procedure.

Initially, strong outlying values will be removed from the dataset (assigned as ‘missing values’ in SPSS). The clustering procedure for the corresponding samples will be performed based on the remaining values of the selected variables. After the clusters are defined, the missing values are restored and the total dataset is re-assigned to the defined clusters. Cluster averages are re-calculated with this new dataset but iteration is not allowed. The cluster averages are only slightly changed with respect to the initial clustering round. By doing this, we can assess whether the samples with missing values are correctly assigned to a cluster during the initial round or that the restored outlier would change its assignment. Clustering was performed for a varying number of clusters. The results were compared and the optimal number of clusters was selected.

3.4. Depth profiles

Depth profiles were made using Grapher software for all cores with more than 5 samples. Based on this constraint, cores X, XI, XIV and XV are excluded. Cores XIV and XV (and one sample from XI) are also the cores for which each sample represents a very large core section (Table 8). For this purpose the most important geochemical parameters were selected, in addition to the grain size distribution.

4. Results chemical analyses

4.1. Chemical composition of Boom clay

The results of the chemical analyses are shown in Appendix B.

4.1.1. Data check

The oxides and several minor/trace elements are measured by two different techniques: XRF and ICP. Both techniques should give the same results. However, three measurements do not show similar results (Figure 4). All three measurements are from the same well: well IX (B48G0159), samples 8, 9 and 10. These measurements are removed from the data set.

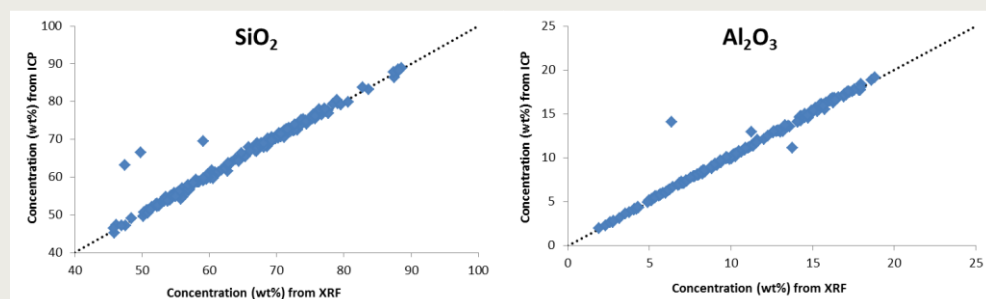


Figure 4. SiO₂ and Al₂O₃ wt% measured by XRF versus the concentration measured by ICP. The dashed lines represent perfect correlations.

4.1.2. Carbon, sulfur and oxide concentrations

The samples consist mostly of SiO₂ (45.8 - 88.6 wt%), with lesser amounts of Al₂O₃ (1.92 - 18.8 wt%), CaO (up to 14.5 wt%), Fe₂O₃ (1.6 - 10.5 wt%), K₂O (3.2 - 5.6 wt%) and MgO (0.3 - 2.9 wt%). The percentile plots, shown in Figure 21 in Appendix B, allow the distinction between normal and lognormal distribution of the components. If the lognormal plot has a better straight fit through the data than the normal plot (visually), the component was treated as lognormal. Most of the oxides have a relatively normal distribution, except for CaO, MnO and SO₃ which have a more lognormal distribution. Na₂O, K₂O and P₂O₅ have a few (2, 3 and 1, respectively) high outliers. The organic and inorganic carbon content are up to 2.5 and 3.5 wt%, respectively. About 35% of the samples has an inorganic carbon content below 0.1 wt%.

Figure 5 (left graph) shows that a positive correlation exists between aluminium and potassium, with a high K/Al ratio at Al₂O₃ < ~8 wt% and a lower K/Al ratio at Al₂O₃ > ~8 wt%. In the graph the K/Al correlations of K-feldspar, muscovite, and illite with maximum and minimum K/Al ratio (based on compositions of KAlMgSi₄O₁₀[(OH)₂(H₂O)] and KAl₄Si₂O₁₀[(OH)₂(H₂O)], respectively) are shown by the dashed lines. Illite with low aluminium (Illite_{max}) has a similar K/Al correlation as K-feldspar. The graph shows that an additional Al source with low or zero K concentration, like kaolinite, is present in the high Al₂O₃ range. The three outliers with high potassium content (samples XI-1, XI-2 and XI-3) also have a significantly high barium content of approximately 2000 ppm (Figure 5). No other correlations with barium can be observed. In the other samples the barium content varies between 100 and 500 ppm, with one exception of 800 ppm, irrespective of the K content (Figure 5).

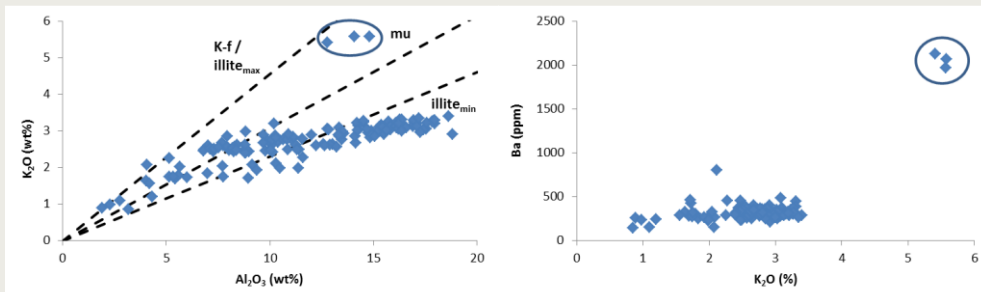


Figure 5. Positive correlation between aluminium and potassium (left) and no correlation between barium and potassium (right). Three outliers are visible (blue circles). K-f = K-feldspar, mu = muscovite.

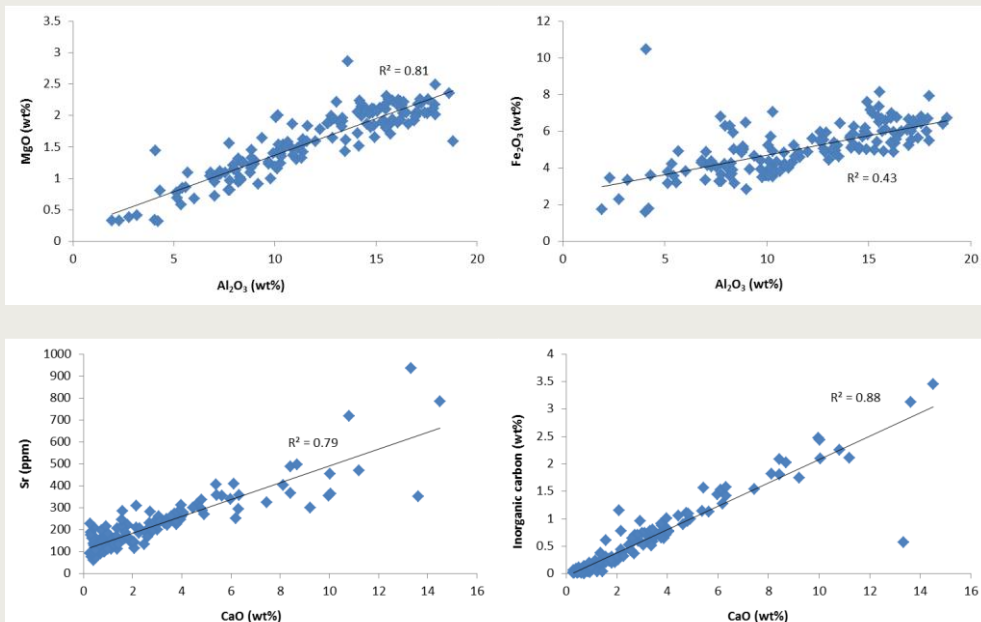


Figure 6. Graphs showing positive correlations. Removing the outlier with high Fe_2O_3 in the graph of Al_2O_3 versus Fe_2O_3 gives a R^2 of 0.57. Removing the one outlier with low inorganic C and high CaO in the graph of CaO versus inorganic carbon gives a R^2 of 0.96.

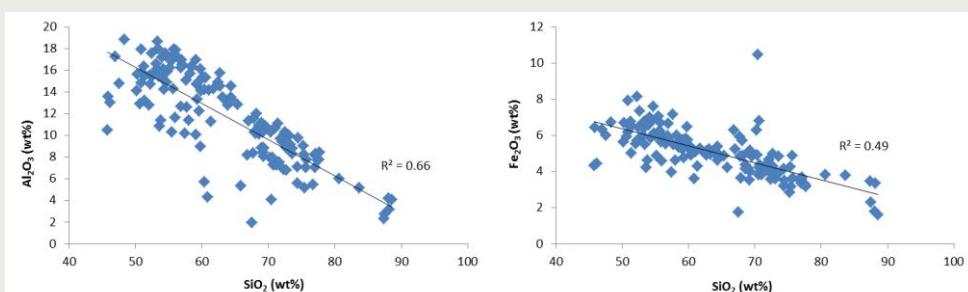


Figure 7. Graphs showing negative correlations between SiO_2 and Al_2O_3 (left) and Fe_2O_3 (right). Removing the one outlier with high Fe in the graph of SiO_2 versus Fe_2O_3 gives a R^2 of 0.57.

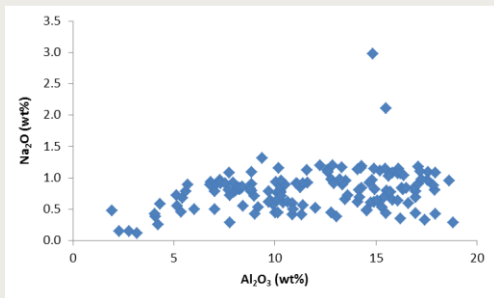


Figure 8. Graph of Na_2O versus Al_2O_3 .

Strong positive correlations exist between MgO and Al_2O_3 and between Fe_2O_3 and Al_2O_3 (Figure 6) suggesting that Mg and Fe are associated with clay minerals. Both MgO and Fe_2O_3 do not correlate with inorganic carbon, indicating that dolomite ($\text{Mg,Ca}(\text{CO}_3)_2$), magnesite (MgCO_3) and siderite (FeCO_3) are not prominently present. One sample (I6) has a significantly high Fe_2O_3 content which is not related to high Al_2O_3 , total S or inorganic C, suggesting the presence of either Fe-(hydr)oxide or (Fe-rich) glauconite. Strong positive correlations exist between CaO and Sr and between CaO and inorganic C (Figure 6), indicating CaCO_3 with significant Sr as substitute for Ca. One sample (IV2) has a significantly low inorganic carbon content with a high CaO content (Figure 6). The sample has a very high P_2O_5 content of 8.22 wt%, suggesting the presence of apatite ($\text{Ca}_5(\text{PO}_4)_3(\text{F,Cl,OH})$). This sample also has the highest Sr content of 937 ppm. Part of the Ca in apatite might be replaced by Sr. Negative correlations exist between SiO_2 and Al_2O_3 and between SiO_2 and Fe_2O_3 (Figure 7).

Figure 8 shows the Al_2O_3 content versus Na_2O . A wide scatter can be observed between 0 and 1.5 wt% Na_2O . In the lower Al_2O_3 range the Na_2O content increases, suggesting an increasing albite content. In the higher range Na_2O is irrespective of Al_2O_3 content. Two samples (VIII4 and VIII5) have a significantly higher Na_2O value of 2.1 and 3.0 wt% respectively which might be caused by local albite enrichment.

Both the total carbon and total sulfur content show a positive correlation with the organic carbon content but the R^2 values are low (Figure 9).

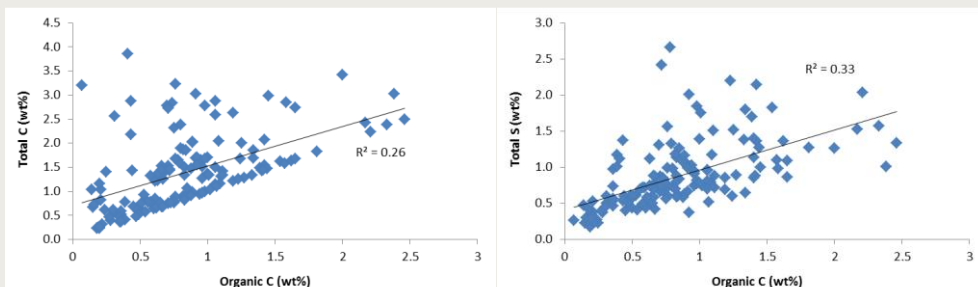


Figure 9. Organic carbon versus total carbon (left) and total sulfur content (right).

4.1.3. Trace elements

The trace elements with the highest concentrations are barium (145-2126 ppm), strontium (70-937 ppm) and zircon (81-760 ppm). The other trace elements are generally below 250 ppm, but lead and zinc both have a few high outliers up to 750 and 450 ppm respectively. The Sr content shows a strong positive correlation with Ca (Figure 6). Many other trace elements (Rb, V, Ce, Ni, Co, La, Cu, Ga, Nb, Th, Pr, Eu, Gd, Cs, Y, Nd, Sm, Sc, Ta, Dy, Er,

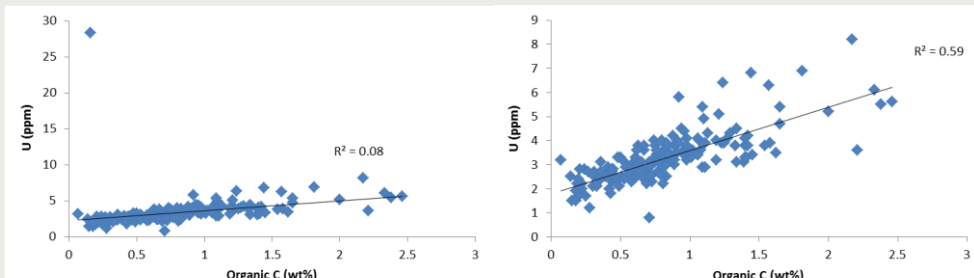


Figure 10. Positive correlation between organic C and U. Note that one outlier significantly affects the R^2 value, which is only 0.08. Removal of the outlier increases R^2 to 0.59.

Yb, Tb, Ho, Lu and Tm) have a (strong) positive correlation ($R^2 > 0.5$) with Al_2O_3 . Zircon has a positive correlation with SiO_2 and a weak negative correlation with Al_2O_3 . The remaining trace elements which do not correlate well with Al_2O_3 are Ba, Sr, U, Zr, Mo, Pb, Zn and As ($R^2 < 0.5$). Cobalt, Cs and Ni show a positive correlation with Fe_2O_3 . A positive correlation exists between organic C and U (Figure 10). The one outlier with extreme U value is the same outlier as in Figure 6, for which a high apatite concentration was suggested.

4.2. Boom clay mineralogy

The XRD results of the bulk rock and the clay fraction for the selected samples are shown in Table 13 of Appendix C. The samples consist mainly of quartz (16.3 - 86.3 wt%) and clay minerals (8.4 - 70.2 wt%, from bulk analysis). Plagioclase and K-feldspar are present in all samples and vary between 0.3 - 5.6 and 2.2 - 11.1 wt% respectively. The carbonate content varies strongly between the samples and consists of calcite (up to 25.9 wt%), aragonite (up to 5.1 wt%) and occasionally small amounts of ankerite/dolomite and siderite. Pyrite and anatase are present in almost all samples with values up to 6.9 and 0.9 wt% respectively. The small amounts of gypsum in most samples can be assumed to have formed during drilling/storage as a result of calcium reaction (from calcite) with oxidized S from pyrite. Also jarosite is assumed to be an artifact of pyrite oxidation.

A strong negative correlation exists between the quartz and total clay mineral content and a moderately positive correlation between quartz and feldspar (K-feldspar plus plagioclase), except for one outlier (Figure 11). Removal of the outlier gives a positive correlation with $R^2 = 0.50$.

The clay mineralogy from the clay fraction analysis varies significantly. Only two samples contain a significant amount of Fe in the 2:1 clays (see Figure 22 and Table 13 of Appendix C). Smectite and illite/smectite mixed layers (ISS) represent the largest part. The chlorite content is very low (1-2% of the clay fraction). In general, except for a few outliers, the samples with a high total clay content (from bulk XRD) contain more kaolinite/smectite mixed layers (KSS) and smectite and less ISS and illite. Kaolinite and illite show a moderately positive correlation, while illite and smectite have a moderately negative correlation (Figure 11). Removal of the one outlier with low smectite and illite contents results in a $R^2 = 0.44$.

XRD analyses show that the three outliers with high K_2O and Ba content (samples XI-1, XI-2 and XI-3) contain 1.6 to 2.2 wt% sylvite (KCl) (Table 13). No other samples which were analyzed by XRD contain this mineral. The high K and Ba content suggest contamination from drilling fluids. Sylvite is an evaporate mineral which is one of the last to precipitate out of a solution. These three samples also contain > 1% of halite, suggesting that formation water and drilling fluids were not removed during core preparation. The evaporites are probably an artifact of this. Since no other samples contain such extreme K and Ba concentrations, this artifact only occurred in core XI.

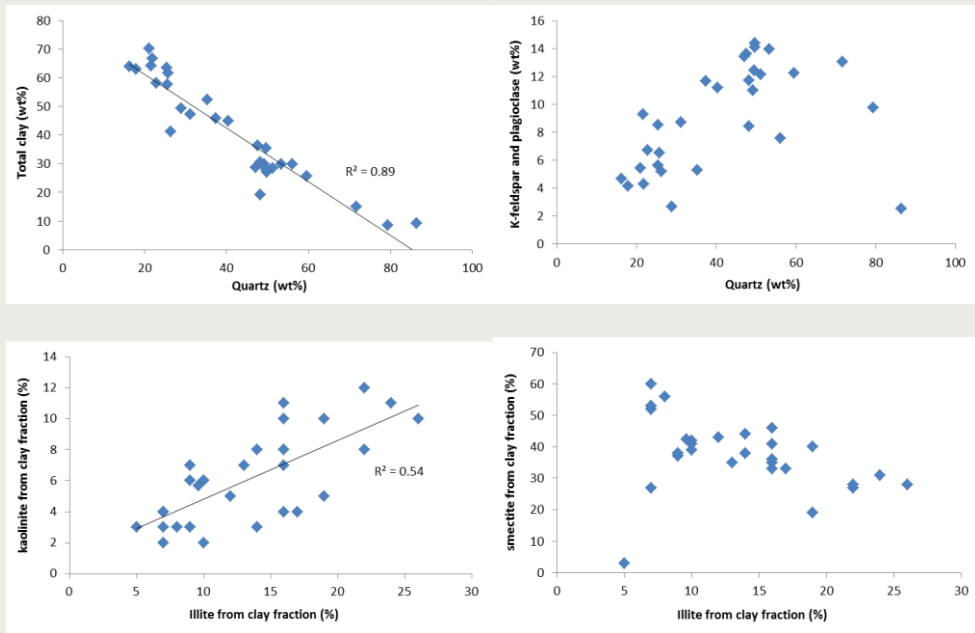


Figure 11. Bulk analysis: quartz versus total clay (upper left) and K-feldspar plus plagioclase (upper right). Clay fraction analysis: illite versus kaolinite (lower left) and smectite (lower right).

4.3. Mineralogy and geochemistry

Since only part of the samples are analysed by XRD, correlations between geochemistry and mineralogy might provide proxies of the mineralogy for the remaining samples. Also, correlations might give additional insight in the specific types of minerals present. A strong positive correlation exists between K-feldspar and Al_2O_3 at Al_2O_3 concentrations up to 8 wt%. Above that value, K-feldspar decreases (Figure 12). The total clay content from the bulk XRD analysis has a very strong positive correlation with Al_2O_3 (Figure 12). The R^2 increases from 0.86 to 0.89 when Al_2O_3 is corrected for K-feldspar and plagioclase. A strong positive correlation exists between Al_2O_3 (corrected for Al in feldspar) and kaolinite and Al_2O_3 (corrected for Al in feldspar) and chlorite (Figure 12). At Al_2O_3 content up to 5 wt% the kaolinite content is stable at around 1%. Above 5 wt% Al_2O_3 the kaolinite content increases.

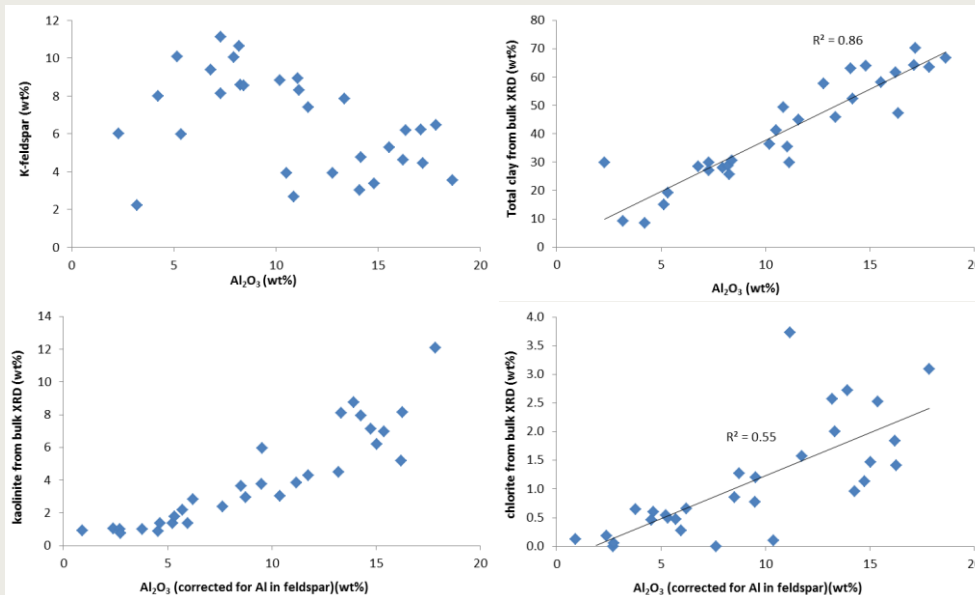


Figure 12. Al_2O_3 versus K-feldspar (upper left) and total clay (upper right). Al_2O_3 (corrected for Al in K-feldspar and plagioclase) versus kaolinite (lower left) and chlorite (lower right)

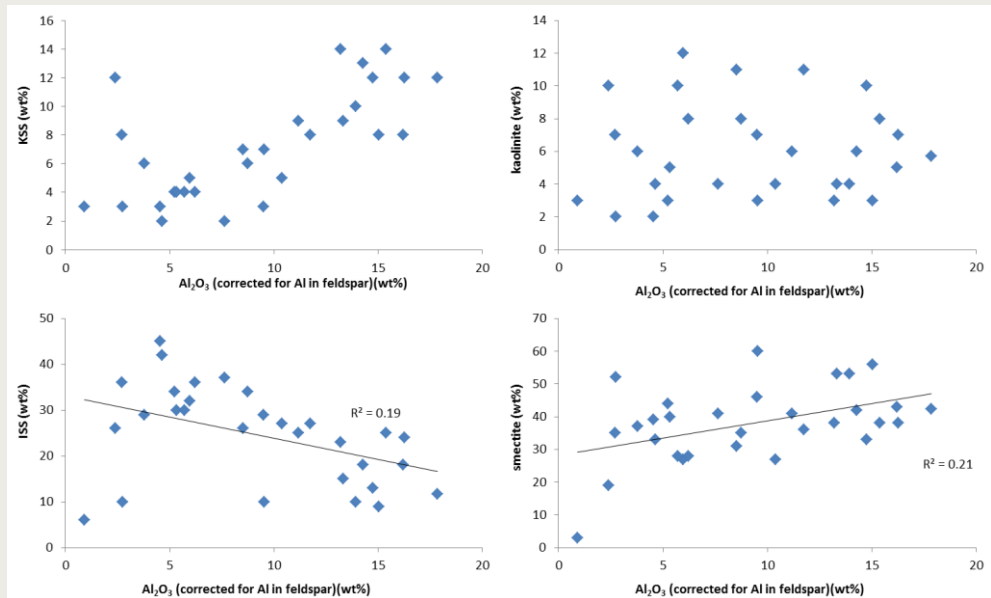


Figure 13. Al_2O_3 corrected for feldspar versus KSS (upper left), kaolinite (upper right), ISS (lower left) and smectite (lower right) from clay fraction XRD.

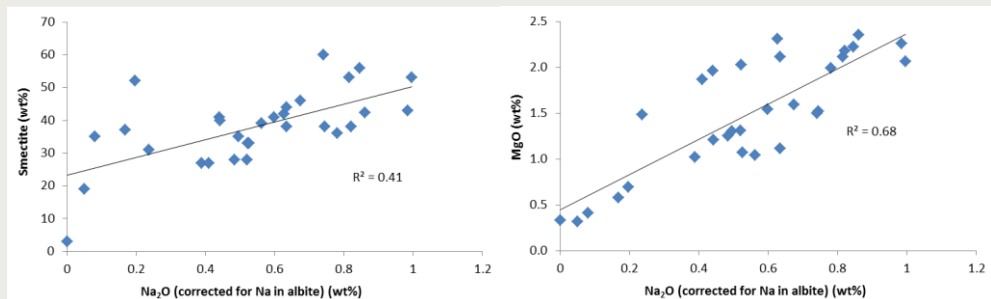


Figure 14. Correlations between Na_2O (corrected for Na in albite) and smectite from clay fraction XRD analysis (left) and MgO (right).

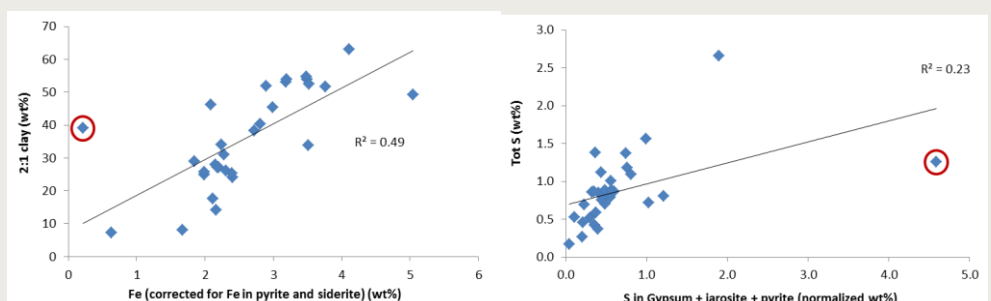


Figure 15. Correlation between Fe from XRF (corrected for Fe in pyrite and siderite from XRD) and 2:1 clays from XRD bulk analysis (left). Without the outlier (red circle) R^2 is 0.66. Correlation between S in S-bearing minerals from XRD and total S measured by XRF (right). Without the outlier (red circle) R^2 is 0.62.

Figure 13 shows the correlation between the clay fraction analysis and Al_2O_3 (corrected for Al in feldspar). Except for a few outliers, KSS shows a positive correlation with Al_2O_3 , while kaolinite shows no correlation at all. The correlation between ISS and Al_2O_3 is weakly negative and weakly positive between smectite and Al_2O_3 . If any, the correlation between CaO and plagioclase is negative indicating that plagioclase does not contain Ca. The

correlation between Na_2O and plagioclase is weak, but positive. A strong positive correlation between Na_2O (corrected for Na in albite) versus smectite and MgO can be observed (Figure 14), suggesting the association of Na and Mg with smectite. This could indicate that the smectite type is Na-montmorillonite, but this would require further analysis, e.g. by FTIR measurement. Positive correlations between KSS/ISS and Na are less strong.

To assess the correlation between iron and clays, the amount of iron measured by XRF was corrected for the amount of Fe in siderite and pyrite measured by XRD. One outlier significantly lowers the R^2 value of the correlation. Without the outlier, the R^2 increases from 0.49 to 0.66 (Figure 15). Corrected Fe does not show any correlation with the clay minerals from the XRD clay fraction analysis. When plotting the S in S-bearing minerals gypsum + jarosite + pyrite, the same sample is an outlier. When removing the outlier, the R^2 increases from 0.23 to 0.62. This outlier (sample III4) has a very high pyrite content of 6.9 wt% as measured by XRD. This indicating that the sample batch measured by XRF contained a smaller amount of pyrite, causing discrepancy between the two analytical techniques.

4.4. Grain size distribution

Plots of the grain size distribution from Sedigraph and Laser Diffraction are shown in Appendix D. The results for the Sedigraph and the laser diffraction are somewhat different. This is partially due to the fact that the distribution for the Sedigraph is measured between 0.5 and 250 μm . The fractions $< 0.5 \mu\text{m}$ and $> 250 \mu\text{m}$ are calculated. The laser diffraction measures the total range, up to 880 μm .

The distributions from both the Sedigraph and the laser diffraction show a division between silt-rich samples and clay-rich samples. The two techniques give different peak locations, which are for Sedigraph and laser diffraction respectively 30 - 70 μm and 80 - 150 μm for the silty samples, and $\sim 3 \mu\text{m}$ and $\sim 8 \mu\text{m}$ for the clay-rich samples.

The group of silty samples comprises of the upper and lower parts of core II to VI, the lower part of cores VII, IX, X, XIII and XVII, and core I and XVI in total. The clay-rich group comprises of the middle part of cores II to VI, the upper part of cores VII, IX, X, XIII and XVII, and cores VIII, XI, XII, XIV and XV in total. In Figure 16 the Al_2O_3 and MgO concentrations are plotted versus the clay fraction from the laser diffraction and sedigraph. Overall, we can conclude that the clay fraction of the Boom Clay is low.

For the sedigraph and the laser diffraction the clay fraction is defined as the wt% $< 2 \mu\text{m}$ and $< 8 \mu\text{m}$, respectively. The value of $< 2 \mu\text{m}$ is the conventional definition for the clay fraction. According to Konert and Vandenberghe (1997) the fraction $< 2 \mu\text{m}$ measured by pipette methodology (as in the sedigraph) corresponds with a grain size of 8 μm by the Laser technique. For a more detailed explanation of the different techniques, see the report of OPERA task 4.1.1 by Vis and Verweij (2013). The graphs in Figure 16 show a strong correlation between Al_2O_3 and the clay fraction. This is especially true for the clay fraction from the laser diffraction, which suggests that this technique is better for these sediments than the sedigraph. The positive correlation between MgO and the clay fraction is moderate. The R^2 is equal for both measurement techniques. The interception of the trendlines with the y-axis might give an indication of the average amount of aluminium and magnesium related to the non-clayminerals. For Al_2O_3 the non-clay fraction is feldspar and for magnesium dolomite or magnesite. For both components the interception is significantly higher for the sedigraph.

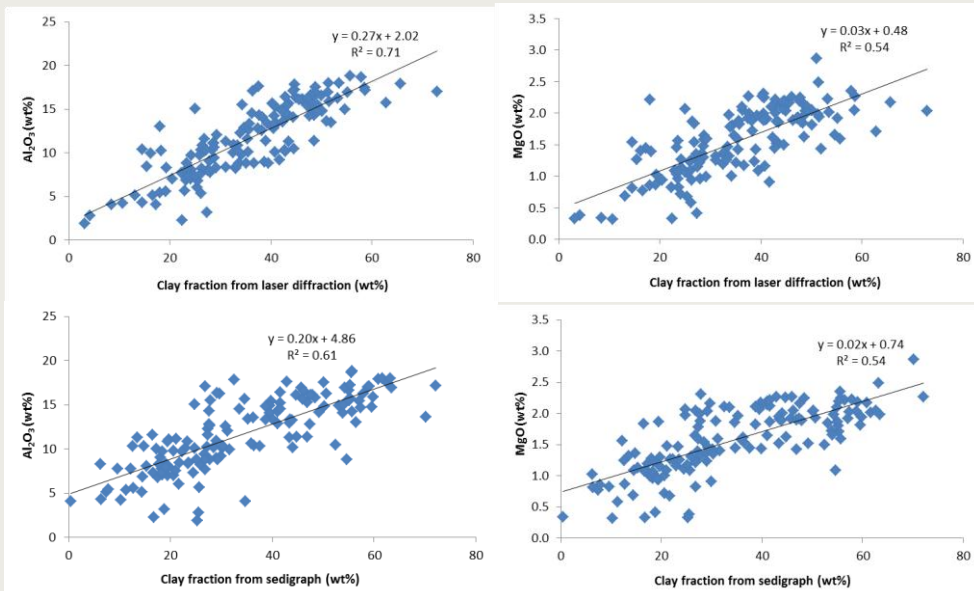


Figure 16. Correlation between the clay fraction and Al₂O₃ (left) and MgO (right). The upper graphs show the clay fraction from the laser diffraction (wt% < 8 µm), the lower graphs from the sedigraph (wt% < 2 µm).

4.5. Depth profiles

The depth profiles of all cores except X, XI, XIV and XV (≤ 4 samples per core) are shown in Appendix E, Figure 25 to Figure 38. The depth interval for each core is 250 m so that the vertical axis is the same for each profile. The actual top and bottom of the profiles differ per core. An onset with a stretched vertical range is provided if necessary. Note that each sample represents up to 3.5 m of core material (Table 8). A description per core is given in the captions.

5. Statistical analyses

5.1. Geochemical data correlation

The geochemical data from XRF and ICP was processed for use in the statistical software program SPSS. All measurements below the detection limit are set at the value of the detection limit divided by two, so that the sum of all these values is valid for a dataset with normal distribution. For the trace elements, the ICP analyses are used instead of the XRF analyses since they have less measurements below the detection limit. The trace elements Be, Sn, W, Ag, Au, Cd, Sb, Bi, Hg, Tl, Au and Se are removed from the dataset due to a high percentage of measurements below the detection limit. For the oxides, the XRF data are chosen for the statistical analyses since these also include SO_3 and V_2O_5 .

Correlation matrices are produced for all remaining variables. These show how well two variables correlate (either positive or negative). Note that any outliers can significantly affect the correlations, as was shown for the relation between P_2O_5 , U and organic C. Due to one sample with high P_2O_5 and U values, a high correlation between these parameters is calculated, while the positive correlation between U and organic C is destroyed due to this same single outlier (Figure 10). The correlations allow the selection of a limited number of variables for the cluster and factor analyses. The results of the correlation matrices for high correlation values ($|R| > 0.6$ and correspondingly $R^2 > 0.36$) are shown in Appendix F. SiO_2 shows negative correlations with Al_2O_3 , Fe_2O_3 and MgO , while these oxides, in turn, show positive correlations with each other and several other oxides (Table 15 in Appendix F). The Al_2O_3 content is also positively correlated with organic C. SiO_2 also shows negative correlations with many trace elements except for Zr, while Al_2O_3 , MgO , Ti_2O and V_2O_5 show positive correlations with almost all trace elements (Table 16). K_2O and Fe_2O_3 show positive correlations with a few trace elements. Inorganic C and CaO show strong positive correlations with only Sr. P_2O_5 shows a strong correlation with only U, but it should be noted that this correlation is based on one outlier with extremely high P_2O_5 and U values. The correlation between U and organic C is not shown in the table because that same outlier significantly reduces the R^2 value (Figure 10 and Table 16). Most trace elements show strong positive correlations with each other. Only Ba, Sr and U do not show any correlations with any other trace element. The trace element Zr shows an (almost perfect) positive correlation with Hf (Table 17).

5.2. Cluster analysis

A selection of variables is made for the cluster analysis and includes all oxides, organic and inorganic C, and several trace elements. Most trace elements are excluded since they correlate highly with Al_2O_3 and/or with each other. Rubidium represents all trace elements which highly correlate with Al_2O_3 (Table 16). Copper and Hf are excluded since they highly correlate with Pb and Zr, respectively (Table 17). Based on the percentile plots of the selected variables (Appendix B) the following are treated as lognormal instead of normal distributed variables: CaO, MnO, SO_3 , inorganic C and all selected trace elements. For these variables the log of the values was used in the analysis. A few high outliers from Na_2O , K_2O , P_2O_5 , U, Ba and Pb were initially removed from the dataset to prevent that these dominate the cluster results. Subsequently, the values of the resulting dataset were standardized.

The cluster analyses for 6, 8, and 10 clusters give varying results. In the case of 6 clusters, the number of samples is well divided over the clusters (3 clusters with 36 samples each, one with 35 samples and 2 with 3 samples each). In the case of 8 clusters, the samples are still well divided, but the results for the sample assignment to the clusters are quite different than for 6 clusters and the average cluster compositions have significantly changed. For the 10-cluster case, the smaller clusters of the 6- and 8-cluster cases are disintegrated into clusters of 1, 2 and 3 samples each. These small clusters then represent

the samples which are outliers. This implies that the formation of separate clusters for the outliers is more relevant than splitting up the larger clusters. Because outliers are not the main interest of this study, the 10-cluster case becomes therefore less relevant.

In the 6-cluster case, many cores are (almost) completely represented in one of the clusters. For the 8-cluster case the results are very different and the samples of each core are more spread over the clusters. Therefore, the 6-cluster case is assessed in more detail. A short description of the clusters is shown in Table 1 and the average cluster compositions are shown in Table 2. The cluster classification is mainly based on the Al, Si and Ca content. For each cluster the average clay and sand fraction and their spread within the cluster are shown in Table 2. In general, a higher SiO₂ content corresponds to a higher sand fraction and a high Al₂O₃ content with a high clay fraction. However, the scatter in the clay and sand fraction is large.

The small clusters 2 and 3 are very similar and represent silica-rich samples. Some consistent differences in the minor components caused the separation into two clusters, but these differences are not crucial. Hence, the two clusters can be seen as one. The four largest clusters of the 6-cluster case are further analyzed by cluster analysis individually (Figure 17). This allows to assess whether the samples of each core remain together when more clusters are formed, without having the problem that the cluster means are shifting significantly when more clusters are formed (like in the 8-cluster case) (Figure 17). The results of the cluster analysis per cluster are shown in Appendix G. Clusters 1, 4 and 6 are each relatively homogeneous, shown by the small variability in parameters for the sub-clusters. Cluster 5 shows a larger variability between the sub-clusters. Four distinct sample groups form. The top parts of cores XI, XII, XIV and XV form a separate sub-cluster (sub-cluster 3 in Table 20) which have the highest SiO₂ and lowest Al₂O₃ content of the cluster. Core VIII (complete) and the middle parts of cores XI, XII, XIII and XV form a separate sub-cluster (sub-cluster 2 in Table 20) with the highest Al₂O₃ and Fe₂O₃ and lowest CaO content of the cluster. The top part of core I forms another sub-cluster (sub-cluster 2 in Table 21) and has intermediate SiO₂, extremely low Al₂O₃ and high CaO. The middle part of core I, top and bottom of core II, and the complete fresh core form a fourth sub-cluster (sub-cluster 3 in Table 21) with intermediate to high SiO₂ and intermediate Al₂O₃ and CaO. The remaining cores and samples are dispersed over de sub-clusters.

Table 1. Cluster description for the 6-cluster case.

Cluster	Nr. of samples	Cores and samples	Description
1	35	Upper and/or lower parts of core I to VII, IX, X, XIII and main (upper) part of core COVRA	Si-rich, intermediate Al, Fe, Mg. High Na and K
2	3	Core IV, samples 1, 9 and 11	Very Si-rich, Al and Fe poor
3	3	Samples II9, IV7 and V10	Very Si-rich, Al and Fe poor
4	36	Cores VIII, XI, XII, XIV and XV, core XIII 1-6, 3 samples from 3 other cores	Si-poor, high in all remaining oxides.
5	36	Core I, fresh core, upper part of core II, several samples from core IV	Si-rich, low Al, high Ca
6	36	Middle part of cores II, III, V, VI and VII, lower sample of COVRA core and core IX almost completely	Si-poor, high Al, Fe, Mg and K. Low Ca.

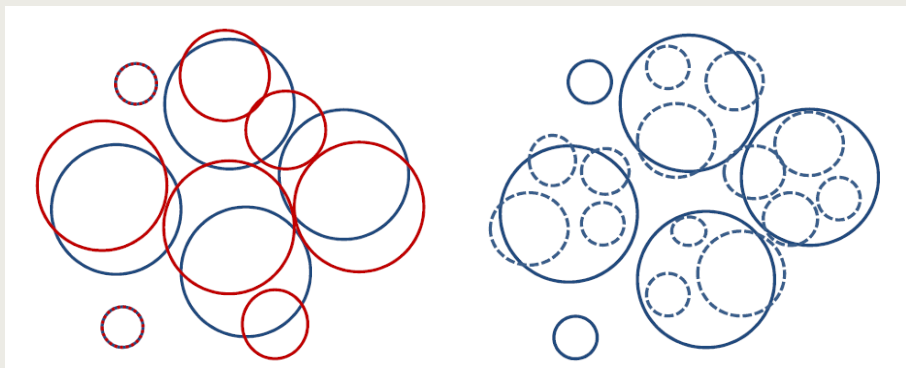


Figure 17. Left: schematic representation of 6- and 8-cluster case in blue en red, respectively. The cluster averages shift significantly, and samples switch between the different clusters. Right: representation of the separate cluster analysis for the four main clusters of the 6-cluster case.

Table 2. Cluster means for the 6-cluster case (in wt%) and corresponding average clay and sand fraction. Spread of the clay and sand fractions within each cluster is shown in brackets.

	Cluster					
	1	2	3	4	5	6
SiO ₂	70.9	87.7	86.8	53.0	69.6	57.8
Al ₂ O ₃	10.4	2.7	4.5	14.1	7.5	16.0
Fe ₂ O ₃	4.3	3.0	2.4	6.1	4.4	5.8
CaO	0.9	1.1	0.3	5.0	4.5	0.9
MgO	1.4	0.4	0.5	2.0	1.1	1.9
Na ₂ O	0.8	0.1	0.4	1.0	0.7	0.7
K ₂ O	2.7	1.0	1.8	2.8	2.3	3.1
MnO	0.02	0.01	0.01	0.04	0.02	0.02
TiO ₂	0.7	0.2	0.3	0.7	0.5	0.8
P ₂ O ₅	0.06	0.07	0.04	0.12	0.07	0.08
Cr ₂ O ₃	0.02	0.01	0.01	0.02	0.02	0.02
S ₂ O ₃	0.3	0.1	0.0	0.6	0.7	0.4
V ₂ O ₅	0.02	0.01	0.01	0.02	0.01	0.03
Organic C	0.6	0.4	0.2	1.0	0.6	1.3
Inorganic C	0.1	0.2	0.1	1.1	0.9	0.1
Ba	336	178	301	272	328	312
Rb	99	36	57	118	80	141
Sr	139	89	81	320	270	148
U	2.9	1.2	1.8	3.7	2.9	4.2
Zr	352	184	364	181	418	216
Mo	0.9	1.1	0.7	1.7	1.7	1.3
Pb	10.5	4.5	11.9	19.2	7.8	18.1
Zn	53	18	19	122	35	68
As	6.8	9.1	4.5	8.0	10.7	11.6
Clay fraction	7.0 (4-14)	5.8 (2-10)	3.9 (4)	8.2 (4-12)	6.8 (0-12)	11.8 (5-25)
Sand fraction	19.1 (3-45)	59.1 (38-89)	78.4 (76-82)	3.2 (0-13)	35.8 (0-91)	3.8 (0-30)
Nr of samples	35	3	3	36	36	36

5.3. Factor analysis

A factor analysis, by principle component extraction, was first performed on all variables minus the trace elements which were removed from the dataset due to a high percentage

of measurements below the detection limit. This results into the extraction of 8 components by Kaiser Normalization (selection of components with eigenvalues > 1) which explain 88.4% of the total variance. The component matrix is huge and complex. Therefore, as a next step, many trace elements were removed which correlate highly with Al₂O₃ or CaO. Factor analysis on the new data set is performed using various types of component extraction methodologies. Also, the rotation methodology is varied. In the literature there is no consensus on which methodology to use in which case. Since the results of the different methodologies vary only slightly and in each case more or less the same factors are found, it does not really matter which one is used. The resulting component matrix is shown in Table 3. Seven principal components are extracted by Kaiser Normalization, which explain 77.1% of the total variance.

Factor 1 represents Al and thus the clay size fraction. Silicon and the sand fraction are negatively associated. Magnesium, TiO₂ and V₂O₅ are highly positively associated. The second factor represents carbonate. The Sr content is not included in the factor analysis, but would be positively correlated, considering the correlation between Sr and CaO. The SiO₂ content is slightly negatively correlation with carbonate. The third component represents organic material, associated with total S, Mo, As and U. This factor is representative of pyrite, even though Fe₂O₃ is not associated with this factor. The trace metals Mo and As, as well as Hg and to a lesser extent Co, Cu, Mn and Ni are commonly pyritized in anoxic marine sediments (Raiswell and Plant 1980; Huerta-Diaz and Morse, 1992). Iron is moderately associated with the clay factor but is in general not strongly representative of a specific component. The association of organic matter and pyrite

Table 3. Varimax rotated component matrix for the 7-factor case. The extraction method used is the unweighted least squares method. Only loadings higher than 0.4 are shown, the loadings higher than 0.6 are in bold.

	Factor						
	1	2	3	4	5	6	7
Clay fraction	.54						
Sand fraction	-.76						
SiO ₂	-.73	-.52					
Al ₂ O ₃	.93						
Fe ₂ O ₃	.56				.52		
log CaO		.88					
MgO	.83						
Na ₂ O					.42		
K ₂ O	.71					.58	
log MnO		.48			.55		
TiO ₂	.91						
P ₂ O ₅							.73
Cr ₂ O ₃	.66						
log SO ₃		.58					
V ₂ O ₅	.87						
Total C		.84					
Total S			.79				
Organic C	.57		.61				
Inorganic C		.94					
log Ba						.88	
log Hf				-.89			
log U	.43						.84
log Zr				-.88			
log Mo			.72				
log Pb					.51		
log Zn	.45				.65		
log As			.63				
% of variance	27.0	12.9	9.7	9.3	7.6	5.3	5.1
Cumulative %	27.0	40.0	50.0	59.0	66.7	72.0	77.1

reflect the reducing conditions during the deposition or early burial of the clay (Decler et al., 1983). The fourth factor of Hf and Zr is representative of zircon. Hafnium is a major trace element in this mineral (e.g. Tichomirowa et al., *in press*). The remaining factors represent combinations of elements which do not have significance on their own. The factor analysis was repeated for four factors to assess the correlation of those elements with the main factors. The results are shown in Table 4. The same main factors are defined as in the 7-factor case. These results imply that the main variance between the samples can be explained by clay (and quartz), carbonate, pyrite and zircon.

Table 4. Varimax rotated component matrix for the 4-factor case. The extraction method used is the unweighted least squares method. Only loadings higher than 0.4 are shown, the loadings higher than 0.6 are in bold.

	Factor			
	1	2	3	4
Clay fraction	0.46			
Sand fraction	-0.80			
SiO ₂	-0.76	-0.51		
Al ₂ O ₃	0.93			
Fe ₂ O ₃	0.67			
log CaO		0.93		
MgO	0.89			
Na ₂ O	0.41			
K ₂ O	0.78			
log MnO	0.55	0.57		
TiO ₂	0.92			
P ₂ O ₅				
Cr ₂ O ₃	0.68			
log SO ₃		0.57		
V ₂ O ₅	0.83			
Total C		0.78		
Total S			0.78	
Organic C	0.48		0.71	
Inorganic C		0.92		
log Ba				
log Hf				0.86
log U		0.42		
log Zr	-0.43			0.86
log Mo			0.74	
log Pb	0.51			
log Zn	0.68			
log As			0.52	
% of Variance	30.6	13.6	10.9	8.6
Cumulative %	30.6	44.2	55.0	63.6

The ‘minor’ components which are more dispersed over several factors, are slightly rearranged between the factors compared to the 7-factor case. P₂O₅ and Ba are the only components which are not explained by any of the factors, indicating that they are not associated with either clay, carbonate, pyrite or zircon. The factor plots and the factor scores per sample for the 4-factor case are shown in Appendix H. The plots are the graphical representation of the rotated component matrix in Table 4. They show how much of each component is explained by the different factors. The factor scores indicate how well a sample is explained by the different factors. For example, the samples of core I all score negative for factor 1, indicating the high quartz and feldspar content of these samples. The samples score high on factors 2 and 4 and they are thus rich in carbonate and zircon. The samples of the northern cores all score high on the carbonate factor and mostly positive on the clay factor.

5.4. Mineralogy

A correlation matrix was also produced with SPSS for the mineralogy (Appendix I). Besides the correlations already discussed in sections 4.2 and 4.3, a strong correlation also exists between anatase and different clay minerals. A factor analysis was not performed since N is too low (N = 30).

Kmeans clustering was performed for 3 clusters based on the bulk XRD analyses. The following minerals/components were eliminated: ilmenite (rare occurrence, low amounts), total non-clay (reflected in total clay component) and 2:1 Fe-clay (rare occurrence). The results are shown in Table 5. Clusters 1 and 2 have low quartz and feldspar and a high clay content. The difference between the two clusters is the carbonate content which is much higher in cluster 2. The northern cores and the middle parts of the southern cores belong to these clusters. Cluster 3 has a high quartz and feldspar, low clay and intermediate carbonate content. The new, fresh drilling core XVI and the upper and/or lower part of the southern cores belong to this cluster (Table 5).

Table 5. Results of cluster analysis based on mineralogy (in wt%). *Total 2:1 clay content.

Sample	Cluster	Distance		Cluster		
				1	2	3
III 4	1	4.853	Quartz	27.45	22.98	55.46
III 8	1	2.231	Plagioclase	1.96	1.15	3.09
V 4	1	3.482	K-feldspar	5.50	3.69	8.26
V 6	1	3.217	Clin/Heul	0.00	0.63	0.78
V 8	1	2.493	Calcite	0.50	11.34	2.52
XIII 4	1	1.710	Aragonite	0.42	0.45	1.52
XIII 6	1	2.846	Ank/Dol	0.00	0.39	0.01
XIII 10	1	2.874	Siderite	0.00	0.64	0.11
III 6	2	5.637	Pyrite	1.29	0.65	0.70
IV 8	2	5.242	Anatase	0.78	0.54	0.20
XI 1	2	3.285	Sylvite	0.00	0.96	0.00
XI 2	2	2.407	Halite	0.18	0.63	0.05
XI 3	2	3.798	Gypsum	1.49	0.36	0.58
XIII 2	2	4.060	Jarosite	1.38	0.00	0.05
III 10	3	2.036	Chlorite	2.22	1.43	0.46
III 11	3	1.743	2:1 clay*	49.98	47.80	24.36
IV 7	3	2.765	Kaolinite	6.76	6.35	1.82
IV 9	3	2.786	Total clay	58.96	55.57	26.64
IV 11	3	4.067				
V 2	3	2.642				
V 10	3	2.391				
XIII 8	3	2.608				
XVI	3	1.876				
XVI	3	2.582				
XVI	3	2.399				
XVI	3	2.222				
XVI	3	2.697				
XVI	3	1.986				
XVII 5	3	2.609				

5.5. Mineralogy and geochemistry

Appendix J shows the correlation matrix between the mineralogy and the geochemistry. Besides the correlations described in section 4.3 most trace elements correlate negatively with quartz, and positively with anatase and clays. Plagioclase and K-feldspar correlate positively with Hf and Zr, and jarosite and halite correlate well with Ba.

6. Discussion and conclusions

6.1. Characterization

The clay mineralogy is a crucial aspect in the safety assessment of radioactive waste storage in clay-type host rocks, as will be explained in the next section. The quantification of clay mineralogy is difficult to assess in detail, but the analysis was performed based on advanced interpretation techniques (Zeelmaekers, 2011). The bulk rock XRD analysis gives a general idea of the clay mineral content. The clay fraction XRD analysis results in a more detailed insight in the clay mineralogy. Furthermore, the clay fraction is based on grain size ($<2\text{ }\mu\text{m}$) (see section 3.1.2 on XRD methodology). Hence, it contains very small quartz and feldspar grains while larger clay grains are excluded from the analysis (Zeelmaekers, 2011). A combination of (bulk and clay fraction) XRD and geochemical analysis provides additional information.

The strong positive correlation between Al_2O_3 and the total clay fraction from bulk XRD suggests that the bulk XRD gives a good representation of the clay mineral fraction. Hence, the Al_2O_3 content (even if not corrected for Al in feldspar) is a good qualitative proxy for the clay mineral fraction. This proxy allows the quantitative interpretation of the clay fraction XRD analysis by plotting the clay mineralogy against the Al_2O_3 .

The positive correlation between Al and K in combination with the XRD analyses shows the presence of K-feldspar in samples with relatively low Al (and thus clay) content. In samples with higher Al (clay) content kaolinite is present in addition to K-feldspar, which decreases the K/Al ratio. K-feldspar has a lower content in these samples, while the illite content is positively correlated with kaolinite (Figure 11). These correlations imply that the Al_2O_3 content in Boom Clay can be used as an indicator for the relative amounts of K-feldspar, illite and kaolinite if XRD analyses are not available.

The Mg and Fe content show a strong positive correlation with Al, suggesting that they are mainly associated with clays (e.g. smectite, illite or chlorite) and not with carbonates like dolomite or siderite. This is confirmed by the limited presence of these carbonate minerals in the XRD analyses.

Besides clay minerals, Fe is present in (generally) small amounts of pyrite in most of the samples and jarosite in a few of the samples. Jarosite (as well as gypsum, sylvite and halite) have probably been formed during storage of the core due to drying and/or oxidation. The one sample in core III4 with very high pyrite content plots as an outlier in the iron and sulfur graphs. This indicates that potentially the two batches of the sample, which are analysed by XRD and XRF are slightly different. The batch analysed by XRD seems to have had a significantly higher pyrite content than the batch analysed by XRF.

The strong correlation between inorganic carbon and CaO indicate the presence of CaCO_3 . The XRD results show that CaCO_3 is present mainly as calcite and to a lesser extent as aragonite, except for the samples of the fresh core (XVI) which contain rather consistent and similar amounts of calcite and aragonite (~3 wt% each). Strontium is a common trace element in CaCO_3 . The correlation factor between Sr and calcite ($R^2 = 0.47$) is much higher than Sr and aragonite ($R^2 = 0.03$). This is unexpected, since Sr is known to have a preference for aragonite.

The weakly negative correlation between Ca and plagioclase suggests that the plagioclase is Na-rich (albite). This is also shown by the position and intensity of the X-ray diffraction peaks. The correlation between Na and plagioclase is weak but positive, suggesting that another source of Na is present besides albite. The Na content correlates with Mg, suggesting that Na/Mg-montmorillonite is the smectite variant present or that Na and Mg are adsorbed to the smectite mineral surface.

Most of the trace elements are highly associated with Al_2O_3 , MgO , TiO_2 and V_2O_5 . The correlation matrix between the mineralogy and the trace elements shows that these trace elements are highly associated with anatase (TiO_2), clay and kaolinite. V_2O_5 is associated with clay and anatase and is probably a trace element in these minerals. Unclear is whether the trace elements have a preference for specific clay types. Cs, Ga, Pb, Ni and As are correlated with chlorite.

In Decleer et al. (1983) the results of a very similar statistical study are published for the Belgian Boom Clay for the clay products industry. The strong positive correlation between the chemical constituents of clay minerals and the clay size fraction, and their negative correlation with SiO_2 , quartz and the sand fraction was also found in the outcrops in the clay pits of Sint-Niklaas, Terhagen and Kruibeke (Belgium). Furthermore, they also concluded the presence of CaCO_3 by the strong correlation between CaO and CO_2 (inorganic carbon in our study).

Table 6 shows a combined overview of the cluster analysis and the grain size and mineralogy interpretations. The clustering analysis based on the bulk rock XRD mineralogy is very consistent with the factor analysis. The factor analysis shows that the main part of the variance between the samples can be explained by four factors: clay content, carbonate, pyrite and zircon. The clay factor represents also the (inverse) quartz and feldspar contents since these are highly negatively correlated with clay. The (weak) negative correlation between carbonate and the SiO_2 content from the factor analysis was also observed in some of the depth profiles shown in Appendix E. Decleer et al. (1983) found the same factors, except for zircon since trace elements were not measured. According to their analysis, a positive correlation exists between the clay minerals and pyrite and organic carbon. This correlation is not as clear in the samples of our study.

The six clusters from the cluster analysis based on the geochemical composition are mainly defined by the clay (e.g. Al_2O_3), quartz (SiO_2) and carbonate (CaO and inorganic C) components. Furthermore, the organic C content is generally low in the clusters with high SiO_2 . The clustering also shows a clear correlation with the grain size distribution. The samples of the cluster with high quartz, plagioclase and K-feldspar and low clay content all have a grain size distribution with a clear peak between 30 and 70 μm (Sedigraph). This is comparable to samples from Belgium (Honty, 2008). The samples of the cluster with low quartz and feldspar contents and high clay content have a much lower grain size. The correlations between quartz and SiO_2 and between Al_2O_3 and total clay are almost perfect, indicating that these oxides can serve as a proxy for the quartz and clay content. CaO and inorganic C are almost perfectly correlated with calcite, indicating that these can serve as a proxy as well.

The clustering analysis based on the geochemical composition resulted in a clear geographical and depth-related subdivision of the different cores and samples. All samples of the cores in the northern part of the country, except the lower 4 samples of core XIII, form a separate cluster. The samples have a low SiO_2 content and they are rich in Al_2O_3 , Fe_2O_3 , CaO , MgO , Na_2O , inorganic carbon and Sr. The CaO , inorganic carbon and Sr content are representative of high CaCO_3 contents of the samples and the high MgO is representative of the montmorillonite and/or chlorite content. All these samples fall into the group of lower grain sizes and the few samples analyzed by XRD (except for sample XIII 2) in the mineralogy cluster with low quartz and feldspar but high clay and calcite content. The upper and/or lower parts of the cores in the southern part of the country, as well as the lower part of core XIII in the northern part of the country, form a separate cluster which is rich in SiO_2 , intermediate in Al_2O_3 , Fe_2O_3 and MgO . They have intermediate to large grain sizes. Only few of the samples in this cluster were analyzed by XRD, and these belong to the cluster with high quartz and feldspar and low clay content. The carbonate content is intermediate.

The middle parts of the southern cores form a separate cluster with a very low SiO₂ and high Al₂O₃, Fe₂O₃, MgO and K₂O contents, indicating high clay content. The main difference with the cluster of the cores in the northern part of the country is that these samples have a low CaO, inorganic carbon and Sr content, and they are therefore low in CaCO₃. The few samples of the cluster which are analysed by XRD show low quartz and carbonate and high clay content, which is consistent with the geochemical clustering. Assuming that these samples are representative of the cluster, the high K₂O content does not seem correlated to K-feldspar or sylvite and is probably the result of potassium-rich illite or muscovite.

The cores in the most eastern region of the country, core I (except for 2 samples in the lower part of the core), the upper part of core II and several samples of core IV form a separate cluster together with the fresh core (XVI). This cluster has a relatively high SiO₂ content and intermediate Al₂O₃, Fe₂O₃, CaO, MgO, Na₂O and K₂O. It has a similar composition to the cluster of the upper and/or lower parts of the cores in the southern part of the country, except that it has a higher CaO content and slightly lower Al₂O₃. Hence, the carbonate content is higher and the clay content lower. The grain size distributions show peaks around 30-70µm (Sedigraph) and low clay fraction content (max 12%). The few samples analyzed by XRD (mainly from the fresh core) fall in the mineralogy cluster with high quartz and feldspar and low clay content.

The two remaining clusters each contain three samples with very high SiO₂ content. They probably represent sandy layers within the Boom Clay, which is also reflected by their coarse grain sizes. The two clusters have not very distinct differences and can be considered as one. Four of the samples in these clusters are from core IV, the other two are from cores II and V. These cores are all in the province of Limburg.

Based on the clustering, combined with the grain size and mineralogy analyses the cores are divided into 3 groups (Table 6). Overall, we have a clear division between the northern and the southern part of the Netherlands. The northern part is much more clay-rich, is fine grained and relatively homogeneous with depth. The samples have a relatively high carbonate content. In the southern part of the country the Boom Clay is more silty. Here, the upper and/or lower parts of the Boom Clay are coarser grained and contain more quartz and feldspar. The middle parts of the Boom Clay are finer grained and more clay-rich with an occasional sandy layer. In the southeastern part, the Boom Clay is in general more sandy and carbonate-rich than the southwestern part. This results in the division of the following groups: North, Southeast and Southwest (Table 6).

Geochemical and grain size analyses of Boom Clay samples in Belgium are presented in Honty (2008). The samples in this study were taken from the Mol-1 borehole and from the HADES URL location, both located in Mol. The depth range of the samples is 204.3 - 286.7 m. The upper and lower parts of the cores are coarse silt, the middle part is more clay rich. Core III south of Tilburg, being most closely located to Mol and having a depth range of 340 - 485 m, has a similar grain size distribution with depth.

XRD analyses were performed on part of the samples from Mol. These analyses were performed by two different laboratories for cross analysis. The upper part of the Boom Clay is more quartz-rich with concentrations around 50 wt% and K-feldspar and plagioclase contents between 6 - 11 and 2 - 4 wt%, respectively. This is consistent with the samples of cluster 1 and 5 in our analysis. Also the total clay content and clay mineralogy is similar. The lower part of the Belgian cores have lower quartz and feldspar and higher clay mineral contents, which is similar to clusters 4 and 6 in our analysis but the 2:1 clay content can reach higher values in the Dutch samples. The lowest part of the core from Mol was not analyzed by XRD but the results of the grain size analysis (silty) indicate quartz contents in the higher range.

Hence, the Boom Clay in Mol has silty upper and lower parts and a fine grained, clay-rich middle part. The same depth relation is observed in the southern cores II, III, V and VII. The Belgian Boom Clay samples are all carbonate poor with contents ≤ 1.2 wt%, while the carbonate content in the Dutch samples is up to 26 wt%. The samples with high carbonate

content all belong to clusters 4 and 5 which represent the northern and part of the southeastern cores.

Table 6. Overview of clusters and characteristics. * IV8 fits better with cluster 4.

Core	Location/group	Cluster 1	Cluster 2 + 3	Cluster 4	Cluster 5	Cluster 6
I	Southeast	10,12			1-9, 11, 13	
II	Southeast	6	11	9	1-3, 10	4, 5, 7, 8
III	Southeast	2, 10, 11		6	1	3-5,7-9
IV	Southeast	3,4	1,7,9,11		2,6,8*,10	5
V	Southeast	2-4, 9, 11, 12	10			1,5-8
VI	Southeast	1,2,4-6			3	7-12
VII	Southwest	6,7		1	8	2-5
VIII	North			1-10		
IX	Southwest	11,12				1-7
X	Southwest	1-4				5
XI	North			1-3		
XII	North			1-8		
XIII	North	7-9		1-6		10
XIV	North			1-4		
XV	North			1,2		
XVI	unspecified				1-14	
XVII	Southwest	1,3-6				2
Nr. of samples		35	6	36	36	36
Description		Si-rich, intermediate Al, Fe, Mg. High Na and K	Very Si-rich, Al and Fe poor	Si-poor, high in all remaining oxides.	Si-rich, low Al, high Ca	Si-poor, high Al, Fe, Mg and K. Low Ca.
Mineralogy		intermediate clastic and clay and low carbonate content	(very) high clastic, low clay and carbonate content	low clastic, high clay and carbonate content	intermediate clastic, high carbonate and low clay content	low clastic and carbonate, high clay content
Grain size		intermediate - high	intermediate - very high	low	high	low

6.2. Implications for geological radioactive waste disposal

Clayrocks are investigated as potential host rock for the geological disposal of radioactive waste due to their low porosity, high cation exchange capacities (CEC) and high specific surface areas of the clay minerals (Altmann et al., 2012). These characteristics, which are mainly defined by the clay minerals, influence the diffusion of potentially released radionuclides through the sediment. The high CEC is mainly due to the presence of smectite. The results for this task of the OPERA program show that the mineralogical clay content of the Boom Clay is much larger in the northern part of the Netherlands than in the south. The smectite content in the XRD clay fraction analysis reaches the highest values (>50 wt%) for the samples in the north.

The presence of pyrite in the Boom Clay is important. Oxidation of pyrite as a result of the excavation of a repository, or due to gamma radiolysis of the interstitial water can result in the formation of hematite and sulfuric acid, thereby reducing the pH of the pore water (Ladrière et al., 2009). Changes in pH of the pore water will affect the gas-water-rock interactions of the Boom Clay and correspondingly the geomechanical properties. These effects need to be investigated. However, during excavation of the repository, oxidizing conditions will probably be limited due to installation of concrete walls. The carbonate content of the Boom Clay, which is particularly high in the northern part of the Netherlands, is an important factor in acidifying environments because of its buffering potential. The results of the factor analysis show that pyrite is one of the factors which determine the variance between the different samples. The pyrite content of the Boom Clay varies considerably but it does not show a geographical or depth-related dependence. The organic carbon content of 0.1 to 2.5 wt% is similar to the values in the Belgian Boom Clay samples which have an average of 1.7 wt% (Decleer et al., 1983). Organic carbon in immature sedimentary rocks is usually dominated by kerogen, i.e., the complex high-molecular fraction of sedimentary organic matter that is insoluble in non-polar solvents, alkali and non-oxidizing acids. Upon heating from radioactive waste, the immature kerogen may release components, like hydrocarbons, ketones and alkanoic acids, and complex radioactive elements released from the repository (Deniau et al., 2004). The factor analysis showed that organic carbon is associated with pyrite. Thus, like pyrite, the organic carbon content does not show a geographical or depth related dependence. Hence, the potential effects of pyrite oxidation and of thermal stress on kerogen is relevant for radioactive waste storage in Dutch Boom Clay, regardless of the location of the repository. In the Belgian Boom Clay, pyrite and also organic matter are mainly enriched in the black beds of the Belgian Putte Member. Unfortunately, a stratigraphic sequence is not (yet) available for the Dutch Boom Clay to confirm this correlation in the Netherlands.

In the Boom Clay in Belgium (Figure 18), up to 18 horizons have been found with the presence of septarian carbonate concretions (Figure 19; De Craen et al., 1999). These concretions formed as a result of bacterial activity during early diagenesis (De Craen et al., 1999). They have typical flattened spheroidal shapes with a thickness of 10-20 cm and a diameter of 30-100 cm and vertical, partly open cracks which formed as a result of either dewatering or physical compactional stresses and tension failure (de Craen et al., 1999b). These septarian concretions have not yet been identified and analyzed in the Netherlands. Their presence can be expected, at least in the south of the Netherlands. According to De Craen et al. (1999), the processes which involved the deposition of the concretions were active over large areas and they were insensitive to sedimentary facies. Hence, the presence in the north of the Netherlands is possible. These septarian layers might influence fluid flow at the reservoir scale, forming more or less continuous, horizontal high permeability layers within the low permeable Boom Clay member. However, this has not been observed in the studies on Belgian Boom Clay so far (de Craen and Vandenberghe, personal communication). Nonetheless, the effect of these septarian layers should be further investigated in (reactive) transport modelling.



Figure 18. The Boom Clay as it appears in a quarry near Antwerp (Belgium) showing its horizontally layered structure.



Figure 19. A typical carbonate concretion in the Boom Clay as observed in a quarry near Leuven (Belgium).

6.3. Limitations and considerations

For the purpose of this task within the OPERA program, we had to use core material from the core house of TNO in Zeist. These cores have been drilled at different times over the past few decades. Over time, drilling fluids and core preparation methodologies have evolved. This implies that the sample material has experienced varying conditions of drilling and preparation. These conditions might have had an impact on the mineralogical analyses of the material and possibly the organic content. The nature and extent of this impact is currently not well known.

Furthermore, these cores have been stored at the core house in oxidizing conditions. Oxidation reactions are thought to have prevailed, resulting in the presence of varying amounts of gypsum, halite, sylvite and jarosite, as explicitly observed in some samples.

For future research we advise to focus on fresh material from new drillings. A drilling fluid with minimal (and known) geochemical influence should be selected or developed for this purpose. This material should be analysed in detail as well for reference reasons. Also, the sample material should immediately be stored in anoxic conditions.

Besides the possible geochemical impact of drilling, preparation and storage it should be noted that the material which was sampled for this task represents varying interval lengths of the core. The core house regulations with regard to preservation of core material limit the sampling options. Each sample used for this task represents between 10 cm and 37 m of core material, but the main part of the samples represent <3.5 m of core material.

The samples were divided in two batches for geochemical analysis at ACME and for XRD and grain size analysis at Qmineral. Some heterogeneity between the two batches could not be prevented as was shown by the mismatch in pyrite and FeO content in sample III-4.

With the clay and silt variations with depth, in the South of the Netherlands and in Belgium, in mind, we recommend the development of a detailed stratigraphic characterization. This would allow more considerate sample selection for future research.

References

- Altmann S., Tournassat C., Goutelard F., Parneix J., Gimmi T. and Maes N. (2012). Diffusion-driven transport in clayrock formations. *Applied Geochemistry* 27, p. 463-478.
- Decleer J., Viaene W. and Vandenberghe N. (1983). Relationships between chemical, physical and mineralogical characteristics of the rupelian Boom Clay, Belgium. *Clay Minerals* 18, p. 1-10.
- De Craen M., Swennen R., Keppens E.M., Macaulay C.I. and Kiriakoulakis K. (1999a). Bacterially mediated formation of carbonate concretions in the Oligocene Boom Clay of northern Belgium. *Journal of Sedimentary Research* 69 (5), p. 1098-1106.
- De Craen M., Swennen R. and Keppens E. (1999b). Petrography and geochemistry of septarian carbonate concretions from the Boom Clay Formation (Oligocene, Belgium). *Geologie en Mijnbouw* 77, p. 63-76.
- Deniau I., Derenne S., Beaucaire C., Pitsch H. and Largeau C. (2004). Occurrence and nature of thermolabile compounds in the Boom Clay kerogen (Oligocene, underground Mol Laboratory, Belgium). *Organic Geochemistry* 35, p. 91-107.
- Honty M. (2008). SMARAGD - The study of mineral alterations of clay barriers used for radwaste storage and its geological disposal. External report SCK-CEN-ER-58, 08/Mho/P-12.
- Huerta-Diaz M.A. and Morse J.W. (1992). Pyritization of trace metals in anoxic marine sediments. *Geochimica et Cosmochimica Acta* 56, (7), p. 2681-2702.
- Konert M. and Vandenberghe J. (1997). Comparison of laser grain size analysis with pipette and sieve analysis: a solution for the underestimation of the clay fraction. *Sedimentology* 44, p. 523-535.
- Ladrière J., Dussart F., Dabi J., Haulotte O., Verhaege S. and Regout J. (2009). Mössbauer study of the Boom clay, a geological formation for the storage of radioactive wastes in Belgium. *Hyperfine Interact* 191, p. 1-9.
- Raiswell R. and Plant J. (1980). The incorporation of trace elements into pyrite during diagenesis of black shales, Yorkshire, England. *Economic Geology* 75, p. 684-699.
- Tichomirowa M., Whitehouse M.J., Gerdes A., Götze J., Schulz B. and Belyatsky B.V. (in press). Different zircon recrystallization types in carbonatites caused by magma mixing: Evidence from U-Pb dating, trace element and isotope composition (Hf and O) of zircons from two Precambrian carbonatites from Fennoscandia. *Chemical Geology*.
- Zeelmaekers E. (2011). Computerized qualitative and quantitative clay mineralogy - introduction and application to known geological cases. PhD thesis Katholieke Universiteit Leuven, ISBN 978-90-8649-414-9.

Appendix A

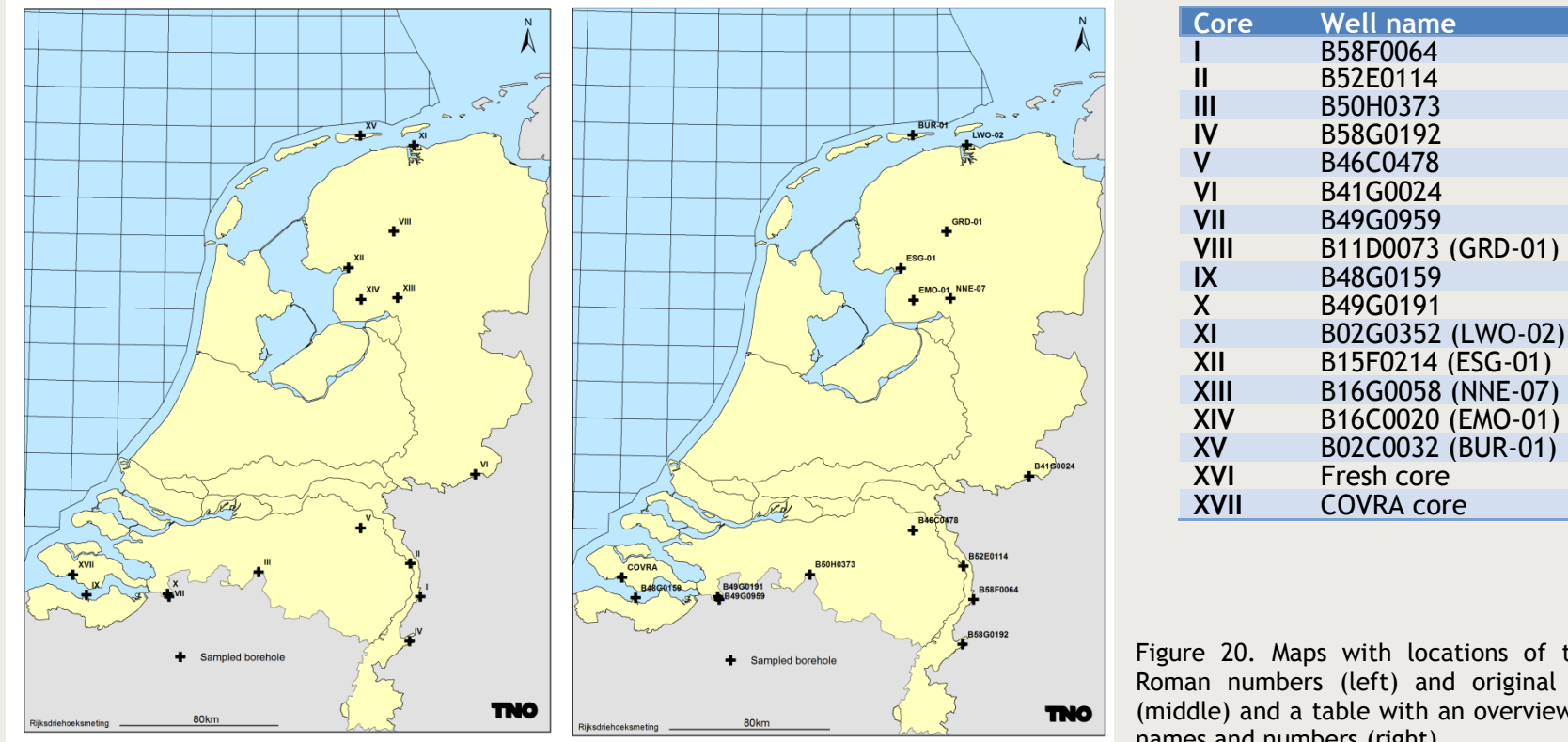


Figure 20. Maps with locations of the boreholes in Roman numbers (left) and original borehole names (middle) and a table with an overview of the wellbore names and numbers (right).

Table 7. Overview of depth (m) of selected samples. The samples in orange are analysed by XRD. * The data from XRF and ICP are inconsistent and removed from the dataset.

Sample number	I	II	III	IV	V	VI	VII	VIII	IX	X	XI	XII	XIII	XIV	XV	XVI	XVII
1	498	396	340	168	153	45	88	454	21	93	610	610	432	613	584	500	27
2	511	414	346	186	168	53	100	460	23	94	632	620	442	625	649	510	79
3	519	434	364	208	183	60	119	489	25	95	650	630	453	638	520	72	
4	540	452	381	222	196	68	125	507	27	96		640	465	660	530	73	
5	561	459	398	233	213	75	141	520	29	98		650	477		540	75	
6	586	476	410	247	226	84	167	529	31			660	489		550	76	
7	607	495	423	262	240	95	175	541	33			670	504		560		
8	624	507	440	277	252	106	182	553	35*			680	514		570		
9	645	520	458	288	280	116		562	37*				523		580		
10	672	534	471	294	312	124		575	39*			537			585		
11	697	539	485	306	330	134			41						590		
12	717			?	143				43						600		
13	736														610		
14															620		

Table 8. Core length represented per sample in meters.

Sample number	I	II	III	IV	V	VI	VII	VIII	IX	X	XI	XII	XIII	XIV	XV	XVI	XVII
1	3.0	2.5	2.0	3.0	1.0	0.5	1.0	0.0	1.0	1.0	0.0	0.0	2.0	5.0	9.0	0.0	37.2
2	1.0	2.5	2.0	3.0	1.0	0.5	1.0	0.0	1.0	1.0	0.0	0.0	1.0	10.0	8.0	0.0	0.0
3	3.0	2.5	1.0	0.5	1.0	1.0	1.0	3.0	1.0	1.0	20.0	0.0	2.0	5.0	0.0	0.0	0.1
4	3.0	2.0	2.0	1.8	1.0	1.0	2.0	3.0	1.0	0.6		0.0	2.0	10.0		0.0	0.0
5	3.5	2.0	3.0	1.2	1.0	0.5	3.0	0.0	1.0			0.0	3.0		0.0	0.0	
6	3.1	1.3	3.0	3.5	1.0	0.5	2.0	0.0	1.0			0.0	3.0		0.0	0.0	
7	3.0	2.0	1.0	3.0	1.0	0.5	1.0	0.0	1.0			0.0	1.0		0.0		
8	3.3	1.5	1.0	2.6	1.0	0.5	2.0	0.0	1.0			0.0	3.0		0.0		
9	3.0	0.5	1.0	0.1	1.0	0.5		0.0	1.0				1.0		0.0		
10	3.0	2.5	2.0	3.0	1.0	0.5		0.0	1.0			2.0			0.0		
11	0.6	3.0	2.0	1.0	1.0	1.0			1.0						0.0		
12	3.0			?	0.5				1.0						0.0		
13	0.8														0.0		
14															0.0		

Appendix B

Table 9. Whole rock XRF data (wt%).

	LOI	SiO ₂	Al ₂ O ₃	Fe ₂ O ₃	CaO	MgO	Na ₂ O	K ₂ O	MnO	TiO ₂	P ₂ O ₅	Cr ₂ O ₃	Ba	Cu	Ni	Pb	Sr	Zn	Zr	SO ₃	V ₂ O ₅	SUM
I 1	6.15	75.5	5.14	3.18	4.63	0.77	0.72	1.74	0.02	0.52	0.06	0.012	0.03	0.003	<0.001	<0.001	0.024	0.003	0.069	0.861	0.011	98.45
I 2	13.17	60.9	4.32	3.6	13.62	0.81	0.58	1.2	0.03	0.45	0.05	0.01	0.02	<0.001	<0.001	<0.001	0.033	0.003	0.059	0.96	0.009	98.72
I 3	6.23	76.7	5.43	3.56	3.97	0.85	0.68	1.69	0.02	0.53	0.06	0.015	0.03	0.005	<0.001	<0.001	0.02	0.004	0.063	0.232	0.01	99.73
I 4	6.75	74.4	5.58	3.21	4.8	0.86	0.78	1.79	0.02	0.49	0.05	0.014	0.04	<0.001	<0.001	<0.001	0.025	0.004	0.053	0.614	0.01	98.79
I 5	12.22	60.4	5.67	4.91	10.8	1.09	0.89	2.01	0.02	0.43	0.08	0.017	0.04	<0.001	<0.001	<0.001	0.061	0.003	0.069	1.013	0.015	98.59
I 6	7.46	70.5	4.08	10.45	2.08	1.44	0.38	2.07	0.03	0.2	0.36	0.018	0.02	<0.001	<0.001	<0.001	0.009	0.005	0.019	0.266	0.03	99.04
I 7	5.77	75.7	7.03	4.88	1.69	0.94	0.78	2.6	0.01	0.45	0.07	0.015	0.04	0.002	<0.001	0.003	0.02	0.003	0.046	0.117	0.015	100.01
I 8	7.17	70.3	7.96	6.3	2.25	1.15	0.77	2.86	0.02	0.51	0.07	0.019	0.04	<0.001	<0.001	<0.001	0.021	0.003	0.053	0.324	0.017	99.42
I 9	8.55	68.6	10.1	4.36	3.27	1.16	0.76	2.61	0.01	0.63	0.06	0.016	0.04	<0.001	0.001	<0.001	0.02	0.006	0.036	0.315	0.015	100.18
I 10	5.17	77.6	7.76	3.29	1.02	0.96	0.72	2.59	0.02	0.52	0.07	0.015	0.03	<0.001	0.001	<0.001	0.02	0.003	0.034	0.204	0.015	99.72
I 11	7.7	77	7	3.35	0.71	0.72	0.5	1.83	0.01	0.52	0.06	0.014	0.03	<0.001	<0.001	<0.001	0.005	0.004	0.031	0.313	0.018	99.43
I 12	6.28	74.5	9.78	3.49	1.36	1	0.64	2.46	0.01	0.68	0.04	0.017	0.03	<0.001	<0.001	<0.001	0.009	0.006	0.029	0.131	0.02	100.26
I 13	13.38	58	11.4	4.63	6.19	1.42	0.56	2.49	0.02	0.65	0.06	0.016	0.03	<0.001	0.002	<0.001	0.023	0.007	0.023	0.525	0.021	98.85
II 1	8.31	69.3	8.05	4	4.9	1.13	0.8	2.47	0.02	0.55	0.07	0.018	0.05	<0.001	<0.001	<0.001	0.027	0.004	0.043	0.48	0.015	99.61
II 2	4.98	77.4	7.69	3.28	1.26	0.82	0.81	2.67	0.02	0.55	0.07	0.015	0.04	<0.001	<0.001	<0.001	0.014	0.003	0.042	0.225	0.014	99.61
II 3	11.24	61.4	11.27	4.28	5.63	1.52	0.85	2.61	0.02	0.7	0.09	0.014	0.03	<0.001	0.001	0.002	0.031	0.006	0.024	0.476	0.02	99.7
II 4	11.51	55.8	17.91	6.68	0.67	2.17	0.81	3.27	0.02	0.86	0.08	0.023	0.04	<0.001	0.005	<0.001	0.013	0.009	0.013	0.177	0.034	99.8
II 5	11.25	57	16.97	6.64	0.66	2.03	0.78	3.24	0.02	0.81	0.09	0.021	0.04	<0.001	0.005	<0.001	0.012	0.009	0.015	0.212	0.032	99.56
II 6	8.81	73.3	9.16	3.92	0.28	0.91	0.53	2.08	0.01	0.56	0.06	0.019	0.04	<0.001	0.006	<0.001	0.006	0.005	0.028	0.103	0.017	99.67
II 7	11.04	63.1	13.48	5.25	0.75	1.43	0.66	2.76	0.01	0.76	0.07	0.024	0.03	<0.001	0.002	<0.001	0.004	0.008	0.018	0.275	0.028	99.38
II 8	9.08	62.7	15.73	4.92	0.4	1.71	0.77	3.26	0.02	0.88	0.06	0.022	0.03	<0.001	0.002	<0.001	0.015	0.008	0.02	0.139	0.029	99.62
II 9	17.54	45.9	13.59	6.43	9.97	2.86	0.72	2.92	0.04	0.66	0.06	0.013	0.02	<0.001	0.002	0.001	0.031	0.006	0.011	0.221	0.02	100.73
II 10	5.38	80.6	6.02	3.81	1.14	0.68	0.5	1.72	0.02	0.46	0.04	0.016	0.04	<0.001	<0.001	0.018	0.008	0.01	0.048	0.195	0.014	100.44

II 11	2.34	88.6	4.04	1.62	0.34	0.34	0.42	1.64	<0.01	0.31	0.03	0.011	0.03	<0.001	<0.001	0.004	0.013	0.002	0.034	0.041	0.007	99.69
III 1	8.3	67.9	10.29	3.64	3.42	1.24	0.76	2.8	0.02	0.65	0.08	0.016	0.04	<0.001	0.005	<0.001	0.024	0.005	0.028	0.533	0.016	99.11
III 2	7.94	69.2	10.28	3.54	2.6	1.36	0.79	2.86	0.02	0.69	0.08	0.014	0.04	<0.001	0.001	<0.001	0.015	0.007	0.032	0.528	0.015	99.36
III 3	11.21	58.5	16.27	5.36	0.46	2.16	0.84	3.31	0.02	0.82	0.07	0.023	0.05	<0.001	0.007	<0.001	0.014	0.009	0.019	0.594	0.026	99.09
III 4	10.54	58.4	16.36	5.57	0.87	2.03	0.82	3.31	0.02	0.92	0.07	0.022	0.04	<0.001	0.005	0.002	0.013	0.009	0.018	0.589	0.031	98.99
III 5	13.69	55.4	16.9	6.06	0.5	1.92	0.84	3.13	0.02	0.87	0.11	0.024	0.04	<0.001	0.005	<0.001	0.017	0.009	0.017	0.3	0.034	99.51
III 6	12.62	52.3	15.53	8.14	2.93	2.31	0.8	2.91	0.05	0.84	0.19	0.018	0.04	<0.001	0.003	<0.001	0.02	0.009	0.016	1.012	0.028	98.69
III 7	12.09	58.2	15.68	5.98	0.44	1.85	0.77	3.02	0.02	0.83	0.09	0.019	0.03	<0.001	0.003	0.001	0.02	0.012	0.021	0.502	0.026	99.03
III 8	12.07	56.1	17.84	6	0.47	2.11	0.88	3.26	0.02	0.87	0.11	0.022	0.04	<0.001	0.005	<0.001	0.015	0.011	0.016	0.166	0.032	99.75
III 9	11.65	56.6	17.09	5.51	1.8	2.04	0.9	3.19	0.02	0.89	0.07	0.021	0.04	<0.001	0.005	0.002	0.018	0.009	0.016	0.291	0.03	99.78
III 10	6.8	71.4	11.06	4.01	0.74	1.3	0.91	2.77	0.02	0.7	0.05	0.016	0.04	<0.001	<0.001	0.003	0.013	0.006	0.035	0.281	0.018	99.77
III 11	5.72	75.4	8.25	4.27	1.37	1.02	0.82	2.44	0.02	0.61	0.06	0.019	0.04	<0.001	0.002	<0.001	0.011	0.005	0.063	0.083	0.017	100.02
IV 1	3.53	87.5	2.76	2.31	2.48	0.38	0.15	1.1	<0.01	0.24	0.04	0.011	0.02	<0.001	<0.001	<0.001	0.017	<0.001	0.035	0.291	0.01	100.48
IV 2	3.94	67.5	1.92	1.73	13.33	0.33	0.48	0.89	0.01	0.2	8.22	0.007	0.03	<0.001	<0.001	<0.001	0.087	0.003	0.032	0.321	0.008	98.63
IV 3	6.03	75.3	9.01	2.84	1.16	1.28	0.42	2.44	0.02	0.7	0.05	0.014	0.03	<0.001	<0.001	<0.001	0.019	0.004	0.035	0.356	0.015	99.29
IV 4	7.53	73.1	10.02	3.6	0.43	1.19	0.45	2.47	0.01	0.72	0.07	0.017	0.03	<0.001	<0.001	<0.001	0.009	0.006	0.033	0.244	0.015	99.64
IV 5	8.97	67	11.32	5.22	1.58	1.32	0.41	2.49	0.01	0.7	0.05	0.018	0.03	<0.001	0.003	<0.001	0.014	0.007	0.026	0.669	0.025	99.14
IV 6	8.3	75.8	7.76	3.64	0.72	0.82	0.29	1.74	<0.01	0.47	0.05	0.016	0.03	<0.001	0.003	<0.001	0.014	0.005	0.025	0.184	0.015	99.62
IV 7	2.67	88.1	4.21	1.78	0.4	0.32	0.26	1.56	<0.01	0.32	0.03	0.007	0.02	<0.001	<0.001	<0.001	0.012	0.001	0.023	0.023	0.006	99.65
IV 8	14.22	53.6	10.87	4.22	10.04	1.87	0.41	2.49	0.03	0.61	0.05	0.011	0.03	<0.001	<0.001	<0.001	0.034	0.006	0.012	1.217	0.017	98.46
IV 9	4.31	87.4	2.3	3.45	0.41	0.33	0.15	0.98	0.01	0.12	0.02	0.005	0.02	<0.001	<0.001	<0.001	0.009	0.002	<0.002	0.092	0.009	99.55
IV 10	9.36	65.9	5.34	4.22	9.22	0.58	0.46	1.75	0.01	0.45	0.03	0.018	0.03	<0.001	<0.001	<0.001	0.028	0.002	0.041	2.208	0.011	97.36
IV 11	3.29	88.2	3.18	3.35	0.5	0.41	0.12	0.85	0.01	0.17	0.15	0.01	0.01	<0.001	<0.001	<0.001	0.007	0.002	0.002	0.047	0.012	100.22
V 1	10.95	61.8	14.28	5.28	0.95	1.99	0.84	3.15	0.02	0.8	0.07	0.021	0.04	<0.001	0.005	<0.001	0.018	0.008	0.02	0.319	0.023	100.2
V 2	7.75	69	11.13	4.18	1.7	1.48	0.9	2.84	0.02	0.76	0.17	0.014	0.04	<0.001	0.001	<0.001	0.02	0.006	0.03	0.121	0.018	100.01
V 3	7.01	72.5	10.27	3.98	0.7	1.39	0.87	2.87	0.02	0.64	0.08	0.017	0.04	<0.001	0.001	<0.001	0.015	0.005	0.036	0.196	0.016	100.39
V 4	9.59	63.3	13.36	4.94	1.04	1.96	0.89	3.08	0.03	0.87	0.08	0.021	0.05	<0.001	0.003	<0.001	0.014	0.012	0.025	0.405	0.021	99.19
V 5	11.75	57.1	16.52	5.88	1.38	2.04	0.84	3.11	0.03	0.91	0.11	0.023	0.04	<0.001	0.004	0.001	0.017	0.009	0.018	0.283	0.03	99.68
V 6	12.27	53.3	18.63	6.41	0.91	2.35	0.95	3.4	0.02	0.89	0.1	0.024	0.04	<0.001	0.005	0.001	0.016	0.012	0.015	0.628	0.036	99.24
V 7	12.78	54.5	17.56	6.78	0.72	2.03	0.96	3.06	0.02	0.82	0.09	0.024	0.04	<0.001	0.002	0.003	0.012	0.01	0.017	0.212	0.029	99.36

V 8	12.78	61.1	14.16	5.1	0.35	1.52	0.81	2.67	0.02	0.74	0.07	0.023	0.03	<0.001	0.003	<0.001	0.014	0.008	0.017	0.401	0.023	99.32
V 9	9.4	64.4	13.52	4.6	0.99	1.61	0.95	2.98	0.01	0.81	0.06	0.018	0.04	<0.001	0.002	<0.001	0.013	0.007	0.022	0.333	0.02	99.35
V 10	3.05	83.7	5.15	3.77	0.28	0.69	0.55	2.25	0.01	0.4	0.05	0.017	0.03	<0.001	0.001	<0.001	0.009	0.001	0.041	0.035	0.011	99.92
V 11	7.41	70.7	7.74	6.79	1.56	1.56	1.08	2.04	0.03	0.77	0.05	0.022	0.04	0.001	0.003	<0.001	0.022	0.007	0.032	0.167	0.023	99.83
V 12	6.92	72.1	9.38	4.66	0.92	1.64	1.31	1.92	0.02	0.94	0.07	0.017	0.03	<0.001	0.001	<0.001	0.022	0.007	0.027	0.159	0.02	99.97
VI 1	6.03	77.7	8.42	3.17	0.35	1.26	0.55	2.62	0.01	0.58	0.05	0.014	0.03	<0.001	<0.001	<0.001	<0.002	0.003	0.029	0.138	0.014	100.82
VI 2	7.24	73.1	9.93	3.59	0.41	1.4	0.57	2.73	0.02	0.64	0.05	0.014	0.04	<0.001	0.001	<0.001	0.01	0.005	0.032	0.212	0.017	99.68
VI 3	13.07	57.5	10.15	3.98	8.42	2	0.45	2.42	0.02	0.56	0.06	0.013	0.03	<0.001	<0.001	<0.001	0.033	0.005	0.019	0.986	0.018	98.7
VI 4	8.42	70.6	10.4	3.8	0.44	1.54	0.61	2.69	0.01	0.63	0.06	0.014	0.04	<0.001	0.002	<0.001	0.009	0.005	0.024	0.36	0.019	99.19
VI 5	7.59	71.1	10.65	3.82	0.86	1.58	0.62	2.77	0.02	0.68	0.06	0.016	0.03	<0.001	0.003	<0.001	0.013	0.005	0.037	0.708	0.018	99.77
VI 6	6.87	72.4	10.1	3.58	0.84	1.42	0.65	2.75	0.01	0.65	0.06	0.019	0.03	<0.001	0.003	<0.001	0.008	0.005	0.026	0.482	0.016	99.34
VI 7	10.16	62.4	14.9	5.01	0.61	1.84	0.62	3	0.02	0.77	0.08	0.022	0.03	<0.001	0.003	<0.001	0.015	0.007	0.018	0.323	0.031	99.49
VI 8	13.25	59.9	14.11	5.74	0.29	1.72	0.62	2.86	0.02	0.71	0.07	0.026	0.04	<0.001	0.006	<0.001	0.005	0.008	0.021	0.301	0.025	99.37
VI 9	13.33	59.2	14.74	5.75	0.34	1.81	0.61	2.94	0.02	0.78	0.06	0.025	0.04	<0.001	0.003	<0.001	0.007	0.009	0.02	0.168	0.03	99.6
VI 10	12.8	54.8	15.84	6.1	2.06	1.94	0.65	3.03	0.01	0.85	0.08	0.026	0.02	<0.001	0.004	<0.001	0.009	0.01	0.017	1.259	0.03	98.18
VI 11	10.95	60.2	15.4	5.43	0.59	1.92	0.69	3.16	0.02	0.84	0.05	0.02	0.03	<0.001	0.001	<0.001	0.012	0.008	0.019	0.415	0.027	99.31
VI 12	10.35	60.4	14.2	5.19	1.94	2.24	0.69	3.21	0.02	0.72	0.05	0.017	0.03	<0.001	0.003	<0.001	0.016	0.007	0.018	0.817	0.022	99.02
VII 1	16.76	46.2	13.04	4.44	11.2	2.21	0.38	2.64	0.04	0.7	0.1	0.017	0.03	<0.001	0.003	<0.001	0.043	0.007	0.012	1.172	0.02	97.75
VII 2	11.05	60.6	15.29	4.99	0.72	1.9	0.53	3.1	0.02	0.91	0.09	0.021	0.05	<0.001	0.005	<0.001	0.011	0.008	0.021	0.182	0.028	99.21
VII 3	16.22	52.7	15.49	7.33	0.64	1.8	0.44	3.01	0.02	0.87	0.11	0.024	0.04	<0.001	0.007	<0.001	0.012	0.01	0.02	0.621	0.031	98.69
VII 4	10.51	59.8	16.08	5.39	0.43	1.89	0.64	3.22	0.02	0.96	0.09	0.025	0.04	<0.001	0.005	<0.001	0.014	0.008	0.022	0.114	0.028	99.1
VII 5	13.79	55.6	16.95	6.17	0.47	1.98	0.69	3.16	0.02	0.88	0.09	0.023	0.04	<0.001	0.005	0.001	0.017	0.009	0.018	0.194	0.031	99.85
VII 6	4.67	77	8.19	3.56	0.59	0.94	0.83	2.53	0.02	0.65	0.06	0.015	0.03	<0.001	<0.001	<0.001	0.014	0.004	0.056	0.11	0.015	99.1
VII 7	4.82	77.1	8.29	3.66	0.47	0.96	0.84	2.56	0.02	0.63	0.04	0.018	0.03	<0.001	0.004	<0.001	0.01	0.003	0.035	0.181	0.014	99.4
VII 8	6.18	73.6	8.31	3.89	2.01	0.99	0.84	2.49	0.02	0.59	0.06	0.015	0.04	<0.001	<0.001	<0.001	0.02	0.004	0.038	0.439	0.016	99.02
VIII 1	11.9	55.7	14.28	6.24	3.5	2.14	1.19	3.02	0.02	0.74	0.17	0.02	0.04	<0.001	0.006	0.001	0.021	0.009	0.018	0.386	0.025	98.9
VIII 2	12.67	54.3	14.25	5.85	4.05	2.19	1.16	3.02	0.03	0.77	0.13	0.019	0.04	<0.001	0.006	<0.001	0.024	0.031	0.014	0.719	0.025	98.45
VIII 3	13.57	51	15.83	6.57	4.76	2.24	1.08	3.12	0.1	0.79	0.12	0.024	0.03	<0.001	0.013	0.001	0.022	0.012	0.012	0.545	0.028	99.21
VIII 4	13.44	51.5	15.51	6.51	3.67	2.1	2.11	2.94	0.06	0.77	0.14	0.022	0.04	<0.001	0.008	<0.001	0.026	0.007	0.013	0.998	0.026	98.83
VIII 5	14.44	50.9	14.84	6.18	3.96	2.04	2.98	2.81	0.06	0.75	0.16	0.018	0.03	<0.001	0.009	<0.001	0.027	0.001	0.012	0.377	0.026	99.17

XIII 1	14.17	52.3	14.69	5.7	5.39	2.02	0.92	3.05	0.02	0.79	0.07	0.02	0.03	<0.001	0.007	<0.001	0.034	0.027	0.013	0.735	0.026	99.21
XIII 2	16.46	45.8	10.5	4.32	14.51	1.5	0.89	1.98	0.04	0.6	0.08	0.016	0.03	<0.001	0.004	<0.001	0.071	0.007	0.013	2.128	0.019	96.75
XIII 3	14.8	51.4	13.21	5	8.69	1.89	0.98	2.57	0.04	0.71	0.1	0.016	0.03	<0.001	0.005	<0.001	0.048	0.009	0.014	0.16	0.022	99.4
XIII 4	11.52	56.9	16.23	5.96	1.56	2.22	1.07	3.2	0.03	0.85	0.09	0.018	0.03	<0.001	0.006	0.002	0.026	0.012	0.014	0.199	0.026	99.71
XIII 5	13.03	50.9	17.95	7.91	2.16	2.49	1.08	3.28	0.06	0.89	0.33	0.025	0.04	<0.001	0.007	0.004	0.028	0.014	0.012	0.044	0.036	100.07
XIII 6	12.4	55	17.1	5.99	1.59	2.18	1.18	3.13	0.02	0.82	0.07	0.019	0.04	<0.001	0.005	0.001	0.029	0.014	0.015	0.089	0.027	99.51
XIII 7	9.3	65.4	12.85	4.88	0.43	1.64	1.2	3.03	0.01	0.79	0.07	0.019	0.04	<0.001	0.002	0.001	0.019	0.008	0.026	0.195	0.026	99.67
XIII 8	8.82	68.1	10.19	5.71	0.31	1.54	1.16	3.2	0.01	0.7	0.06	0.026	0.04	<0.001	0.003	<0.001	0.021	0.007	0.037	0.327	0.021	99.9
XIII 9	6.8	72.7	8.84	4.97	0.3	1.45	1.09	2.98	0.01	0.71	0.05	0.026	0.03	<0.001	0.002	<0.001	0.015	0.004	0.056	0.344	0.022	99.95
XIII 10	13.97	54	17.19	6.56	0.28	2.26	1.1	3.35	0.02	0.84	0.07	0.025	0.04	<0.001	0.004	0.002	0.024	0.01	0.014	0.168	0.041	99.72
XIV 1	11.4	59.6	12.25	5.59	3.06	1.78	1.2	2.6	0.02	0.72	0.13	0.03	0.04	<0.001	0.003	0.003	0.022	0.008	0.02	0.705	0.019	98.42
XIV 2	11.79	57.7	12.6	5.48	4.04	1.88	1.12	2.63	0.02	0.74	0.1	0.031	0.04	<0.001	0.003	0.003	0.026	0.011	0.021	1.022	0.02	98.14
XIV 3	12.26	56.9	12.64	5.96	3.75	1.88	1.09	2.6	0.02	0.75	0.11	0.033	0.04	<0.001	0.004	0.002	0.03	0.009	0.019	1.421	0.018	98
XIV 4	13.49	51.3	16.37	6.76	3.98	2.21	1.04	3	0.06	0.8	0.11	0.027	0.03	<0.001	0.007	0.001	0.034	0.012	0.013	0.746	0.027	99.2
XV 1	11.55	59.1	10.06	5.24	6.31	1.97	0.93	2.47	0.02	0.6	0.12	0.017	0.03	<0.001	0.001	<0.001	0.025	0.006	0.019	0.563	0.017	98.37
XV 2	13.98	53.8	11.39	4.6	10.02	1.62	0.91	1.99	0.06	0.59	0.1	0.015	0.03	<0.001	0.004	<0.001	0.05	0.007	0.014	0.445	0.02	99.1
XVI 1	6.68	72.3	6.83	4.41	3.23	1.09	0.93	2.49	0.01	0.41	0.07	0.015	0.04	<0.001	<0.001	<0.001	0.021	0.003	0.034	0.36	0.012	98.51
XVI 2	6.65	72.7	6.79	4.28	3.38	1.04	0.89	2.45	0.01	0.42	0.07	0.016	0.04	<0.001	<0.001	<0.001	0.021	0.003	0.033	0.148	0.012	98.7
XVI 3	6.26	74.4	7.11	4.14	2.7	1.03	0.9	2.5	0.01	0.45	0.07	0.016	0.04	<0.001	<0.001	<0.001	0.015	0.003	0.038	0.22	0.01	99.61
XVI 4	7.26	70.8	7.28	4.36	3.86	1.11	0.97	2.44	0.02	0.47	0.07	0.017	0.03	<0.001	0.001	<0.001	0.019	0.004	0.038	0.553	0.015	98.65
XVI 5	6.86	71.3	7.27	4.23	3.69	1.08	0.93	2.46	0.02	0.48	0.08	0.017	0.04	<0.001	<0.001	<0.001	0.022	0.003	0.04	0.371	0.012	98.44
XVI 6	6.72	71.1	7.3	4.08	3.56	1.07	0.91	2.5	0.02	0.51	0.07	0.016	0.03	<0.001	0.001	<0.001	0.02	0.003	0.038	1.08	0.01	97.9
XVI 7	6.7	71.6	7.54	4.02	3.12	1.09	0.91	2.55	0.01	0.53	0.07	0.016	0.03	<0.001	0.001	<0.001	0.028	0.005	0.041	0.835	0.011	98.21
XVI 8	6.94	70.7	7.94	4.22	3.31	1.21	0.92	2.57	0.01	0.55	0.08	0.012	0.03	<0.001	0.001	<0.001	0.021	0.004	0.036	0.878	0.016	98.46
XVI 9	7.24	67.7	8.34	5.94	3	1.25	0.84	2.51	0.02	0.51	0.08	0.015	0.04	<0.001	0.002	<0.001	0.013	0.005	0.028	1.418	0.013	97.48
XVI 10	7.51	66.8	8.2	6.3	3.78	1.31	0.85	2.5	0.03	0.52	0.08	0.017	0.03	0.009	<0.001	<0.001	0.022	0.005	0.03	1.998	0.013	97.9
XVI 11	7.62	69	8.83	5.06	3.42	1.32	0.9	2.51	0.02	0.54	0.08	0.016	0.04	<0.001	<0.001	0.002	0.019	0.004	0.032	0.489	0.016	99.32
XVI 12	7.39	69.2	8.4	5.03	3.75	1.25	0.86	2.47	0.02	0.51	0.09	0.012	0.04	<0.001	0.001	<0.001	0.024	0.005	0.033	0.679	0.015	98.96
XVI 13	7.46	69.3	8.84	5.17	2.82	1.21	0.8	2.4	0.02	0.52	0.08	0.018	0.04	<0.001	<0.001	<0.001	0.018	0.005	0.027	0.623	0.017	98.66
XVI 14	7.66	69.3	8.8	5.12	2.6	1.17	0.78	2.39	0.02	0.51	0.08	0.015	0.04	<0.001	0.002	<0.001	0.009	0.005	0.025	1.02	0.016	98.46

XVII 1	8.79	64.4	13.32	5.39	1.34	1.82	1.17	2.88	0.02	0.77	0.06	0.015	0.04	<0.001	0.002	<0.001	0.016	0.009	0.018	0.202	0.022	100.02
XVII 2	11.35	57.6	15.07	7.15	1.78	2.07	0.64	2.85	0.03	0.77	0.06	0.016	0.03	<0.001	0.003	<0.001	0.012	0.009	0.015	0.294	0.028	99.39
XVII 3	6.48	73.6	8.79	4.84	0.6	1.09	0.83	2.62	0.01	0.57	0.08	0.014	0.04	<0.001	0.002	<0.001	0.011	0.018	0.04	0.376	0.015	99.56
XVII 4	7.18	71.8	9.7	4.38	0.59	1.26	0.79	2.67	0.01	0.56	0.06	0.015	0.04	<0.001	<0.001	<0.001	0.014	0.005	0.03	0.087	0.019	99.07
XVII 5	8.5	67.8	11.58	4.83	0.44	1.59	1.12	2.78	0.02	0.7	0.05	0.021	0.04	<0.001	0.007	<0.001	0.009	0.006	0.025	0.215	0.017	99.39
XVII 6	7.08	70.4	10.31	4.92	0.48	1.35	0.95	2.81	0.02	0.66	0.08	0.019	0.04	<0.001	<0.001	<0.001	0.011	0.012	0.033	0.208	0.017	99.13

Table 10. Leco (Total C, Total S and organic C) and ICP-ES results (in wt%).

	TOT/C	TOT/S	C/ORG	SiO2	Al2O3	Fe2O3	MgO	CaO	Na2O	K2O	TiO2	P2O5	MnO	Cr2O3	LOI
I 1	1.04	0.47	0.14	76.55	5.27	3.2	0.77	4.61	0.7	1.9	0.53	0.07	0.02	0.012	6.2
I 2	3.2	0.26	0.07	61.2	4.29	3.53	0.81	13.37	0.53	1.45	0.44	0.05	0.03	0.011	14.1
I 3	1.04	0.38	0.21	76.53	5.6	3.59	0.85	4.02	0.69	1.81	0.56	0.07	0.02	0.015	6
I 4	1.16	0.34	0.2	75.02	5.7	3.19	0.86	4.91	0.77	1.94	0.51	0.06	0.02	0.014	6.8
I 5	2.56	0.5	0.31	61.67	5.83	4.96	1.1	10.95	0.88	2.3	0.46	0.09	0.02	0.016	11.5
I 6	1.4	0.23	0.25	71.44	4.16	10.28	1.44	2.08	0.39	2.11	0.2	0.35	0.02	0.019	7.4
I 7	0.58	0.6	0.31	75.46	7.12	4.82	0.95	1.69	0.75	2.72	0.46	0.08	0.01	0.016	5.8
I 8	0.78	1.17	0.39	70.42	8.01	6.26	1.15	2.24	0.76	2.93	0.53	0.07	0.01	0.016	7.4
I 9	1.23	1.12	0.63	68.07	10.14	4.29	1.15	3.27	0.73	2.69	0.65	0.06	0.01	0.015	8.7
I 10	0.63	0.44	0.5	77.54	7.86	3.26	0.95	1.02	0.69	2.62	0.53	0.08	0.01	0.014	5.3
I 11	0.94	1.03	0.94	77.26	7.11	3.36	0.73	0.71	0.49	1.85	0.51	0.06	<0.01	0.015	7.8
I 12	0.73	0.72	0.59	74.14	9.97	3.45	1	1.37	0.63	2.56	0.69	0.05	0.01	0.014	6
I 13	2.85	0.98	1.58	59.26	11.47	4.6	1.4	6.28	0.52	2.55	0.65	0.09	0.02	0.015	13
II 1	1.43	0.6	0.44	69.73	8.11	3.9	1.1	4.82	0.77	2.54	0.55	0.08	0.02	0.015	8.2
II 2	0.52	0.74	0.36	77.4	7.88	3.26	0.83	1.27	0.79	2.71	0.56	0.08	0.01	0.014	5
II 3	2.02	1.08	0.89	61.13	11.35	4.25	1.5	5.68	0.8	2.66	0.7	0.1	0.02	0.017	11.6
II 4	1.62	1.83	1.54	54.26	17.68	6.76	2.1	0.66	0.78	3.39	0.84	0.09	0.02	0.021	13.2
II 5	1.49	1.7	1.39	56.49	17.12	6.52	2.02	0.65	0.74	3.26	0.81	0.09	0.02	0.02	12.1
II 6	1.58	1.1	1.57	73.26	9.15	3.86	0.91	0.27	0.52	2.09	0.56	0.07	<0.01	0.017	9.2
II 7	2.39	1.57	2.33	63.42	13.56	5.29	1.43	0.74	0.64	2.76	0.77	0.08	0.01	0.022	11.1
II 8	0.98	0.63	0.89	61.61	15.55	4.83	1.67	0.38	0.73	3.24	0.86	0.06	0.02	0.018	10.9
II 9	3.23	0.99	0.76	45.18	13.58	6.2	2.77	9.83	0.67	3.14	0.66	0.07	0.04	0.014	17.7
II 10	0.59	0.97	0.36	79.87	6.14	3.78	0.69	1.15	0.48	1.76	0.47	0.05	0.01	0.013	5.4
II 11	0.23	0.28	0.2	88.88	4.08	1.6	0.35	0.33	0.41	1.64	0.31	0.05	<0.01	0.009	2.2
III 1	1.25	0.78	0.67	68.43	10.47	3.61	1.24	3.44	0.74	2.84	0.66	0.09	0.01	0.015	8.3
III 2	0.93	0.61	0.53	69.23	10.34	3.47	1.35	2.62	0.76	2.82	0.67	0.1	0.01	0.016	8.4
III 3	0.85	1.14	0.83	58.69	16.31	5.45	2.16	0.47	0.82	3.31	0.82	0.07	0.02	0.018	11.7
III 4	0.93	1.26	0.85	58.69	16.78	5.65	2.03	0.89	0.79	3.36	0.93	0.09	0.02	0.019	10.5

III 5	1.64	1.36	1.62	55.96	16.94	6.15	1.89	0.54	0.82	3.18	0.88	0.12	0.02	0.02	13.3
III 6	2.04	0.79	1.08	52.86	16.09	8.25	2.33	2.93	0.78	2.99	0.84	0.2	0.05	0.019	12.5
III 7	1.28	0.89	1.27	58.78	16.05	5.99	1.86	0.47	0.74	3.03	0.85	0.09	0.02	0.02	11.9
III 8	1.45	0.85	1.4	54.72	17.7	5.96	2.07	0.45	0.84	3.24	0.87	0.11	0.02	0.022	13.8
III 9	1.27	0.75	0.96	56.08	17.21	5.52	2.01	1.78	0.87	3.24	0.89	0.08	0.02	0.018	12.1
III 10	0.47	0.52	0.35	71.37	11.12	3.98	1.29	0.73	0.88	2.78	0.71	0.06	0.01	0.015	6.9
III 11	0.62	0.27	0.24	75.53	8.16	4.12	0.99	1.36	0.8	2.49	0.6	0.05	0.02	0.015	5.7
IV 1	0.67	0.23	0.15	86.42	2.62	2.24	0.37	2.4	0.12	1.11	0.22	0.08	<0.01	0.01	4.3
IV 2	0.73	0.3	0.16	68.35	1.95	1.74	0.34	13.58	0.49	0.98	0.22	8.12	0.02	0.009	4
IV 3	0.68	0.4	0.45	75.97	9.19	2.91	1.28	1.2	0.42	2.44	0.66	0.04	0.01	0.013	5.7
IV 4	0.7	0.74	0.67	72.4	9.94	3.53	1.15	0.43	0.44	2.44	0.7	0.04	0.01	0.015	8.7
IV 5	1.31	1.51	1.1	66.77	11.41	5.25	1.33	1.58	0.4	2.54	0.7	0.04	0.01	0.018	9.8
IV 6	1.16	1.17	1.09	76.25	7.84	3.66	0.8	0.74	0.28	1.76	0.48	0.04	<0.01	0.015	8
IV 7	0.24	0.42	0.18	88.53	4.19	1.69	0.32	0.38	0.26	1.56	0.28	<0.01	<0.01	0.007	2.7
IV 8	2.84	0.83	0.74	54.48	11.11	4.3	1.88	10.28	0.38	2.6	0.59	0.04	0.03	0.012	14.1
IV 9	0.75	0.87	0.71	87.76	2.28	3.41	0.34	0.4	0.16	0.96	0.11	<0.01	<0.01	0.005	4.5
IV 10	2.18	1.37	0.43	67.95	5.59	4.35	0.62	9.7	0.47	1.88	0.46	<0.01	0.01	0.012	8.8
IV 11	0.39	0.37	0.28	88.11	3.14	3.2	0.41	0.5	0.12	0.85	0.18	0.13	<0.01	0.006	3.3
V 1	1.22	0.85	1.19	61.99	14.2	5.25	1.97	0.97	0.82	3.18	0.79	0.06	0.02	0.018	10.6
V 2	0.84	0.46	0.61	69.22	11.22	4.13	1.47	1.7	0.89	2.96	0.77	0.14	0.02	0.017	7.3
V 3	0.61	0.54	0.48	72.27	10.16	3.9	1.36	0.69	0.84	2.86	0.65	0.08	0.01	0.016	7
V 4	0.9	1.18	0.82	63.94	13.54	4.92	1.96	1.07	0.89	3.21	0.89	0.06	0.02	0.018	9.3
V 5	1.69	0.65	1.34	56.68	16.73	5.95	2.03	1.42	0.82	3.18	0.92	0.1	0.02	0.02	11.9
V 6	1.15	0.81	1.06	53.64	18.82	6.47	2.35	0.91	0.94	3.46	0.89	0.08	0.02	0.021	12.2
V 7	1.54	1.36	1.42	54.48	17.8	6.88	2.04	0.73	0.96	3.19	0.85	0.07	0.02	0.022	12.8
V 8	1.68	1.09	1.65	60.83	14.23	5.2	1.52	0.35	0.78	2.67	0.73	0.04	0.01	0.021	13.4
V 9	0.89	0.61	0.76	64.9	13.59	4.61	1.6	1	0.92	2.96	0.81	0.04	0.02	0.016	9.3
V 10	0.25	0.17	0.19	83.22	5.15	3.82	0.68	0.28	0.54	2.25	0.4	0.05	0.01	0.013	3.5
V 11	0.82	0.53	0.21	70.65	7.86	6.83	1.57	1.58	1.05	2.1	0.79	0.02	0.03	0.021	7.3
V 12	0.47	0.39	0.27	72.04	9.46	4.6	1.62	0.92	1.32	2.01	0.94	0.07	0.02	0.017	6.8

VI 1	0.57	0.41	0.54	76.8	8.37	3.11	1.23	0.34	0.53	2.64	0.58	0.03	0.01	0.014	6.2
VI 2	0.65	0.56	0.62	73.31	9.85	3.5	1.38	0.41	0.56	2.77	0.65	0.04	0.01	0.015	7.4
VI 3	2.78	0.77	0.98	57.9	10.34	3.96	2	8.64	0.44	2.52	0.58	0.05	0.02	0.015	13.4
VI 4	0.77	0.7	0.75	70.95	10.42	3.77	1.52	0.45	0.6	2.71	0.63	0.03	0.02	0.015	8.8
VI 5	0.79	0.77	0.75	70.52	10.7	3.88	1.57	0.85	0.62	2.77	0.66	0.03	0.02	0.017	8.2
VI 6	0.9	0.62	0.84	72.79	10.24	3.6	1.4	0.85	0.62	2.73	0.64	0.04	0.01	0.014	6.9
VI 7	1	0.82	0.98	62.28	14.98	4.99	1.83	0.63	0.61	3.05	0.77	0.06	0.02	0.019	10.6
VI 8	1.47	1.27	1.44	60.15	14.16	5.74	1.71	0.28	0.61	2.9	0.71	0.05	0.02	0.021	13.5
VI 9	1.83	1.27	1.81	59.2	14.52	5.65	1.76	0.35	0.59	2.97	0.78	0.03	0.02	0.022	13.9
VI 10	2.43	1.53	2.17	55.83	16.25	6.44	1.96	2.16	0.64	3.08	0.82	0.07	0.02	0.026	12.5
VI 11	0.97	0.94	0.96	59.88	15.48	5.36	1.9	0.6	0.69	3.23	0.84	0.04	0.02	0.019	11.8
VI 12	1.06	0.84	0.85	60.56	14.59	5.32	2.26	2.03	0.7	3.36	0.73	0.03	0.02	0.017	10.2
VII 1	3.02	0.66	0.91	47.27	12.98	4.65	2.23	11.57	0.35	2.83	0.66	0.1	0.04	0.014	17.1
VII 2	1.03	0.75	1.02	59.68	15.32	4.86	1.85	0.73	0.5	3.15	0.92	0.09	0.02	0.019	12.7
VII 3	2.24	2.03	2.21	52.99	15.95	7.44	1.81	0.65	0.43	3.06	0.86	0.12	0.02	0.022	16.5
VII 4	0.92	0.58	0.88	59.82	16.51	5.47	1.9	0.42	0.61	3.25	0.96	0.1	0.02	0.02	10.7
VII 5	1.44	1.14	1.4	55.62	17.28	6.14	1.97	0.47	0.67	3.19	0.88	0.09	0.02	0.022	13.5
VII 6	0.31	0.24	0.22	77.54	8.43	3.79	0.98	0.59	0.79	2.56	0.63	0.07	0.02	0.017	4.4
VII 7	0.26	0.3	0.2	77.68	8.53	3.73	0.98	0.47	0.81	2.6	0.63	0.05	0.02	0.014	4.3
VII 8	0.61	0.45	0.3	74.87	8.52	3.9	0.99	2.07	0.82	2.51	0.59	0.07	0.02	0.014	5.5
VIII 1	1.5	0.88	0.83	56.34	14.74	6.33	2.16	3.56	1.17	3.16	0.76	0.17	0.03	0.018	11.4
VIII 2	1.69	0.99	0.91	55.05	14.66	6.01	2.2	4.2	1.15	3.04	0.76	0.13	0.03	0.018	12.5
VIII 3	1.9	0.73	0.8	51.22	16.22	6.79	2.28	4.9	1.06	3.19	0.78	0.13	0.1	0.018	13.1
VIII 4	1.65	0.96	0.95	52.07	15.87	6.6	2.13	3.77	2.08	3	0.76	0.13	0.05	0.017	13.3
VIII 5	1.53	0.66	0.71	51.19	15.05	6.32	2.07	4.05	2.91	2.94	0.74	0.16	0.06	0.016	14.3
VIII 6	1.5	0.96	1.06	54.06	16.66	7.03	2.27	2.22	1.13	3.18	0.83	0.13	0.04	0.022	12.2
VIII 7	1.36	1.39	1	54.67	15.68	6.96	2.17	2.78	1.1	3.12	0.8	0.15	0.05	0.019	12.3
VIII 8	1.47	1.07	0.88	54.73	16.03	7	2.2	2.97	1.12	3.16	0.82	0.11	0.05	0.019	11.6
VIII 9	1.51	0.91	0.96	53.82	16.59	6.75	2.16	3.1	1.03	3.15	0.81	0.22	0.04	0.018	12.1
VIII 10	1.33	1.75	1.01	55.28	15.34	7.72	2.1	2.35	1.12	3.08	0.8	0.16	0.04	0.019	11.8

IX 1	1.43	1.4	1.4	59.4	15.06	5.81	1.65	0.68	0.79	2.92	0.83	0.11	0.02	0.02	12.5
IX 2	2.5	1.34	2.46	53.78	16.89	6.11	1.89	0.64	0.55	3.07	0.87	0.08	0.02	0.025	15.9
IX 3	1.67	0.6	1.24	53.96	18.39	5.59	2.03	2.61	0.41	3.25	0.9	0.1	0.02	0.022	12.5
IX 4	1.11	0.52	1.07	59.16	17.12	5.34	2.02	0.57	0.42	3.33	0.92	0.06	0.02	0.02	10.8
IX 5	1.26	2.2	1.23	49.15	19.18	6.86	1.62	0.66	0.29	3.01	0.9	0.07	0.01	0.021	18.1
IX 6	1.45	0.88	1.41	56.08	17.56	5.67	2.03	1.27	0.32	3.08	0.87	0.08	0.02	0.018	12.8
IX 7	1.37	0.42	0.67	55.78	16.78	5.02	1.95	4.1	0.33	3.14	0.88	0.07	0.02	0.019	11.7
IX 11	0.68	0.58	0.66	70.18	10.9	4.72	1.45	0.48	0.57	2.86	0.68	0.06	0.01	0.016	7.9
IX 12	0.64	0.44	0.6	68.79	12.13	4.82	1.59	0.45	0.51	2.93	0.74	0.07	0.01	0.017	7.8
X 1	0.77	0.85	0.73	64.66	13.02	5.02	1.92	1.46	0.44	3.11	0.72	0.08	0.02	0.017	9.4
X 2	0.78	0.49	0.58	69.26	11.09	4.1	1.37	1.84	0.48	2.97	0.63	0.07	0.01	0.018	8
X 3	0.67	0.56	0.62	64.74	14.63	4.89	1.86	0.8	0.47	3.34	0.8	0.08	0.02	0.018	8.2
X 4	0.52	0.61	0.49	73	9.91	3.86	1.23	0.71	0.6	2.95	0.61	0.08	0.02	0.016	6.9
X 5	0.76	0.5	0.65	63.3	14.95	5.03	2.09	1.01	0.48	3.32	0.83	0.08	0.02	0.018	8.7
XI 1	3.02	1.01	2.38	52.8	13.01	5.43	2.01	3.94	0.88	5.75	0.75	0.12	0.02	0.018	14.9
XI 2	2.74	0.86	1.65	49.53	14.09	5.58	2.03	4.8	1.03	6.22	0.76	0.12	0.03	0.017	15.4
XI 3	2.63	0.69	1.19	47.14	14.81	5.9	2.06	5.96	0.9	6.13	0.73	0.19	0.1	0.017	15.7
XII 1	3.42	1.26	2	56.96	12.04	4.66	1.85	6.43	0.91	2.43	0.73	0.12	0.02	0.015	13.6
XII 2	2.88	0.95	1.06	56.08	10.43	7.39	1.42	8.24	0.68	2.22	0.58	0.18	0.05	0.021	12.3
XII 3	2.99	1	1.45	60.69	9.14	6.46	1.24	7.61	0.69	1.88	0.51	0.13	0.05	0.017	11.3
XII 4	1.87	0.7	0.82	59.44	13.49	4.77	1.89	4.46	0.89	2.93	0.74	0.12	0.02	0.017	11.1
XII 5	2.78	1.31	0.7	51.17	13.11	5.93	1.97	8.55	0.9	2.72	0.71	0.13	0.04	0.016	14.5
XII 6	2.31	0.56	0.75	50.72	15.89	6.76	2.28	5.53	1.01	3.14	0.8	0.18	0.1	0.018	13.3
XII 7	2.59	0.7	1.06	47.15	17.46	6.57	2.21	6.21	0.95	3.06	0.77	0.11	0.04	0.018	15.2
XII 8	1.7	0.78	1	52.38	17.7	6.62	2.27	2.77	1.05	3.24	0.82	0.11	0.03	0.019	12.8
XIII 1	2.03	1.16	0.89	52.32	14.82	5.8	2	5.48	0.9	3.09	0.77	0.08	0.02	0.018	14.5
XIII 2	3.86	1.12	0.41	46.47	10.77	4.43	1.51	14.77	0.84	2.42	0.59	0.09	0.03	0.014	17.9
XIII 3	2.73	0.72	0.71	51.56	13.01	5.08	1.9	8.75	0.96	2.82	0.71	0.11	0.04	0.015	14.8
XIII 4	1.42	0.72	1.11	56.89	16.49	6.09	2.26	1.58	1.02	3.27	0.86	0.1	0.03	0.02	11.2
XIII 5	1.7	0.37	0.92	50.56	17.99	7.84	2.45	2.18	1.06	3.4	0.88	0.33	0.06	0.021	13

XIII 6	1.33	0.88	1.11	54.94	17.46	6.03	2.19	1.63	1.18	3.27	0.84	0.08	0.02	0.019	12.2
XIII 7	0.82	0.8	0.83	65.51	13.06	4.96	1.66	0.42	1.19	3.16	0.81	0.08	0.02	0.019	8.9
XIII 8	0.68	0.87	0.67	67.98	10.39	5.76	1.56	0.32	1.13	3.26	0.68	0.07	0.01	0.023	8.6
XIII 9	0.48	0.51	0.47	72.55	8.99	5.09	1.48	0.29	1.05	2.99	0.67	0.07	0.01	0.022	6.6
XIII 10	1.34	1.38	1.33	53.93	17.54	6.63	2.26	0.29	1.08	3.47	0.84	0.08	0.02	0.024	13.6
XIV 1	1.86	1.8	1.34	60.4	12.52	5.54	1.78	3.13	1.18	2.71	0.74	0.15	0.02	0.032	11.6
XIV 2	2.01	1.52	1.25	58.76	12.9	5.46	1.88	4.13	1.1	2.73	0.75	0.11	0.02	0.03	11.9
XIV 3	2.07	2.14	1.42	57.79	13.03	6.06	1.91	3.9	1.1	2.68	0.76	0.12	0.02	0.032	12.4
XIV 4	1.85	0.6	0.84	51.29	16.59	6.8	2.2	4.05	1.01	3.06	0.8	0.11	0.06	0.026	13.8
XV 1	2.38	0.98	0.8	59.62	10.16	5.21	1.97	6.38	0.92	2.59	0.61	0.13	0.02	0.015	12.2
XV 2	2.87	0.54	0.43	53.62	11.36	4.5	1.59	10.06	0.83	2.29	0.59	0.11	0.05	0.013	14.8
XVI 1	1.36	0.6	0.65	73.17	6.96	4.38	1.08	3.23	0.91	2.55	0.43	0.06	0.01	0.016	7
XVI 2	1.34	0.59	0.83	73.84	6.94	4.2	1.04	3.38	0.87	2.53	0.43	0.06	0.01	0.015	6.5
XVI 3	1.21	0.58	0.61	74.51	7.14	4.04	1.02	2.7	0.88	2.56	0.45	0.07	0.01	0.016	6.4
XVI 4	1.53	0.7	0.66	71.54	7.32	4.36	1.11	3.87	0.93	2.49	0.48	0.08	0.02	0.017	7.6
XVI 5	1.43	0.75	0.72	72.25	7.4	4.21	1.09	3.78	0.91	2.5	0.48	0.08	0.02	0.017	7.1
XVI 6	1.36	0.75	0.63	72.24	7.36	4.15	1.07	3.64	0.89	2.53	0.49	0.07	0.01	0.017	7.4
XVI 7	1.32	0.72	0.58	72.63	7.73	4.22	1.09	3.19	0.89	2.61	0.52	0.07	0.01	0.018	6.9
XVI 8	1.44	0.88	0.66	71.41	8.12	4.4	1.2	3.38	0.91	2.62	0.52	0.08	0.02	0.017	7.1
XVI 9	1.46	2.42	0.72	69.03	8.44	5.95	1.24	3.05	0.82	2.54	0.51	0.05	0.02	0.016	8.2
XVI 10	1.65	2.66	0.78	67.11	8.31	6.41	1.33	3.84	0.85	2.53	0.51	0.07	0.02	0.016	8.8
XVI 11	1.59	1.33	0.79	68.9	8.87	5.05	1.29	3.37	0.89	2.63	0.54	0.07	0.02	0.018	8.2
XVI 12	1.67	1.56	0.76	69.25	8.57	5.03	1.25	3.84	0.85	2.59	0.53	0.07	0.02	0.017	7.8
XVI 13	1.68	1.84	0.98	70.1	8.75	5.13	1.17	2.82	0.78	2.46	0.52	0.07	0.02	0.017	8
XVI 14	1.56	2.01	0.92	69.73	8.95	5.28	1.19	2.68	0.77	2.43	0.52	0.09	0.02	0.014	8.2
XVII 1	0.78	0.69	0.56	64.16	13.68	5.42	1.85	1.37	1.16	2.97	0.78	0.07	0.02	0.015	8.4
XVII 2	0.75	0.6	0.51	58.36	15.4	7.21	2.1	1.8	0.63	2.87	0.78	0.07	0.03	0.016	10.6
XVII 3	0.41	1.01	0.39	73.97	8.93	4.99	1.12	0.61	0.81	2.69	0.57	0.09	0.01	0.015	6.1
XVII 4	0.37	0.46	0.36	72.98	10.05	4.49	1.31	0.61	0.8	2.84	0.59	0.07	0.01	0.016	6.1
XVII 5	0.37	0.53	0.35	68.85	11.75	4.88	1.6	0.44	1.1	2.86	0.71	0.06	0.01	0.015	7.6

XVII 6

0.38	0.56	0.36	71.56	10.46	4.98	1.36	0.48	0.93	2.86	0.64	0.09	0.01	0.015	6.5
------	------	------	-------	-------	------	------	------	------	------	------	------	------	-------	-----

Table 11. ICP-MS results (in ppm)

	Ba	Be	Co	Cs	Ga	Hf	Nb	Rb	Sn	Sr	Ta	Th	U	V	W	Zr	Y	La	Ce	Pr	Nd	Sm
I 1	310	<1	5.1	2.2	6	20.9	11.7	54.5	<1	318.5	0.6	7.2	2.5	57	0.7	759.9	17.1	21.1	47.3	5.09	20.5	3.81
I 2	245	<1	5.8	2.1	4.8	17.1	10.2	45.8	<1	350.8	0.8	5.8	3.2	47	10.7	662.7	14.6	19.9	44.1	4.75	19	3.44
I 3	283	<1	5.8	2.6	6.2	19.6	11.5	57.1	<1	275.3	1	7.1	2.8	65	<0.5	741.4	15.6	22.4	52.6	5.36	21.2	3.36
I 4	307	<1	5.7	2.5	6.2	14.5	10.1	58.2	<1	336.7	0.7	6.8	2.2	55	<0.5	597.3	15.7	22.1	51.8	5.53	22	3.84
I 5	290	3	8.1	3.3	6.7	18.5	9.3	67.9	<1	718.5	0.6	8.3	2.7	64	<0.5	711.2	18.1	28	67.2	7.12	26	4.92
I 6	150	3	9.6	1.9	4	5.6	4.7	62.1	<1	142.6	0.2	6.2	1.7	161	0.5	213.1	11.3	25	82.4	7.19	28.3	5.04
I 7	346	3	7.2	3.4	8.4	13.4	9.5	83	<1	160.6	0.7	7	2.5	80	1.1	522.2	15.2	24.9	65.8	6.6	25.3	4.79
I 8	345	<1	7.9	4.1	10	14	10.6	93.2	<1	183.9	0.7	6.9	2.6	86	0.8	561.8	19.6	30.7	86.1	8.04	34.6	5.7
I 9	316	6	8.8	6.4	12	10.3	13.3	101.7	1	234.7	1	8.5	3.8	94	1.2	378.2	18.9	27	57.8	6.5	23.6	4.35
I 10	336	<1	6.9	5.5	8.7	10.6	11.6	89.3	<1	131.6	0.7	6.8	3.3	73	1	419.3	16.9	25	54.3	5.76	23.7	4.36
I 11	253	7	4.4	7.4	7.7	7.2	10.7	80	1	91.7	0.7	7	4.5	78	<0.5	350.6	19.7	22.2	44.4	5.5	20.6	3.83
I 12	310	<1	7.8	12.1	10.9	9	12.8	106.7	1	112.8	0.8	8.6	2.4	95	1.1	308.6	19.9	29.3	54.2	6.46	24.4	4.51
I 13	233	4	12.6	17.3	13.5	5.2	13	130	3	250.9	0.7	9.3	3.9	140	1.7	234.1	20.7	27.9	52.2	6.35	24.9	4.36
II 1	455	7	7.6	3.8	9.1	12.6	11.3	78.4	<1	270.6	0.7	7.4	2.3	74	<0.5	471.3	18.7	24.9	57.5	6.33	24.9	4.16
II 2	405	<1	5.7	3.4	8.6	12.4	11.3	76.7	<1	132.6	0.7	6.7	2.5	69	<0.5	430.5	15.3	23.3	52.8	5.49	19.7	3.91
II 3	322	3	9.6	7.4	14.4	8.1	14.7	114.4	<1	353.1	0.9	10.1	3	110	0.8	306.9	23.3	30.7	66.6	7.28	27.2	5.17
II 4	302	9	15.6	13.7	22.1	5.2	18.1	169.3	2	153.3	1.3	12.8	3.8	176	1.6	177.5	25.1	40.9	84.6	9.73	35.1	6.48
II 5	317	7	14.3	14	21.1	4.8	18	170.8	2	147.3	1.2	12	3.1	169	1.7	189.7	26	39.1	78.2	9.06	36.6	6.08
II 6	267	3	5.8	6.9	10.3	8.3	10.7	90.6	<1	91.3	0.9	7.5	6.3	90	1.3	291.1	18.9	25.1	50.4	6.03	24.2	4.38
II 7	282	3	9.6	11.9	17	6.5	15.3	142.7	2	128.4	0.9	11.1	6.1	160	1	233	26.2	34.9	69.5	8.57	32.8	5.9
II 8	327	3	12	15.6	18.3	6.4	16.5	158.8	1	136	1.4	11.4	3.2	150	1.1	226.7	23.9	37.4	74.8	8.5	28.4	6.12
II 9	210	3	12.1	14.6	16.6	4.6	13.5	154	2	353.3	1.1	9.6	3.3	104	0.8	145.4	19.5	30	57	6.66	25.9	4.62
II 10	425	<1	5.2	6	6.6	14.4	9	65.6	<1	111.5	0.7	6.2	3.1	58	0.6	501.9	13.2	19.4	40.7	4.55	16.7	3.06
II 11	327	<1	2.9	3.3	4.1	8.5	6.1	50.8	2	77	0.5	4.2	1.7	35	<0.5	368	8.8	13	26.7	2.89	10.8	2.01
III 1	360	<1	8.3	6.2	12.6	8.9	13.5	94.9	<1	237.5	0.9	8	2.7	82	<0.5	314.2	18.3	26.1	59.1	6.44	24.5	4.47
III 2	344	3	9.5	5.8	10.4	8.9	12.7	99.1	<1	200.9	1	8.9	3.1	84	<0.5	352.3	22.2	29.6	61.8	6.85	27.5	4.97
III 3	450	<1	16.3	11.2	19.3	7	18	142.8	2	147.3	1.2	12.6	3.7	137	0.8	214.4	22.9	38.3	83.7	8.85	34	6.48

XVII 5	297	1	9.9	5.9	12.7	7	12	94.7	2	98.1	0.8	8.7	2.4	86	0.9	252.2	15.3	28.4	59.3	5.69	20.5	3.94
XVII 6	320	3	9.7	4.9	10.3	8.8	11.1	87.7	1	107.8	0.7	8.6	2.7	81	0.8	323.3	17	27.2	57.9	5.74	21.6	4.42

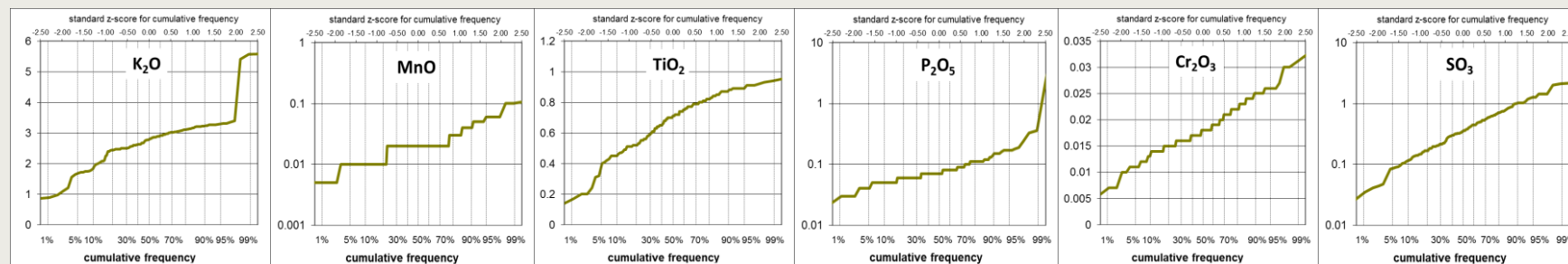
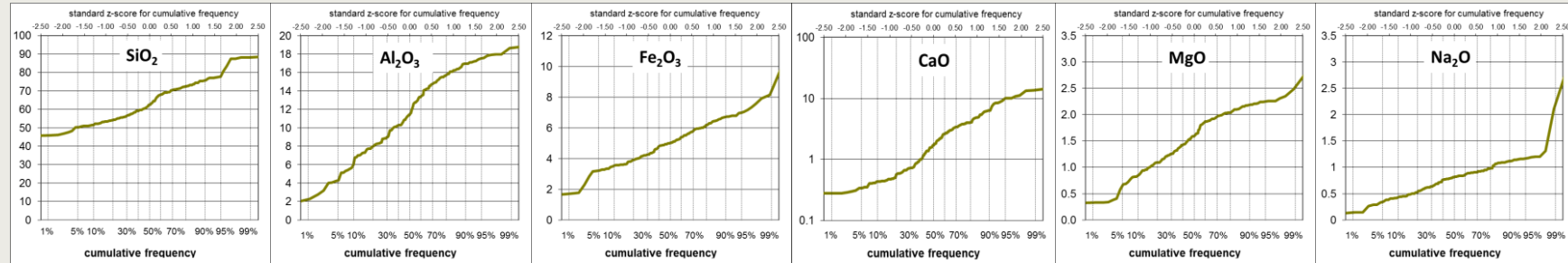
Table 12. ICP-MS results (in ppm) (continued). * values in ppb.

	Eu	Gd	Tb	Dy	Ho	Er	Tm	Yb	Lu	Mo	Cu	Pb	Zn	Ag	Ni	As	Au*	Cd	Sb	Bi	Hg	Tl	Se	Ni	Sc
I 1	0.66	3.28	0.45	3	0.67	1.96	0.35	2.19	0.32	0.7	3	4	31	<0.1	10.4	11.7	0.5	<0.1	0.2	<0.1	<0.01	<0.1	<0.5	<20	5
I 2	0.57	2.83	0.43	2.51	0.55	1.94	0.28	1.8	0.3	0.3	4.6	3.6	26	<0.1	9.6	6.6	2.1	<0.1	<0.1	<0.1	<0.01	<0.1	<0.5	<20	4
I 3	0.68	3.02	0.45	2.8	0.57	1.82	0.28	2.05	0.36	0.3	4.3	4.7	34	<0.1	11.9	7.6	2.7	<0.1	<0.1	<0.1	<0.01	<0.1	<0.5	<20	5
I 4	0.65	3.18	0.47	2.77	0.61	1.6	0.28	1.76	0.28	0.5	4.1	6.9	31	<0.1	11.6	7.3	1.1	<0.1	0.1	<0.1	<0.01	<0.1	0.6	<20	5
I 5	0.83	3.96	0.59	3.37	0.61	2.17	0.31	2.01	0.33	0.4	4.1	5.8	28	<0.1	14.9	11.2	2.7	<0.1	0.1	<0.1	<0.01	<0.1	0.5	25	6
I 6	1	3.71	0.51	2.5	0.46	1.21	0.17	1.23	0.16	0.3	2	6.5	42	<0.1	11.2	16.9	1.1	<0.1	0.2	<0.1	<0.01	<0.1	<0.5	<20	7
I 7	0.9	3.71	0.55	2.97	0.65	1.74	0.24	1.97	0.26	0.4	4.7	6.1	26	<0.1	15.6	12.4	0.8	<0.1	0.1	<0.1	<0.01	<0.1	<0.5	23	7
I 8	1.06	4.33	0.67	3.88	0.71	2	0.33	2.47	0.32	1	6	7.1	32	<0.1	18.3	28.7	0.8	<0.1	0.1	<0.1	0.01	<0.1	<0.5	22	9
I 9	0.94	4	0.63	3.55	0.73	2.24	0.32	2.37	0.33	3.2	9.6	9.4	39	<0.1	22.2	7.7	0.7	0.1	0.1	<0.1	0.02	0.1	0.9	36	10
I 10	0.8	3.72	0.55	3.31	0.76	2.05	0.31	2.26	0.34	2.3	8.6	6.4	29	<0.1	18.4	4.3	2.1	<0.1	0.1	0.3	<0.01	0.2	<0.5	29	7
I 11	0.76	3.48	0.56	3.13	0.69	2.12	0.31	2.43	0.33	6.8	10.7	5.9	33	<0.1	20.1	11.6	1.3	0.5	0.2	0.2	0.02	0.2	1.5	25	7
I 12	0.83	4.05	0.6	3.46	0.82	2.36	0.33	2.37	0.3	0.9	7.5	9.3	38	<0.1	16.9	4.3	2	0.1	<0.1	0.1	0.02	<0.1	0.7	27	9
I 13	1	4.24	0.63	3.4	0.65	2.09	0.27	2.39	0.32	3.8	11.9	13.3	40	<0.1	34.6	15	1.3	0.2	0.1	0.2	0.06	0.3	1.1	49	11
II 1	0.81	3.57	0.58	3.47	0.67	1.91	0.31	1.84	0.33	0.6	6.3	6.9	32	<0.1	16	7.4	<0.5	<0.1	<0.1	<0.1	0.02	<0.1	<0.5	22	8
II 2	0.78	3.25	0.51	2.97	0.59	1.68	0.28	2	0.27	0.5	5.7	6.3	27	<0.1	13.5	9.7	<0.5	<0.1	0.1	<0.1	0.02	<0.1	<0.5	<20	7
II 3	1.06	4.8	0.72	4.19	0.86	2.65	0.4	2.75	0.42	1.3	11.7	12.2	45	<0.1	25.1	4.9	1.7	<0.1	0.1	0.1	0.02	<0.1	0.6	37	11
II 4	1.47	5.93	0.92	5.84	0.97	3.06	0.42	3.07	0.43	0.7	24.6	19.5	70	<0.1	46.9	12.6	0.9	<0.1	0.1	0.3	0.04	0.1	1.3	65	17
II 5	1.31	5.35	0.88	4.61	0.98	2.81	0.44	2.61	0.4	0.4	24.6	17	75	<0.1	44	9	1.1	<0.1	0.1	0.2	0.03	0.1	1.7	55	16
II 6	0.87	3.89	0.6	3.33	0.72	2.26	0.32	2.1	0.33	8.4	18.4	8	42	<0.1	27.5	14.4	0.7	0.5	0.3	0.1	0.04	0.2	2.8	34	9
II 7	1.18	4.94	0.85	4.93	1.01	2.9	0.43	2.98	0.44	2.7	22.2	12.1	66	<0.1	34.9	13.7	0.9	0.6	0.3	0.2	0.04	0.2	3.7	47	14
II 8	1.21	5.33	0.8	5.1	0.94	2.73	0.44	2.89	0.44	0.2	14.6	14.2	57	<0.1	25.4	4.4	<0.5	0.1	0.1	0.2	0.02	<0.1	0.7	43	15
II 9	0.9	4.01	0.63	3.66	0.74	2.26	0.33	2.08	0.33	1.5	11.4	12.7	34	<0.1	22.8	4.8	0.7	0.1	<0.1	0.2	0.03	<0.1	0.6	37	12
II 10	0.59	2.46	0.39	2.42	0.51	1.45	0.25	1.85	0.28	1	26.7	215.3	90	<0.1	12.2	13.3	<0.5	<0.1	0.2	<0.1	0.02	<0.1	<0.5	<20	6
II 11	0.34	1.69	0.26	1.81	0.31	1.08	0.14	1.46	0.17	0.7	7	29	22	<0.1	7.7	4	<0.5	<0.1	0.2	<0.1	<0.01	<0.1	<0.5	<20	3
III 1	0.96	4.13	0.62	3.89	0.67	2.05	0.33	2.08	0.32	0.9	12.5	9.9	42	<0.1	23	5.8	0.6	0.1	<0.1	0.02	<0.1	0.5	29	9	
III 2	1.04	4.25	0.66	4.3	0.76	2.44	0.41	2.5	0.41	0.3	13.1	10.3	49	<0.1	25.3	4.1	0.5	0.1	<0.1	<0.1	0.02	<0.1	<0.5	32	9
III 3	1.22	5.42	0.81	4.62	0.99	2.73	0.41	2.63	0.41	0.5	23.5	19.4	68	<0.1	43.5	7.4	2.3	0.1	0.1	0.2	0.04	0.2	1.1	55	15

V 12	1.05	4.75	0.8	4.9	0.92	3.04	0.44	3.21	0.4	0.3	13.2	10.6	55	<0.1	27.1	3.9	<0.5	0.1	<0.1	<0.1	<0.01	<0.1	<0.5	36	11
VI 1	0.87	3.86	0.59	3.57	0.71	2	0.33	2.17	0.32	2	11.2	7.7	30	<0.1	18.9	3.7	<0.5	<0.1	<0.1	<0.1	0.01	<0.1	<0.5	30	7
VI 2	0.95	4.02	0.64	4.15	0.75	2.41	0.35	2.47	0.38	1.7	11.6	9.1	36	<0.1	21.2	3.7	<0.5	<0.1	<0.1	<0.1	0.01	<0.1	<0.5	34	9
VI 3	0.93	3.95	0.62	3.42	0.69	1.96	0.29	2.1	0.32	1	12.4	11.1	34	<0.1	24.8	4	0.7	<0.1	<0.1	<0.1	0.02	<0.1	0.6	33	10
VI 4	0.88	3.86	0.61	3.59	0.76	2.15	0.31	1.96	0.31	1.4	14.3	10.3	39	<0.1	28.1	3.8	0.8	<0.1	0.1	0.1	<0.01	<0.1	0.6	38	10
VI 5	1.08	4.05	0.67	4.11	0.84	2.19	0.37	2.49	0.35	1.6	13.7	10.4	41	<0.1	26.9	3.7	<0.5	<0.1	0.1	0.1	0.02	<0.1	<0.5	38	10
VI 6	0.97	4.26	0.63	4.12	0.75	2.36	0.35	2.24	0.37	2.7	14.7	11	42	<0.1	27.9	4.5	<0.5	0.2	0.1	0.1	0.02	<0.1	<0.5	45	9
VI 7	1.21	5.52	0.78	4.59	0.92	2.74	0.39	2.69	0.4	0.2	23.9	17.4	62	<0.1	33.3	11.9	0.8	0.1	0.1	0.2	0.04	0.1	0.8	52	14
VI 8	1.28	5.07	0.77	4.12	0.9	2.46	0.39	2.46	0.37	5	28.1	12.7	65	<0.1	37.8	20	<0.5	0.5	0.2	0.2	0.03	0.1	1.9	57	14
VI 9	1.3	5.59	0.87	5.02	1.03	2.88	0.46	2.89	0.4	5.2	22.8	15.8	62	<0.1	33.8	13.1	<0.5	0.3	0.1	0.2	0.02	0.1	1.9	46	15
VI 10	1.48	5.76	0.97	5.39	1.08	3.25	0.45	2.82	0.44	2.5	26.2	14.9	63	<0.1	37.8	14.5	1.3	0.5	0.2	0.2	0.03	0.1	2.2	59	17
VI 11	1.29	5.28	0.83	4.71	1.01	2.68	0.43	2.83	0.44	1.5	16.6	15.9	61	<0.1	26.2	6.1	<0.5	0.2	0.1	0.2	0.02	0.1	0.8	47	15
VI 12	1.01	4.51	0.67	3.82	0.78	2.27	0.36	2.23	0.31	1.7	13.7	13.8	48	<0.1	24.8	7.2	<0.5	0.2	<0.1	0.2	0.01	0.1	<0.5	47	14
VII 1	1.12	4.58	0.73	3.67	0.84	2.16	0.35	2.19	0.34	0.3	16.3	15.3	54	<0.1	31.1	7.2	<0.5	0.2	<0.1	0.2	0.03	0.1	<0.5	48	13
VII 2	1.36	5.28	0.84	4.74	0.98	2.92	0.45	2.74	0.43	0.3	20.7	18.9	72	<0.1	35.7	12.7	<0.5	0.2	<0.1	0.2	0.03	0.1	0.8	47	14
VII 3	1.47	6.05	0.92	4.87	1.11	3.23	0.48	3.18	0.47	1.2	32.7	20.6	80	<0.1	50.6	12.5	<0.5	0.4	0.2	0.3	0.06	0.1	2.9	68	15
VII 4	1.47	5.9	0.92	5	1.18	2.93	0.48	3.45	0.46	0.3	26	20	70	<0.1	35.6	10.2	<0.5	0.2	<0.1	0.2	0.06	0.2	0.7	52	16
VII 5	1.48	5.3	0.89	4.6	0.91	2.9	0.45	2.76	0.47	0.7	28.8	19.8	74	<0.1	41.2	11.4	<0.5	0.2	<0.1	0.2	0.06	0.1	2	60	16
VII 6	0.89	3.82	0.57	3.19	0.66	2.11	0.33	2.35	0.31	0.1	7.7	7.5	38	<0.1	15.2	7.1	1	<0.1	<0.1	<0.1	<0.01	<0.1	<0.5	23	8
VII 7	0.79	3.38	0.54	3.29	0.69	2.13	0.34	1.99	0.33	0.3	8.4	8.1	34	<0.1	15.8	7	<0.5	<0.1	<0.1	<0.1	0.01	<0.1	<0.5	<20	7
VII 8	0.85	3.75	0.57	3.08	0.62	1.86	0.3	1.96	0.3	0.3	9	8.7	37	<0.1	18.9	12.7	<0.5	<0.1	0.1	<0.1	<0.01	0.1	<0.5	29	8
VIII 1	1.25	5.32	0.75	4.27	0.83	2.35	0.42	2.64	0.31	1.4	20.2	19.4	85	<0.1	51.3	6.6	1.9	0.2	<0.1	0.3	0.06	0.2	0.7	63	14
VIII 2	1.28	4.99	0.75	4.84	0.85	2.45	0.37	2.57	0.37	1	22.3	23.8	360	<0.1	54.5	5.8	6.4	0.2	<0.1	0.2	0.04	0.1	0.9	63	14
VIII 3	1.39	5.34	0.85	4.16	0.87	2.5	0.41	2.6	0.36	0.6	23.6	22.7	106	<0.1	79.3	7.4	1.3	0.3	<0.1	0.3	0.08	0.2	1.4	93	16
VIII 4	1.28	5.06	0.77	4.35	0.88	2.36	0.37	2.37	0.35	1	23	27.1	107	<0.1	63.9	9.1	0.7	0.2	<0.1	0.2	0.09	0.2	0.6	73	16
VIII 5	1.32	5.14	0.76	3.72	0.79	2.34	0.32	2.21	0.32	0.5	22.3	19.5	85	<0.1	55.8	7.8	1.1	0.1	<0.1	0.2	0.06	0.2	0.9	70	15
VIII 6	1.34	5.34	0.82	4.63	0.99	2.55	0.4	2.35	0.37	1.1	23.6	22.5	277	<0.1	54.1	10.8	<0.5	0.2	<0.1	0.2	0.11	0.2	0.5	66	17
VIII 7	1.23	5.25	0.81	4.64	0.97	2.76	0.38	2.61	0.4	1.4	22	19.7	110	<0.1	52.8	12.4	<0.5	0.2	<0.1	0.2	0.05	0.2	0.8	65	16
VIII 8	1.31	5.22	0.8	4.41	0.89	2.48	0.44	2.53	0.4	1.3	23.3	20.6	86	<0.1	63	11.3	<0.5	0.3	<0.1	0.2	0.04	0.1	1.1	73	16
VIII 9	1.36	5.39	0.87	4.13	1	2.78	0.39	2.71	0.36	1	23.3	31.7	124	<0.1	59.9	11.5	<0.5	0.2	<0.1	0.2	0.07	0.2	0.7	70	17

VIII 10	1.17	5.18	0.79	4.02	0.85	2.68	0.4	2.8	0.38	1.4	22.4	20.3	85	<0.1	60.4	14.8	<0.5	0.2	<0.1	0.2	0.05	0.2	1.1	72	16		
IX 1	1.3	5.29	0.82	4.8	0.96	3.13	0.43	2.74	0.39	1.3	28.2	18.6	63	<0.1	38.8	11.8	<0.5	0.3	<0.1	0.2	0.03	0.2	1.8	51	14		
IX 2	1.29	5.52	0.83	4.45	0.99	2.87	0.42	2.47	0.42	4.1	34.1	18.2	75	<0.1	45.2	12.6	<0.5	0.4	0.2	0.2	0.03	0.2	3.2	59	16		
IX 3	1.37	5.88	0.89	4.78	1.08	2.93	0.44	3.03	0.46	0.3	23.2	21.9	69	<0.1	34	11.4	<0.5	0.3	<0.1	0.2	0.05	0.2	1	63	18		
IX 4	1.34	5.33	0.85	4.83	1	2.81	0.43	2.69	0.43	0.2	22.4	22.3	70	<0.1	31.9	9.5	0.8	0.3	<0.1	0.2	0.05	0.2	<0.5	51	16		
IX 5	1.35	5.17	0.79	4.5	0.81	2.64	0.4	2.41	0.38	1.6	25.4	26	59	<0.1	37.4	27.1	0.9	0.5	0.1	0.3	0.04	0.3	1.5	56	17		
IX 6	1.39	5.77	0.86	5.03	0.96	2.8	0.38	2.68	0.39	0.6	23.3	21.5	84	<0.1	41.5	7.3	<0.5	0.3	<0.1	0.2	0.05	0.1	1.3	59	16		
IX 7	1.31	5.74	0.82	4.39	0.95	2.55	0.39	2.64	0.39	0.1	19.2	19	67	<0.1	31.6	7.2	<0.5	0.2	<0.1	0.2	0.04	0.1	<0.5	45	15		
IX 11	0.96	4.1	0.66	3.74	0.76	2.31	0.38	2.22	0.38	0.2	10.7	11.4	50	<0.1	23	7.5	<0.5	0.1	<0.1	<0.1	0.02	<0.1	<0.5	31	10		
IX 12	0.96	4.41	0.68	4.26	0.76	2.14	0.34	2.52	0.35	0.1	12.3	13.1	53	<0.1	24.7	6.9	<0.5	<0.1	<0.1	<0.1	0.02	0.1	<0.5	35	11		
X 1	1.18	4.53	0.73	4.32	0.78	2.44	0.39	2.38	0.32	0.5	19.6	15.1	60	<0.1	39.4	7.6	<0.5	0.1	<0.1	0.2	0.04	0.2	<0.5	46	11		
X 2	1.02	4.33	0.67	3.91	0.72	2.38	0.34	2.34	0.33	0.3	14.9	15.3	47	<0.1	25.4	8	<0.5	<0.1	<0.1	<0.1	0.02	0.1	<0.5	31	10		
X 3	1.24	5.22	0.79	4.34	0.87	2.69	0.39	2.32	0.38	0.2	17.9	19.1	54	<0.1	29.6	7.8	1.1	<0.1	<0.1	0.2	0.03	0.1	<0.5	44	13		
X 4	1.05	4.67	0.7	3.83	0.78	2.13	0.37	2.34	0.34	0.4	12.5	10.9	41	<0.1	27.3	8.3	<0.5	0.2	0.1	<0.1	0.02	<0.1	<0.5	34	8		
X 5	1.14	4.89	0.77	4.79	0.86	2.54	0.37	2.43	0.37	0.2	20.2	17.6	64	<0.1	36.5	7.4	<0.5	0.1	<0.1	0.2	0.05	0.1	<0.5	46	13		
XI 1	1.03	4.08	0.65	4.28	0.77	2.26	0.33	2.17	0.35	4.5	17.2	12.9	71	<0.1	42.4	8.6	<0.5	0.3	0.2	0.1	0.03	0.2	1.3	50	12		
XI 2	1.13	4.54	0.83	3.94	0.94	2.78	0.42	2.56	0.42	2.8	18.7	13.4	67	<0.1	45.1	7.1	1.9	0.3	0.1	0.2	0.05	0.2	1.1	58	14		
XI 3	1.27	5.22	0.97	4.15	1.07	3.05	0.46	2.56	0.4	1.1	22.1	16.1	71	<0.1	61.9	6.1	2.2	0.2	0.1	0.2	0.05	0.1	0.5	76	15		
XII 1	0.9	3.79	0.74	3.47	0.87	2.31	0.39	2.05	0.41	5.5	16.7	9.4	60	<0.1	31.7	8.7	2.3	0.3	0.2	0.1	0.03	0.1	1.9	35	11		
XII 2	0.93	3.57	0.72	3.08	0.79	2.35	0.37	2.14	0.36	5.6	100.3	623.8	434	0.1	72.9	11.1	2.9	0.5	0.4	0.3	0.04	0.4	0.7	83	10		
XII 3	0.73	3.14	0.61	2.82	0.61	1.96	0.29	1.7	0.3	6.8	108.3	726.1	444	0.1	45.4	13.5	2.9	0.7	5.4	0.4	0.04	0.5	1.2	56	9		
XII 4	1.07	4.43	0.87	3.97	0.98	2.69	0.43	2.38	0.42	0.2	21.3	41.3	71	<0.1	36.2	2.9	1.3	<0.1	<0.1	0.2	0.04	<0.1	0.6	46	13		
XII 5	1.07	4.31	0.86	3.8	0.93	2.82	0.43	2.4	0.38	0.7	20.3	19.2	58	<0.1	46.6	6.1	1.4	0.2	0.1	0.2	0.05	0.1	1.1	64	13		
XII 6	1.42	5.55	1.06	4.95	1.13	3.16	0.48	2.69	0.45	0.3	29.1	24.8	92	0.1	90.2	5.8	1.3	0.3	0.1	0.2	0.06	0.2	0.8	102	17		
XII 7	1.31	5.22	0.95	4.28	1.03	2.77	0.44	2.43	0.42	0.5	28.6	31.3	95	<0.1	65.5	5.4	1	0.2	<0.1	0.3	0.07	0.2	1	76	19		
XII 8	1.35	5.41	1.01	4.47	1.05	2.94	0.49	2.67	0.43	0.2	26.2	22.2	81	<0.1	46.9	7.8	0.8	0.2	<0.1	0.3	0.04	0.2	0.7	62	19		
XIII 1	1.19	4.46	0.87	3.82	1	2.89	0.44	2.45	0.41	0.4	22.1	16.1	283	<0.1	57.9	3.8	1.2	0.3	<0.1	0.2	0.16	0.1	0.6	65	14		
XIII 2	0.98	4.12	0.77	3.69	0.83	2.51	0.37	2.47	0.4	0.2	17.8	11.2	80	<0.1	34.9	4.7	1.7	0.2	<0.1	0.2	0.07	<0.1	0.7	43	11		
XIII 3	1.02	4.09	0.79	3.68	0.89	2.5	0.38	2.22	0.35	0.2	17.2	15	75	<0.1	44.7	4.9	2	0.2	<0.1	0.2	0.07	0.1	0.6	57	13		
XIII 4	1.23	4.96	0.91	4.33	1.09	3.01	0.46	2.47	0.44	0.2	24.2	18.1	97	<0.1	56.9	7.5	1	0.1	<0.1	0.3	0.09	0.1	1	69	16		

XVII 5	0.82	3.61	0.61	3.05	0.62	2.26	0.3	1.95	0.34	0.3	12.7	12	59	<0.1	26.8	5.2	0.7	<0.1	<0.1	0.1	0.03	<0.1	<0.5	37	11
XVII 6	0.87	3.51	0.68	3.19	0.73	2.23	0.36	2.01	0.38	0.4	12.6	9.3	114	<0.1	25.4	8.1	<0.5	0.1	<0.1	0.1	0.02	<0.1	<0.5	31	10



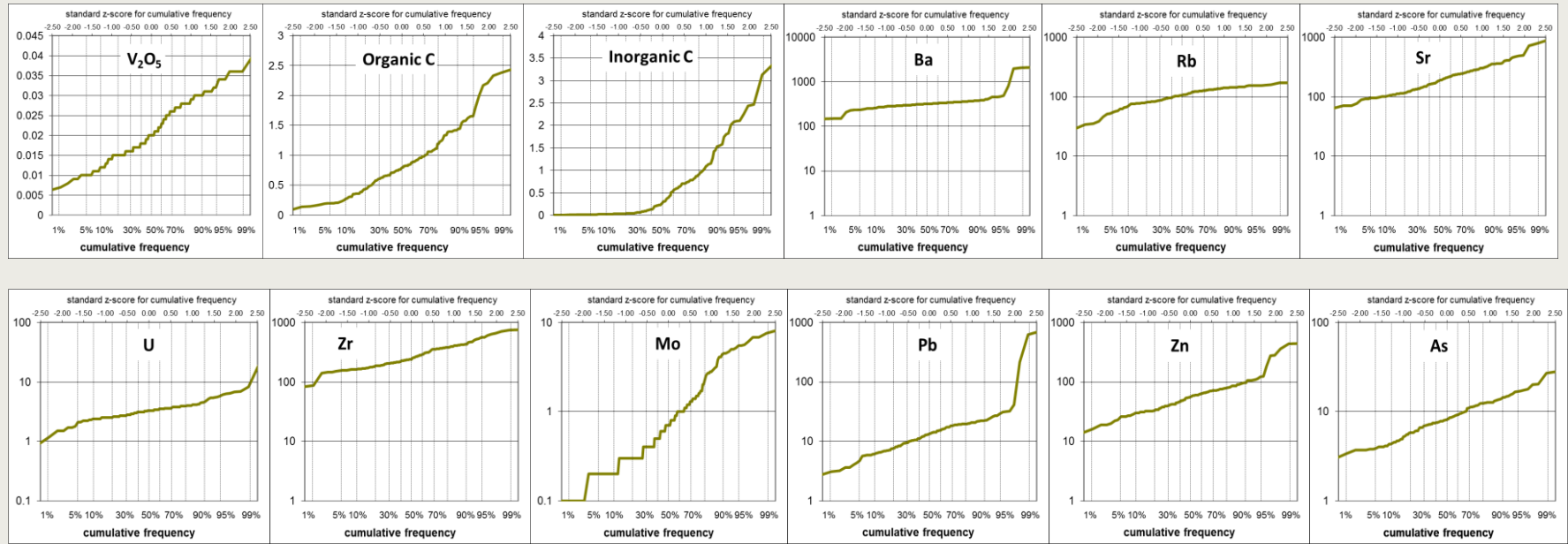


Figure 21. Cumulative frequency, or percentile, plots for the major oxides, organic and inorganic C (in wt%) and for selected trace elements (in ppm). Note that the scale for CaO, MnO, P₂O₅, SO₃ and the trace elements is logarithmic. Except for P₂O₅, these oxides and elements have a lognormal distribution. For P₂O₅ this gives a better view on the data. Except for one outlier in the highest range, the distribution is normal.

Appendix C

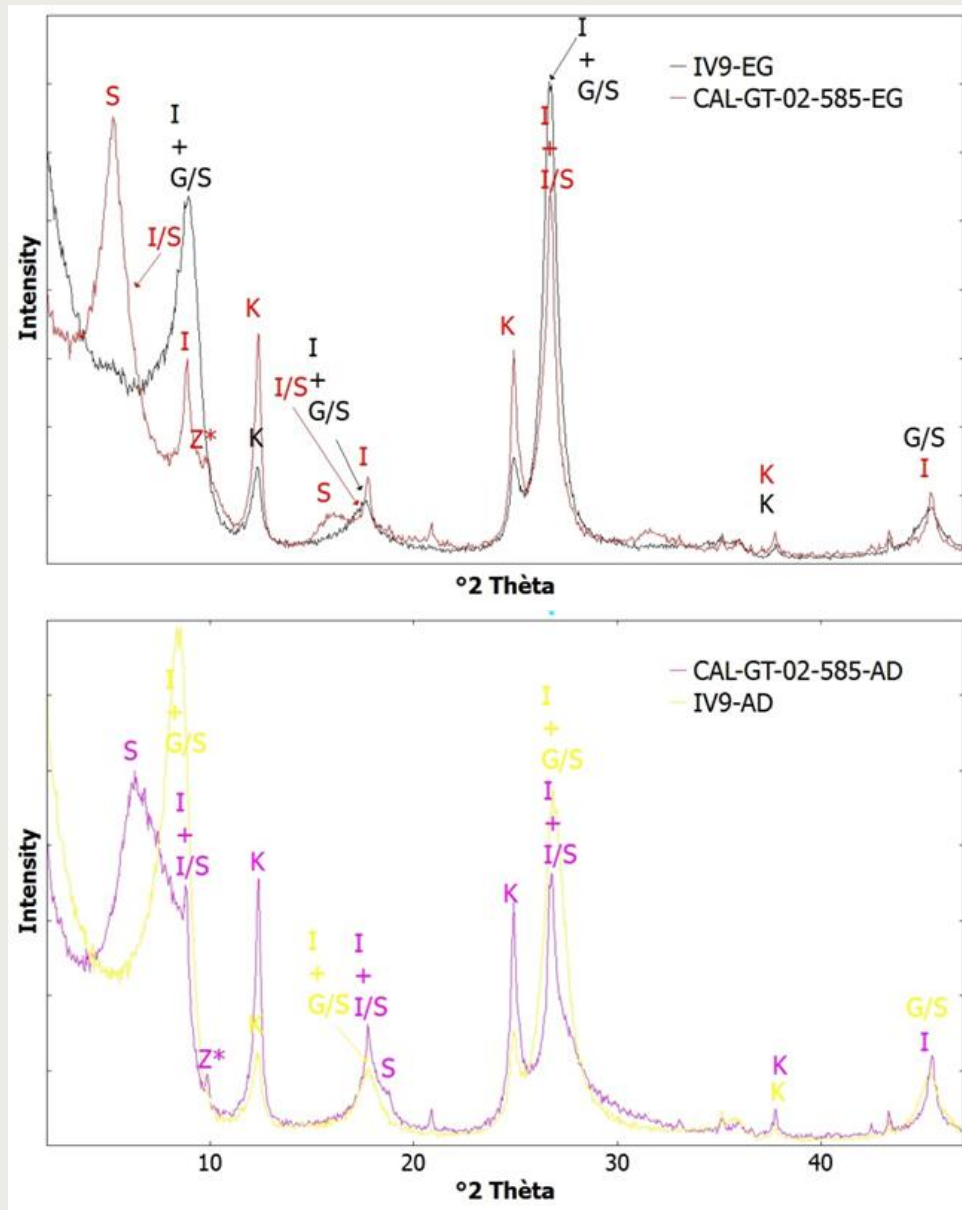


Figure 22. XRD patterns from oriented preparations saturated with ethylene glycol (upper) and from air dried oriented preparations (lower). KSS = Kaolinite/Smectite mixed layers, ISS = Illite/Smectite mixed layers, Glau-smec = Glauconite/Smectite mixed layers.

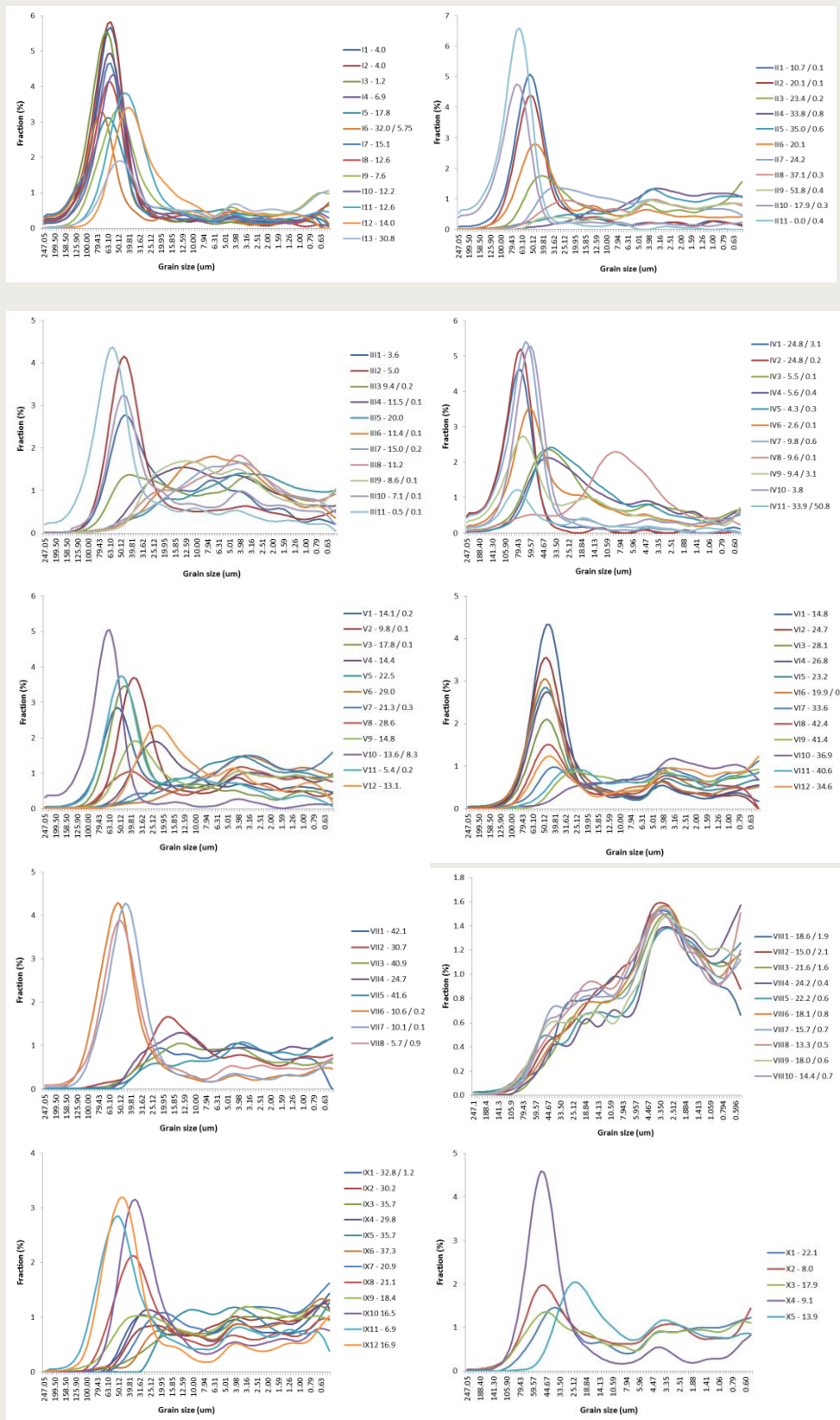
Z* refers to the zeolites which are also found in the clay fraction. The proportion of the peak at 8 - 9 $^{\circ}2\text{theta}$ and 18 $^{\circ}2\text{theta}$ is a measure for the amount of Fe in 2:1 clay minerals. In sample IV 9 the 2:1 clays are much more rich in Fe.

Table 13. Mineralogy from XRD analyses, bulk and clay fraction. KSS = Kaolinite/Smectite mixed layers, ISS = Illite/Smectite mixed layers, Glau-smec = Glauconite/Smectite mixed layers.

Sample	Depth (m)	XRD bulk (wt%)															XRD clay fraction										
		Qtz	Plag	K-f	Clin	Cal	Arag	Ank/Dol*	Sid*	Py	Ana	IIm	Syl*	Hal	Gyp	Jar*	Chl	2:1 clay	Of which 2:1 Fe clay	Kaol	Total Non- clay	Total clay	Kaol	KSS	Chlorite	Smectite	ISS
III4	381	31.2	2.5	6.2					6.9	0.9			2.3	2.6	1.1	39.0		7.1	52.7	47.3	10	12	2	33	13	16	14
III6	410	22.9	1.5	5.3	4.7	0.6		3.9	0.4	0.8		0.2	1.7	1.0	49.3		7.9	41.8	58.2	6	13	1	42	18	1	1	
III8	440	25.4	2.1	6.4		0.7			0.5	0.8			0.7		1.4	53.9		8.1	36.6	63.4	7	12	1	38	24	9	9
III10	471	49.6	3.5	8.9		0.9			0.1	0.5			1.1		1.3	31.1		2.9	64.7	35.3	8	6	1	35	34	16	
III11	485	59.6	3.7	8.6	1.1			0.6	0.2	0.2			0.3		0.3	24.0		1.4	74.3	25.7	12	5	2	27	32	22	
IV7	262	79.3	1.8	8.0	1.1				0.3	0.1			1.0		0.2	7.2		1.0	91.6	8.4	1	12	2	19	26	19	12
IV8	277	28.9	2.7	14.2	2.1	1.5			0.8	0.3			0.1		0.1	46.2		3.0	50.7	49.3	4	5	1	27	27	7	29
IV9	288	56.1	1.6	6.0	2.0	1.6			0.2	0.2			2.4		0.1	28.9	23.9	0.9	70.1	29.9	3	3	1	3	6	5	79
IV10	294	48.3	2.5	6.0	16.2	5.1			0.8	0.2			1.5		0.6	17.6		1.0	80.6	19.3	6	6	2	37	29	9	11
IV11	306	86.3	0.3	2.2		0.6			0.4	0.1			0.8		0.0	8.1		1.0	90.9	9.1	7	8	1	35	36	13	
V2	168	53.3	5.6	8.3	1.6				0.1	0.4			0.2	0.7	0.9	25.3		3.6	70.2	29.8	11	7	1	31	26	24	
V4	196	37.4	3.8	7.9		1.2			0.6	0.6			0.5	2.2	3.7	38.3		3.8	54.1	45.9	6	9	1	41	25	1	8
V6	226	21.9	0.8	3.5					0.5	0.9	0.3		2.4	2.8	3.1	51.6		12.	33.2	66.8	6	12	1	42	11.7	10	17
V8	252	35.3	0.6	4.7		1.4			0.2	0.9	0.4		1.4	2.8	2.6	45.3		4.5	47.6	52.4	3	14	1	38	23	9	12
V10	312	71.7	3.0	10.1									0.2		0.1	14.2	12.4	0.8	85.0	15.0	2	3	1	52	1	7	25
XI1	610	25.5	1.7	3.9	2.1	4.0	0.4	1.0	0.5		2.0	1.2		1.6	51.8		4.3	42.3	57.7	11	8	2	36	27	16		
XI2	632	17.9	1.1	3.0	1.7	8.9	0.5	0.6	0.6		1.6	1.0		2.0	53.0		8.1	36.8	63.1	4	9	1	53	15	7	11	
XI3	650	16.3	1.3	3.4	10.3				0.4	0.6		2.2	1.4		2.7	52.5		8.8	36.0	64.0	4	1	1	53	1	7	15
XII12	442	26.4	1.3	3.9	25.9				0.7	0.4			0.4		1.2	34.0		5.9	58.9	41.1	3	7	1	6	1	7	12
XIII4	465	25.7	1.9	4.6	2.2				1.1	0.7			1.9	0.3	1.5	53.9		6.2	38.4	61.6	3	8	1	56	9	8	15
XIII6	489	21.6	3.0	6.2	1.8				0.5	0.6			0.9	1.1	2.5	54.7		7.0	35.8	64.2	8	14	1	38	25	14	
XIII8	514	47.6	4.8	8.8					0.4	0.3			1.1	0.8	0.0	33.9		2.4	63.7	36.3	4	2	1	41	37	16	
XIII10	537	21.1	1.0	4.4					0.9				2.5	1.8	63.1		5.2	29.8	70.2	5	8	1	43	18	12	13	
XVI12	510	51.3	2.8	9.4	1.9	2.5	2.8	0.1	0.7	0.1			0.5	27.2		0.9	71.5	28.5	2	3	1	39	45	1			
XVI4	530	49.2	2.8	8.1	2.9	3.0	2.8	0.3	0.9	0.2			0.5	28.0		1.4	70.1	29.9	3	4	1	44	34	14			
XVI6	550	49.8	3.2	11.1	2.4	2.8	2.7		0.8	0.1			0.6	25.0		1.4	73.1	26.9	4	2	2	33	42	17			

Sample	Depth (m)	XRD bulk															XRD clay fraction										
		Qtz	Plag	K-f	Clin	Cal	Arag	Ank/Dol*	Sid*	Py	Ana	IIm	Syl*	Hal	Gyp	Jar*	Chl	2:1 clay	Of which 2:1 Fe clay	Kaol	Total Non- clay	Total clay	Kaol	KSS	Chlorite	Smectite	ISS
XVI8	570	49.7	4.1	10.0	2.1	2.7	2.3	0.2		1.0					0.5	25.6		1.8	72.1	27.9	5	4	2	4	3	19	
XVI10	585	47.1	2.8	10.6	1.3	2.8	2.2		0.6	3.5	0.2			0.2		0.5	26.1		2.2	71.3	28.7	1	4	2	28	3	26
XVI12	600	48.2	3.2	8.5	2.0	2.7	2.6		0.2	1.8	0.1					0.7	27.1		2.8	69.4	30.6	8	4	2	28	36	22
XVII5	75	40.4	3.8	7.4		1.9	0.7			0.2	0.3			0.5		0.8	40.4		3.8	55.1	44.9	7	3	1	46	29	16

Appendix D



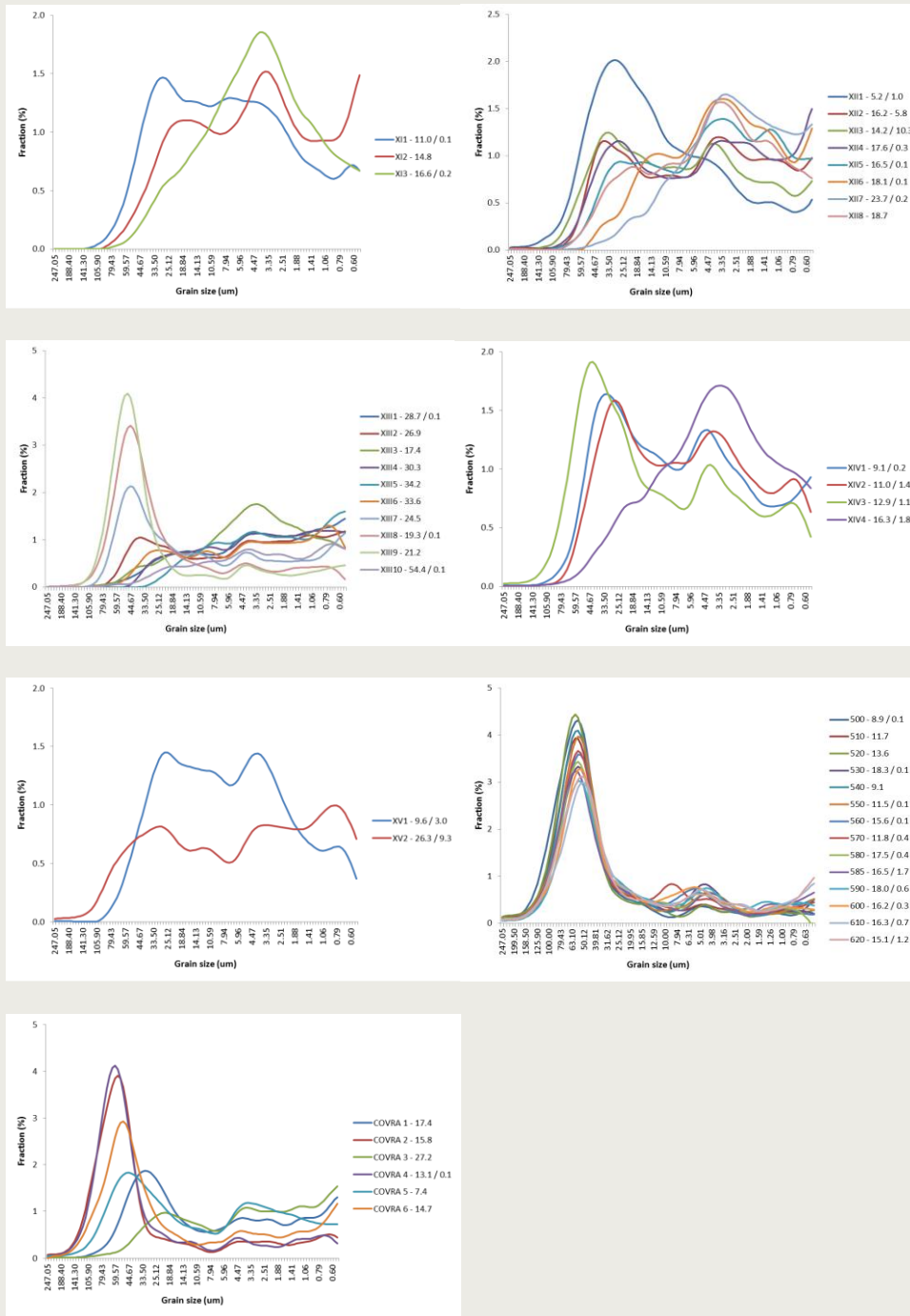
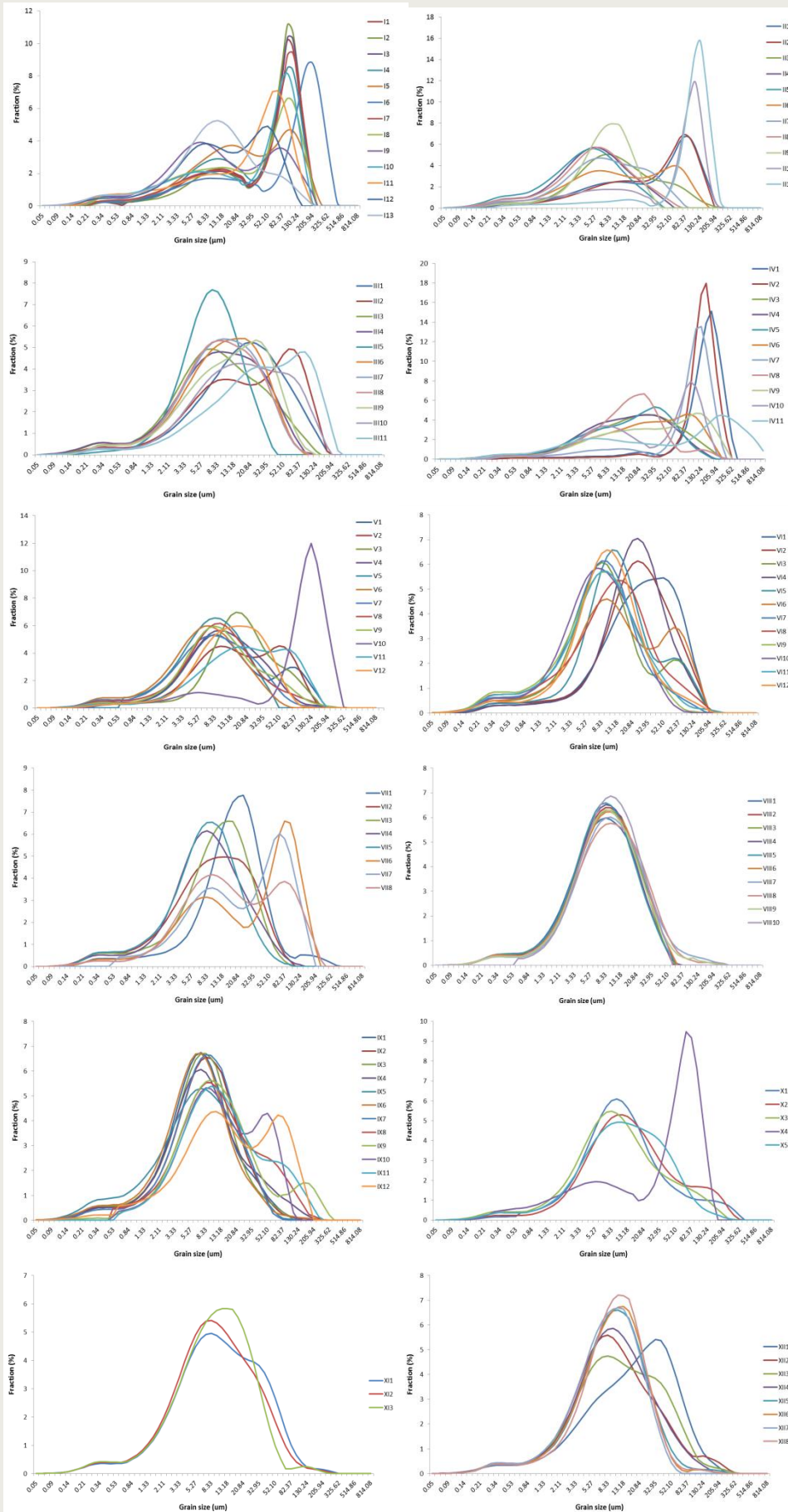


Figure 23. Grain size distribution plots per core from Sedigraph analysis. The numbers in the legend indicate the fraction < 0.516 um and > 250 um. The grain size values are in reversed order for comparison with Honty et al. (2004)



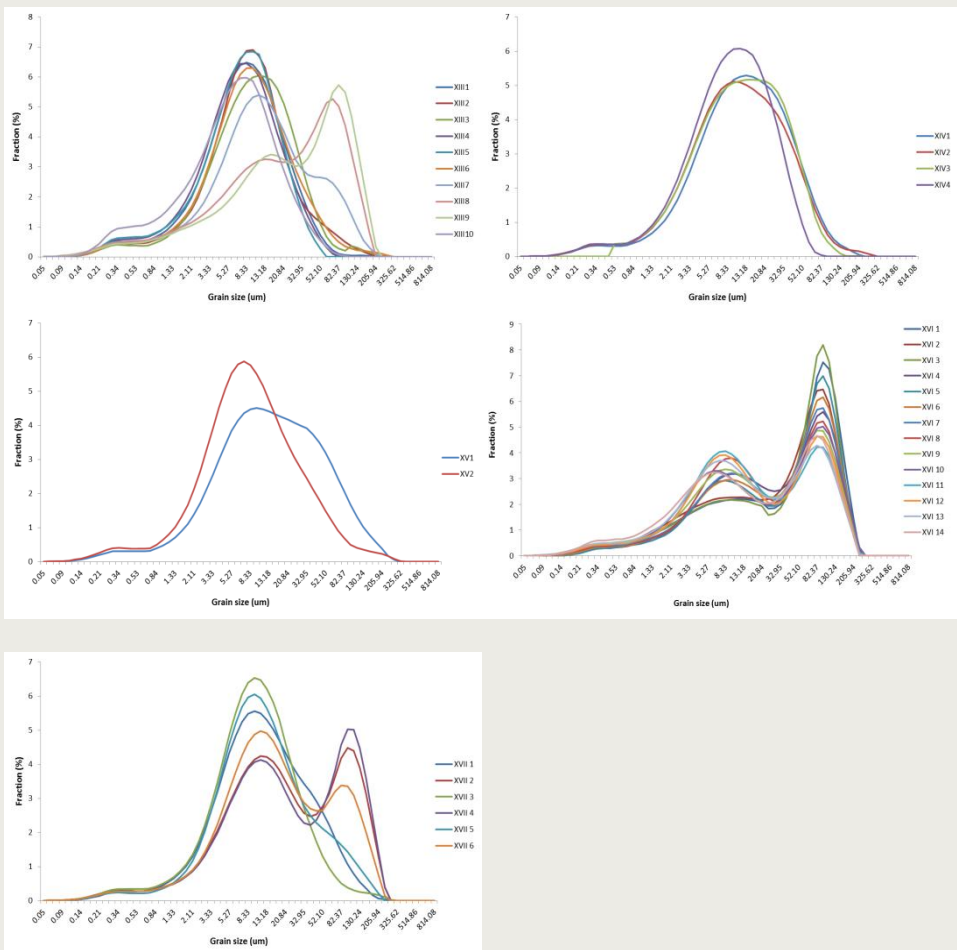


Figure 24. Grain size distribution plots per core from Laser diffraction analysis.

Table 14. Clay, silt and sand volume fraction for each sample based on the sedigraph technique. The fraction of grains >250 µm is included in the sand fraction. The grain size intervals are in accordance to those by Honty (2008).

	Clay (<2 µm)	Silt (2-63 µm)	sand (>63 µm)		Clay (<2 µm)	Silt (2-63 µm)	sand (>63 µm)		Clay (<2 µm)	Silt (2-63 µm)	sand (>63 µm)
I 1A	7.5	54.9	37.7	IV 1A	25.5	20.5	54.0	VII 1A	56.4	43.0	0.6
I 2A	6.4	53.3	40.3	IV 2A	25.3	19.7	55.0	VII 2A	46.8	52.3	0.9
I 3A	7.8	45.5	46.7	IV 3A	18.1	72.6	9.3	VII 3A	55.1	44.7	0.2
I 4A	12.7	52.7	34.6	IV 4A	17.3	75.3	7.4	VII 4A	47.9	52.1	0.0
I 5A	25.7	49.0	25.2	IV 5A	13.5	80.4	6.1	VII 5A	63.4	36.5	0.0
I 6A	34.7	27.7	37.6	IV 6A	9.6	63.1	27.2	VII 6A	19.3	58.9	21.8
I 7A	19.4	45.6	35.0	IV 7A	10.3	40.0	49.7	VII 7A	19.1	67.8	13.1
I 8A	19.7	49.8	30.5	IV 8A	19.5	74.8	5.7	VII 8A	17.8	64.6	17.6
I 9A	23.0	60.2	16.8	IV 9A	16.7	49.3	34.0	VIII 1A	41.1	55.3	3.6
I 10A	18.3	56.7	25.0	IV 10A	11.3	54.6	34.1	VIII 2A	41.0	55.8	3.1
I 11A	20.6	69.7	9.7	IV 11A	18.8	16.1	65.0	VIII 3A	48.4	49.5	2.1
I 12A	20.6	74.6	4.8	V 1A	27.6	59.4	13.0	VIII 4A	54.9	43.9	1.1
I 13A	46.8	45.9	7.3	V 2A	21.1	75.8	3.1	VIII 5A	50.3	47.1	2.6
II 1A	15.3	63.2	21.5	V 3A	27.3	64.9	7.9	VIII 6A	44.7	53.2	2.0
II 2A	26.8	56.9	16.3	V 4A	35.2	64.1	0.7	VIII 7A	41.6	56.4	2.0
II 3A	43.4	53.5	3.1	V 5A	46.3	53.0	0.8	VIII 8A	39.7	57.9	2.3
II 4A	60.8	38.4	0.8	V 6A	55.6	44.2	0.2	VIII 9A	47.5	49.8	2.7
II 5A	58.8	39.4	1.8	V 7A	50.1	48.8	1.1	VIII 10A	39.4	58.4	2.2
II 6A	30.0	60.6	9.4	V 8A	49.2	47.6	3.3	IX 1A	54.0	44.7	1.2
II 7A	39.9	59.5	0.6	V 9A	36.2	61.7	2.1	IX 2A	55.0	45.0	0.0
II 8A	55.3	43.5	1.2	V 10A	14.4	37.5	48.1	IX 3A	61.6	38.0	0.4
II 9A	70.2	29.3	0.4	V 11A	12.2	75.1	12.8	IX 4A	54.3	45.3	0.5
II 10A	21.6	32.0	46.4	V 12A	26.6	72.8	0.6	IX 5A	55.7	44.3	0.0
II 11A	0.5	40.0	59.5	VI 1A	21.8	68.4	9.8	IX 6A	62.6	36.5	0.8
III 1A	12.6	80.3	7.1	VI 2A	31.6	58.5	9.9	IX 7A	50.6	49.3	0.1
III 2A	14.8	75.3	9.9	VI 3A	44.1	49.4	6.5	IX 8A	39.4	57.5	3.1
III 3A	29.6	66.9	3.5	VI 4A	36.4	55.2	8.5	IX 9A	42.8	54.8	2.5
III 4A	29.2	70.4	0.4	VI 5A	35.9	53.4	10.7	IX 10A	32.0	66.4	1.6
III 5A	45.7	53.4	0.9	VI 6A	30.2	58.9	10.9	IX 11A	23.3	61.5	15.1
III 6A	27.9	71.4	0.7	VI 7A	53.1	44.8	2.1	IX 12A	31.2	57.3	11.5
III 7A	34.6	64.5	0.8	VI 8A	53.9	42.4	3.8	X 1A	47.5	49.8	2.7
III 8A	32.6	66.6	0.9	VI 9A	59.5	40.3	0.2	X 2A	29.0	62.9	8.1
III 9A	26.8	72.6	0.6	VI 10A	59.8	39.6	0.6	X 3A	41.6	51.9	6.5
III 10A	19.7	71.8	8.5	VI 11A	57.2	42.0	0.9	X 4A	18.4	68.2	13.4
III 11A	6.2	61.3	32.5	VI 12A	55.7	41.5	2.7	X 5A	33.6	66.2	0.2

	Clay (<2 µm)	Silt (2-63 µm)	sand (>63 µm)		Clay (<2 µm)	Silt (2-63 µm)	sand (>63 µm)
XI 1A	27.6	70.8	1.5	XVI 1	14.5	54.1	31.4
XI 2A	39.5	60.0	0.5	XVI 2	17.5	57.3	25.2
XI 3A	38.7	61.1	0.3	XVI 3	18.4	53.2	28.4
XII 1A	16.5	77.8	5.7	XVI 4	24.5	56.5	19.0
XII 2A	37.6	55.5	6.9	XVI 5	16.7	59.2	24.1
XII 3A	29.1	58.2	12.7	XVI 6	18.3	59.6	22.1
XII 4A	43.5	55.1	1.4	XVI 7	21.0	59.4	19.6
XII 5A	43.3	56.1	0.6	XVI 8	19.0	60.0	21.0
XII 6A	46.0	53.9	0.1	XVI 9	23.4	56.6	20.0
XII 7A	55.2	44.5	0.3	XVI 10	26.0	52.2	21.9
XII 8A	42.9	56.6	0.4	XVI 11	27.7	55.8	16.5
XIII 1A	57.4	42.3	0.3	XVI 12	23.6	59.2	17.2
XIII 2A	52.4	47.1	0.5	XVI 13	26.9	56.6	16.6
XIII 3A	44.0	55.6	0.4	XVI 14	25.2	55.8	19.0
XIII 4A	57.8	42.2	0.0	XVII 1	38.7	59.3	1.9
XIII 5A	63.2	36.8	0.0	XVII 2	24.8	49.0	26.2
XIII 6A	59.0	40.8	0.2	XVII 3	54.6	44.7	0.7
XIII 7A	41.1	55.9	2.9	XVII 4	22.3	51.4	26.4
XIII 8A	28.5	64.3	7.2	XVII 5	27.4	64.7	7.9
XIII 9A	29.3	60.9	9.8	XVII 6	30.3	55.1	14.6
XIII	72.1	27.6	0.3				
XIV 1A	27.4	70.9	1.7				
XIV 2A	30.9	67.0	2.1				
XIV 3A	27.7	65.4	6.9				
XIV 4A	41.6	56.3	2.1				
XV 1A	24.7	71.4	3.9				
XV 2A	44.8	41.7	13.5				

Appendix E

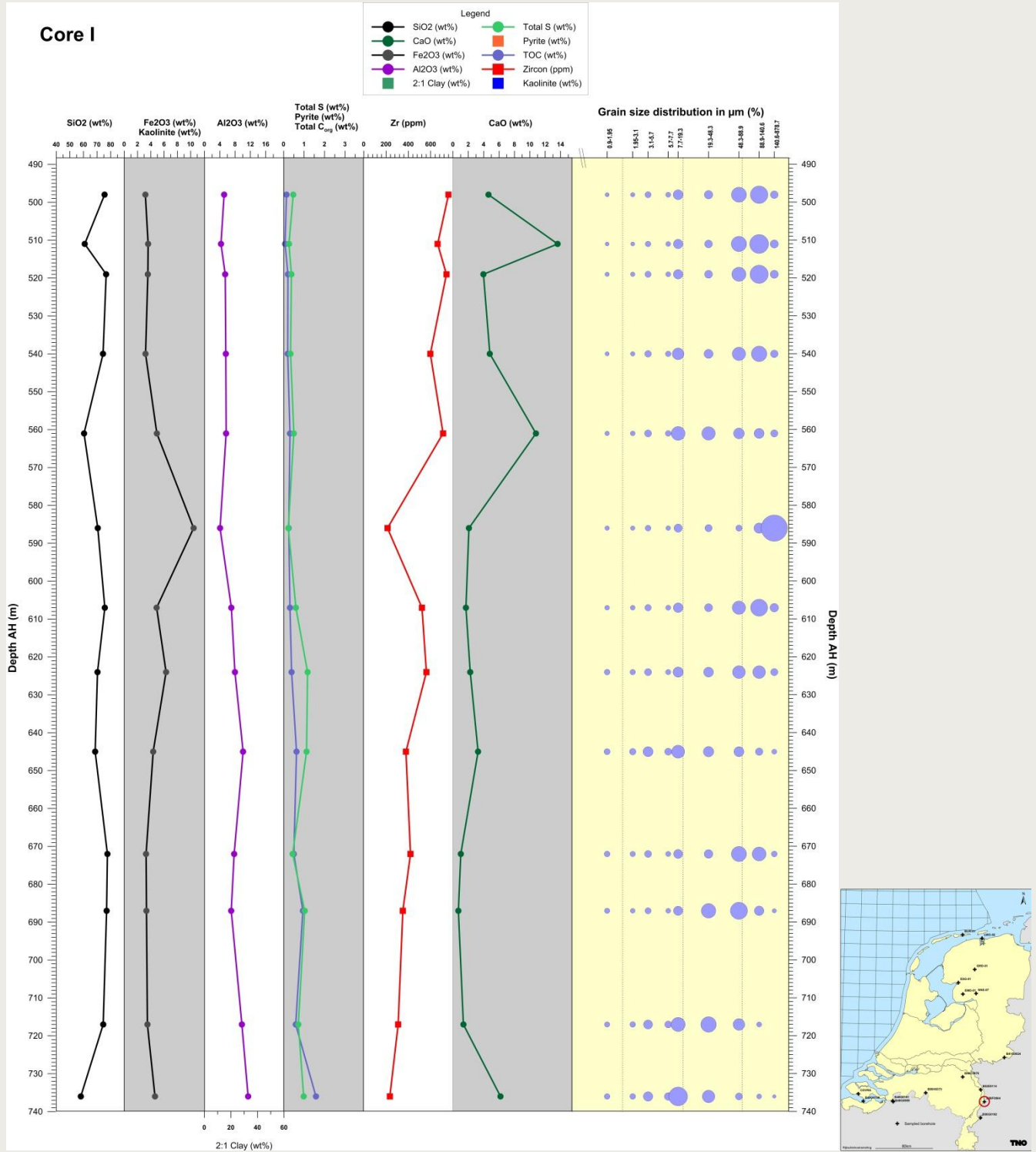


Figure 25. Depth profile of Core I (left) and map with location (right). Fluctuating composition and grain size distribution with depth. The Si content is negatively correlated with Ca. The Ca content has high values in the top and the bottom of the core. One exceptional sample at 586m with high Fe₂O₃ and low Zr content and grain sizes in the silty/sandy interval.

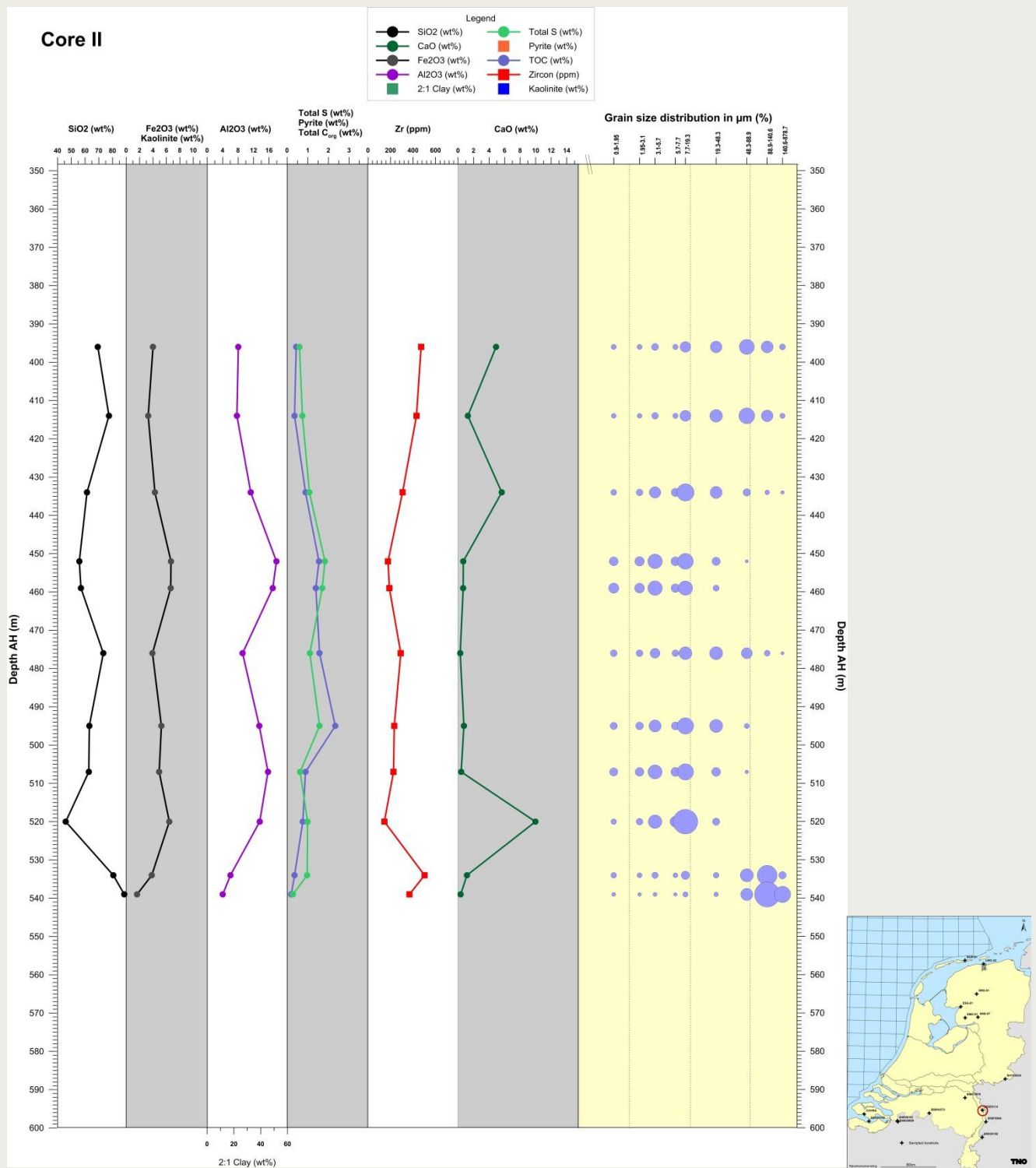


Figure 26. Depth profile of core II (left) and map with location (right). Silty top and bottom, fine-grained and clay-rich in the middle. Aluminium and Fe content are synchronous, and anti-correlate with Si and Zr. Total S and organic C correlate. Local enrichment in Ca.

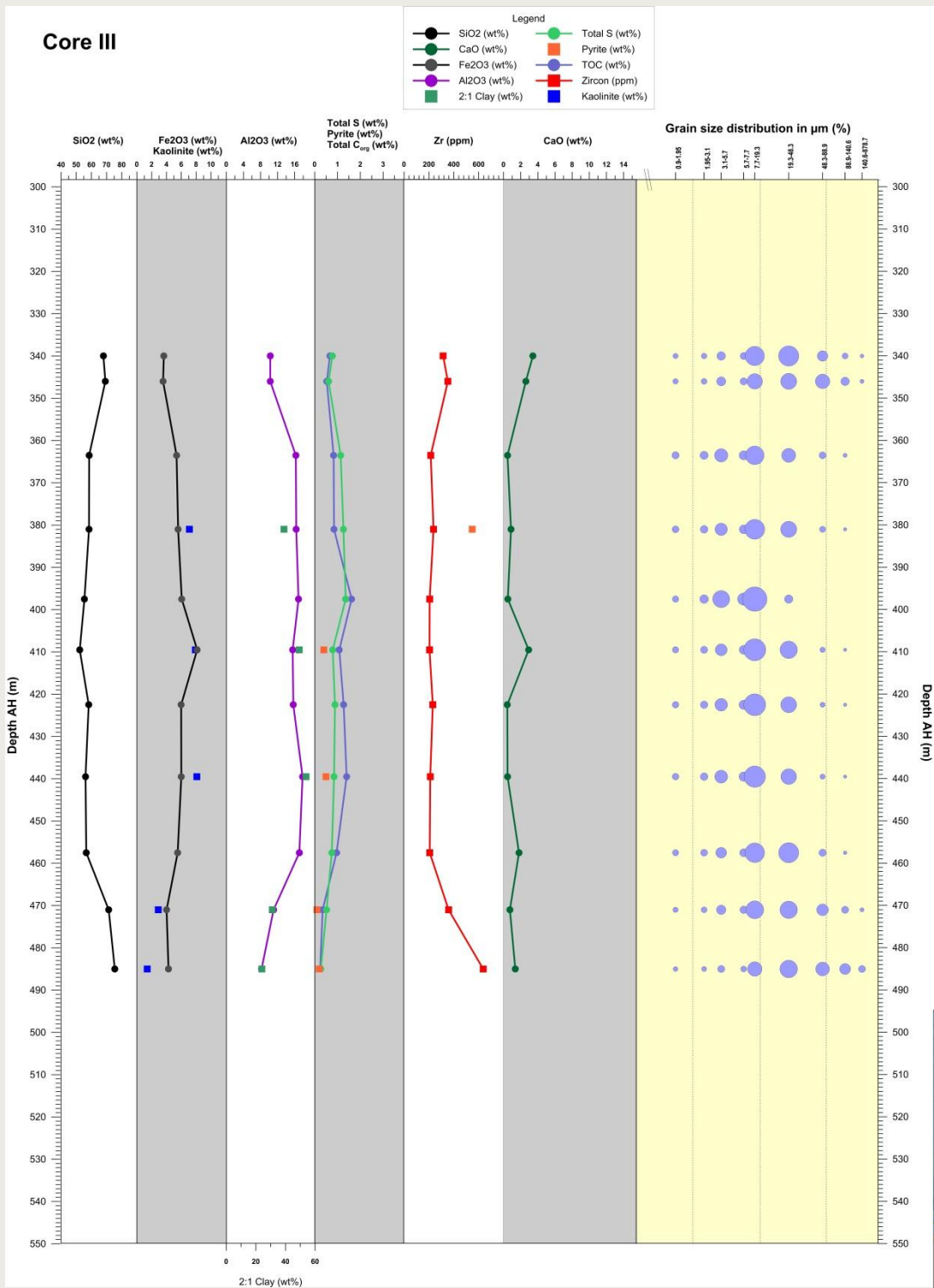


Figure 27. Depth profile of core III(left) and map with location (right). Relatively homogeneous core. Slightly Si-rich, siltier top and bottom, Al and Fe-rich middle part. Kaolinite and 2:1 clay and to a lesser extend Total S and organic C correlate with the Fe₂O₃ and Al₂O₃ profiles. Zircon follows the Si profile. Calcium content is low. The grain size distribution correlates with the Si content.

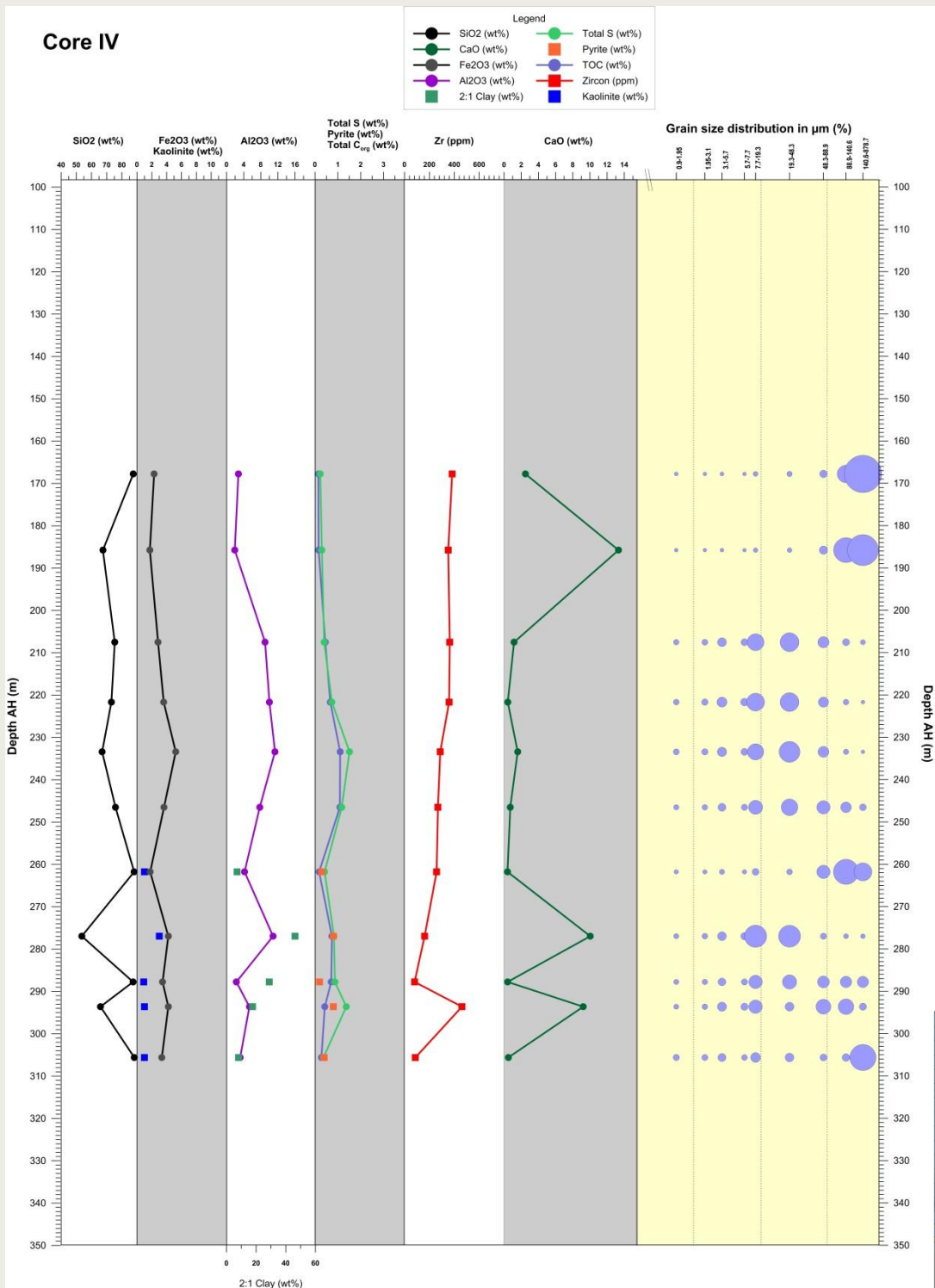


Figure 28. Depth profile of core IV (left) and map with location (right). Very silty/sandy Si-rich top and bottom. More clay-rich in between with an occasional silty/sandy layer. The 2:1 clay and kaolinite, and to a lesser extend Total S and organic C, correlate with the Al and Fe content. Local enrichment in carbonate.

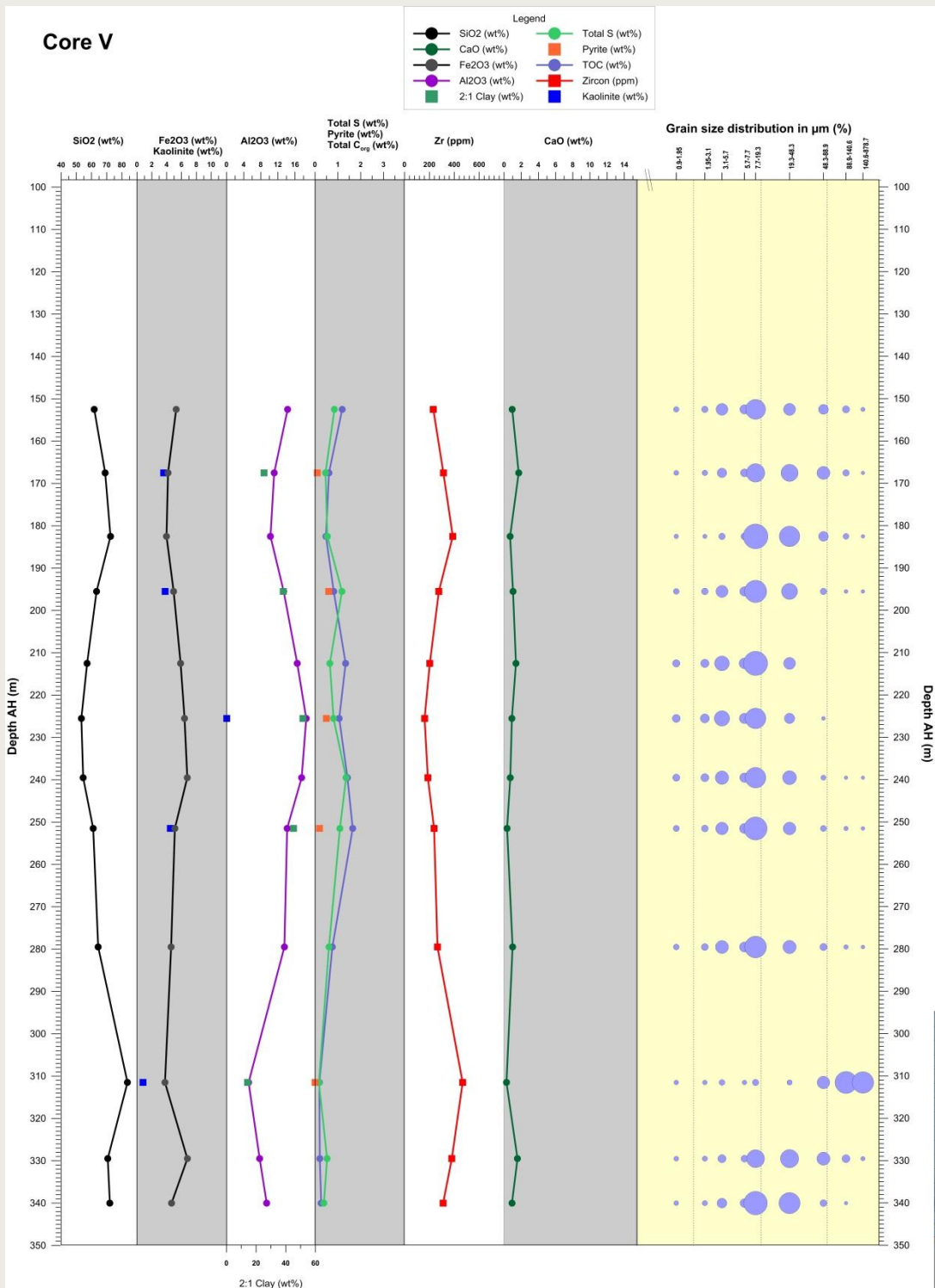


Figure 29. Depth profile of core V (left) and map with location (right). Gradually fluctuating SiO₂ with a Si-rich top and bottom. Zircon and the grain size distribution correlate with the SiO₂ profile. Fe₂O₃, Al₂O₃, kaolinite and 2:1 clay negatively correlate with SiO₂. Total S and organic C are low to intermediate while the pyrite and CaO content are low.

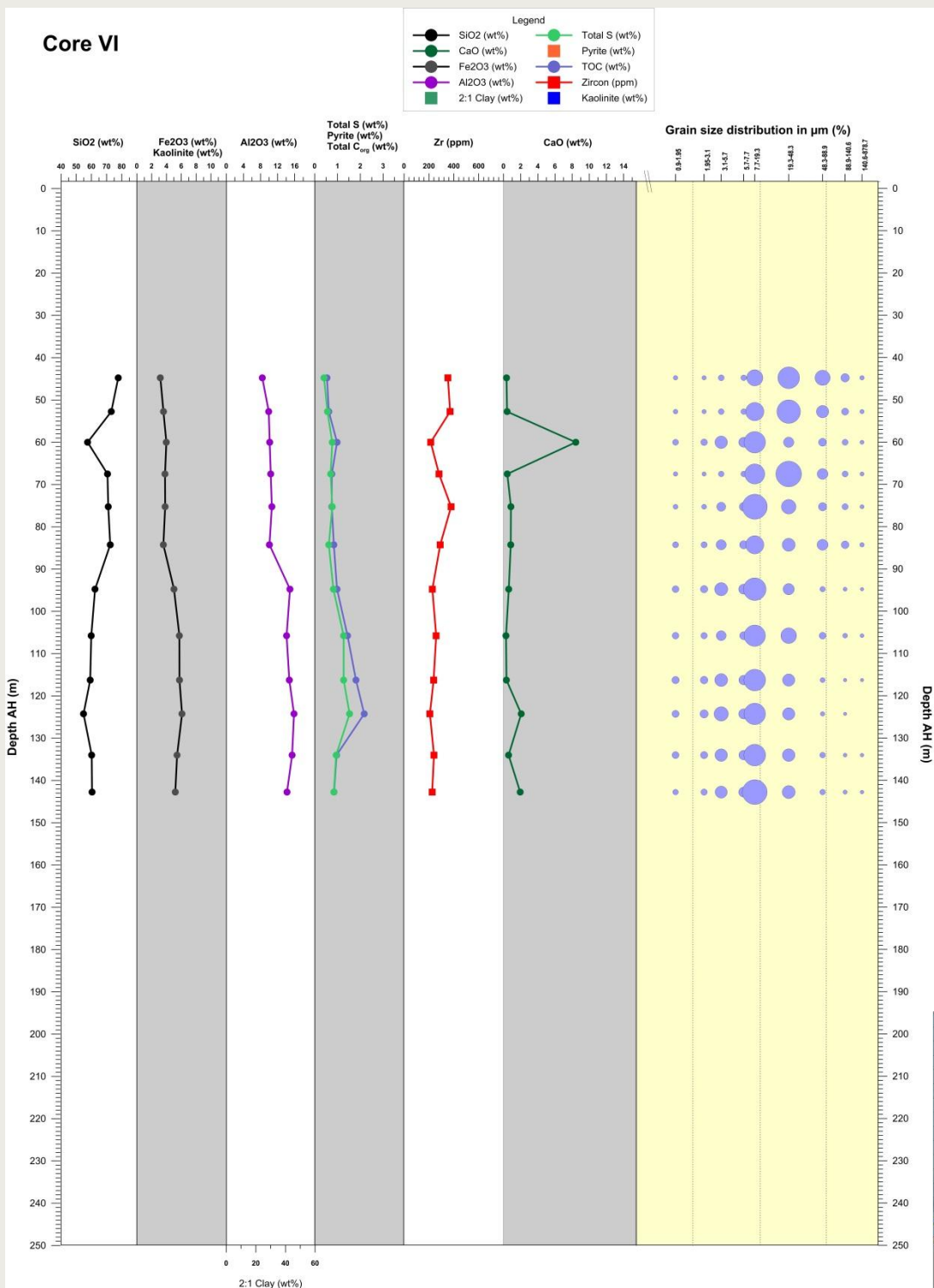


Figure 30. Depth profile of core VI (left) and map with location (right). Relatively homogeneous with depth. The Si content decreases slightly with depth while the Fe and Al content increase slightly. The grain size distribution follows the increased clay fraction. A local carbonate enrichment can be observed in the top.

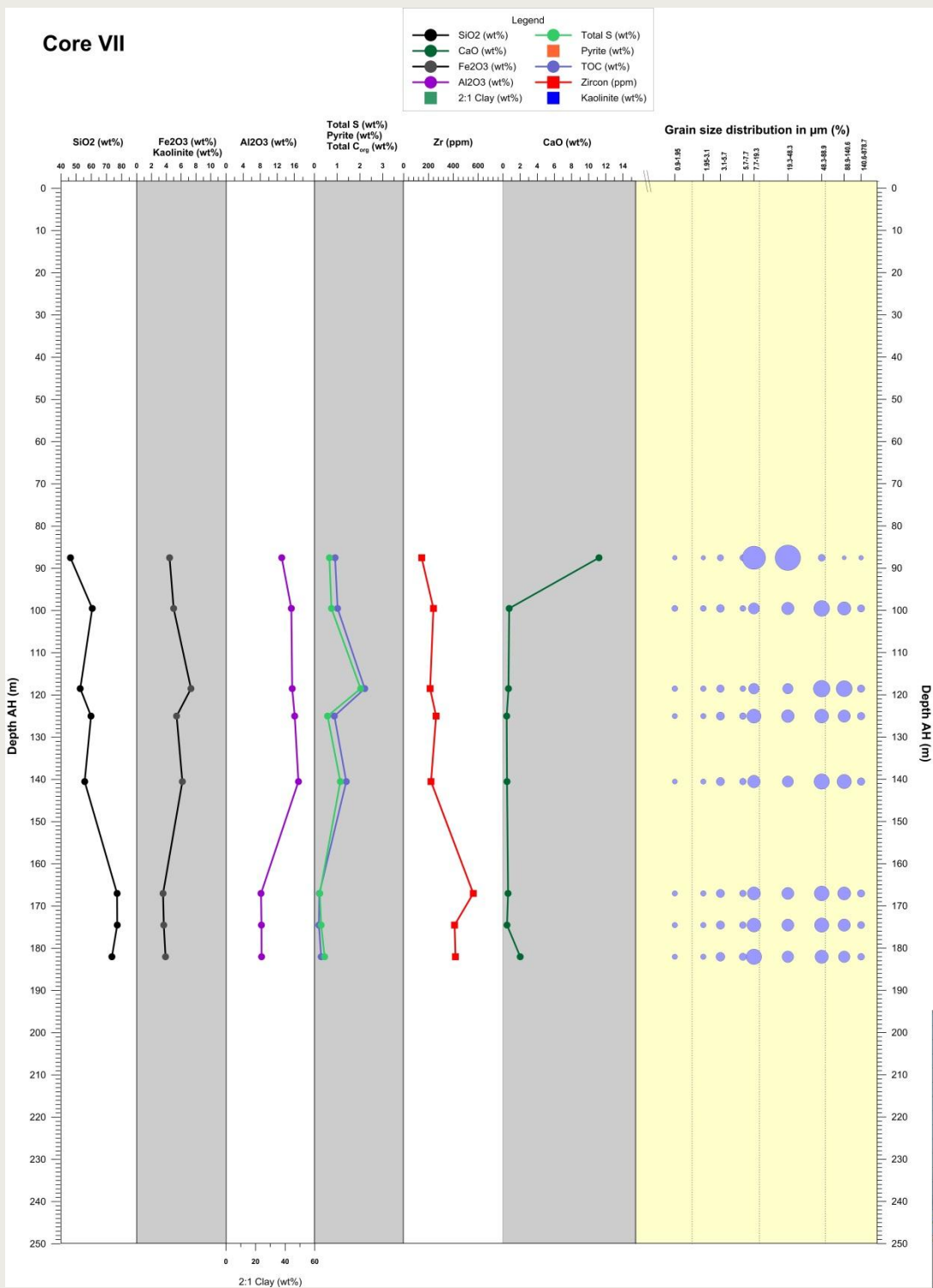


Figure 31. Depth profile of core VII (left) and map with location (right). Al₂O₃ and Fe₂O₃ rich top, SiO₂ rich bottom. Total S correlates with Fe₂O₃ and Zr with SiO₂. Except for the upper sample, the core is CaO poor. The grains are badly sorted.

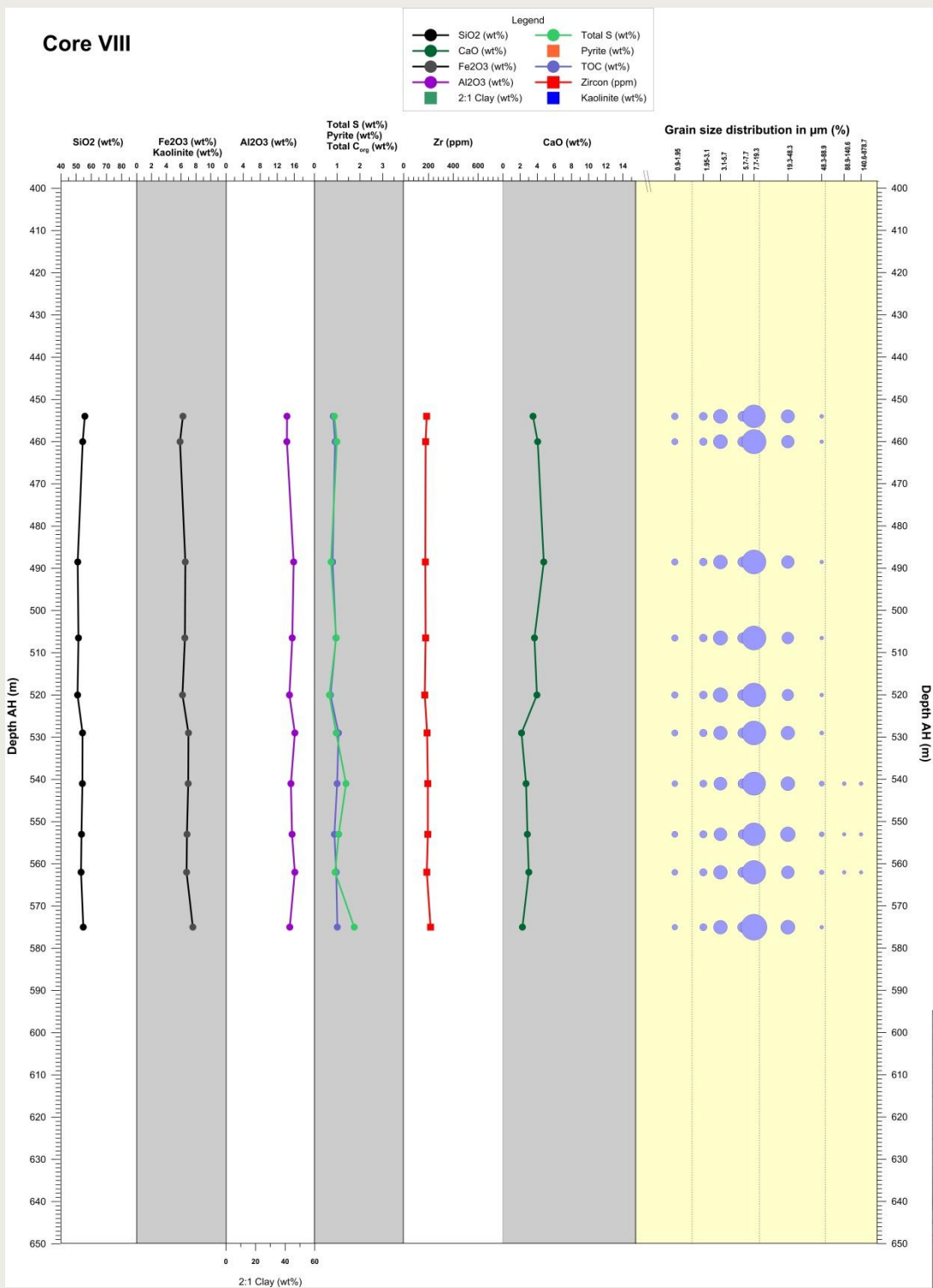


Figure 32. Depth profile of core VIII (left) and map with location (right). Homogeneous over depth. Low SiO₂, high Al₂O₃ and Fe₂O₃, intermediate CaO, total S and organic C content. Grain size distribution homogeneous and well sorted.

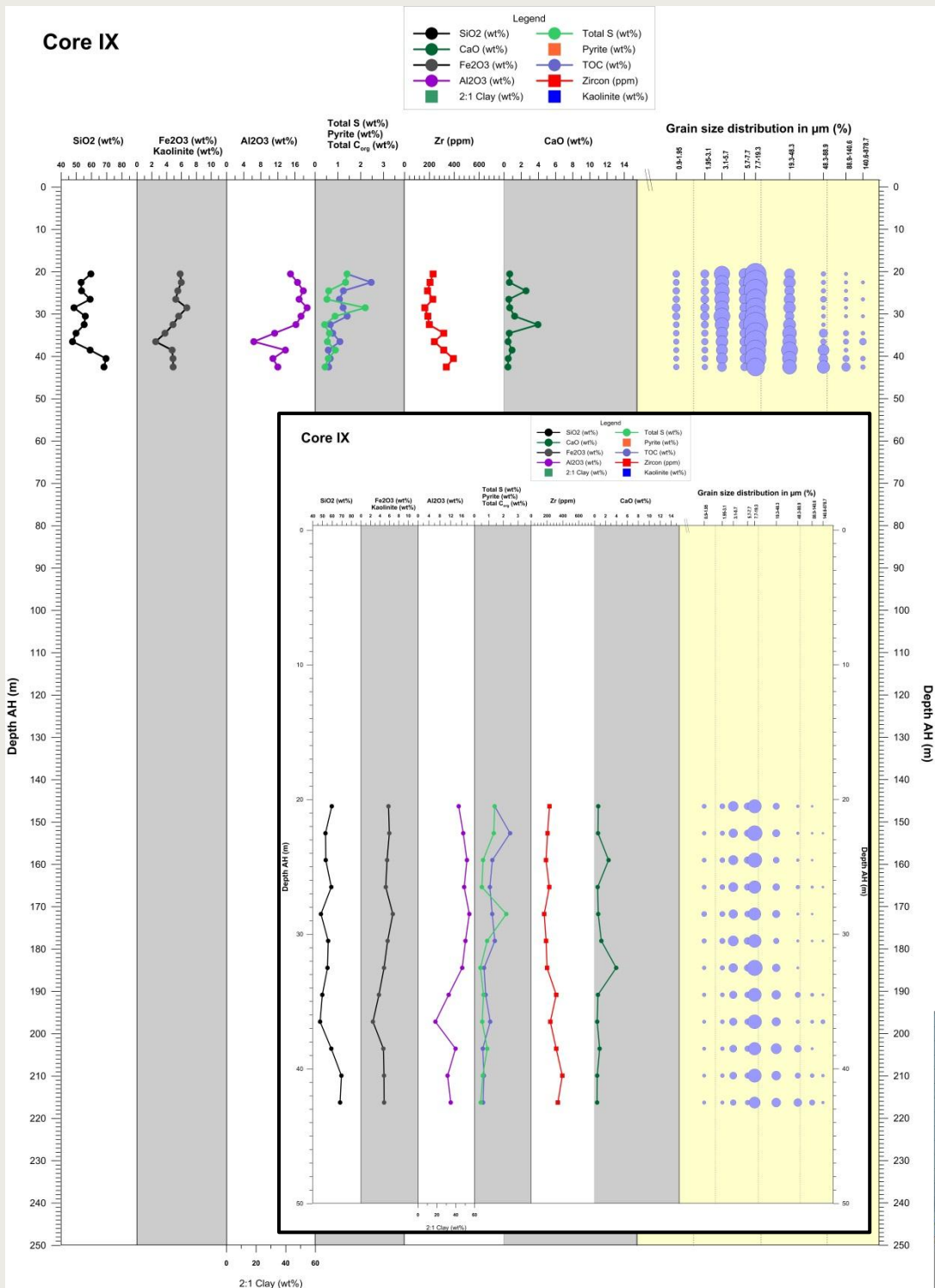


Figure 33. Depth profile of core IX (left) and map with location (right). Since the samples are all on a small depth interval, the interval is stretched in the onset.

Fluctuating composition with depth with more clay-rich top. Local enrichment in total S, organic C and carbonate, without correlations.

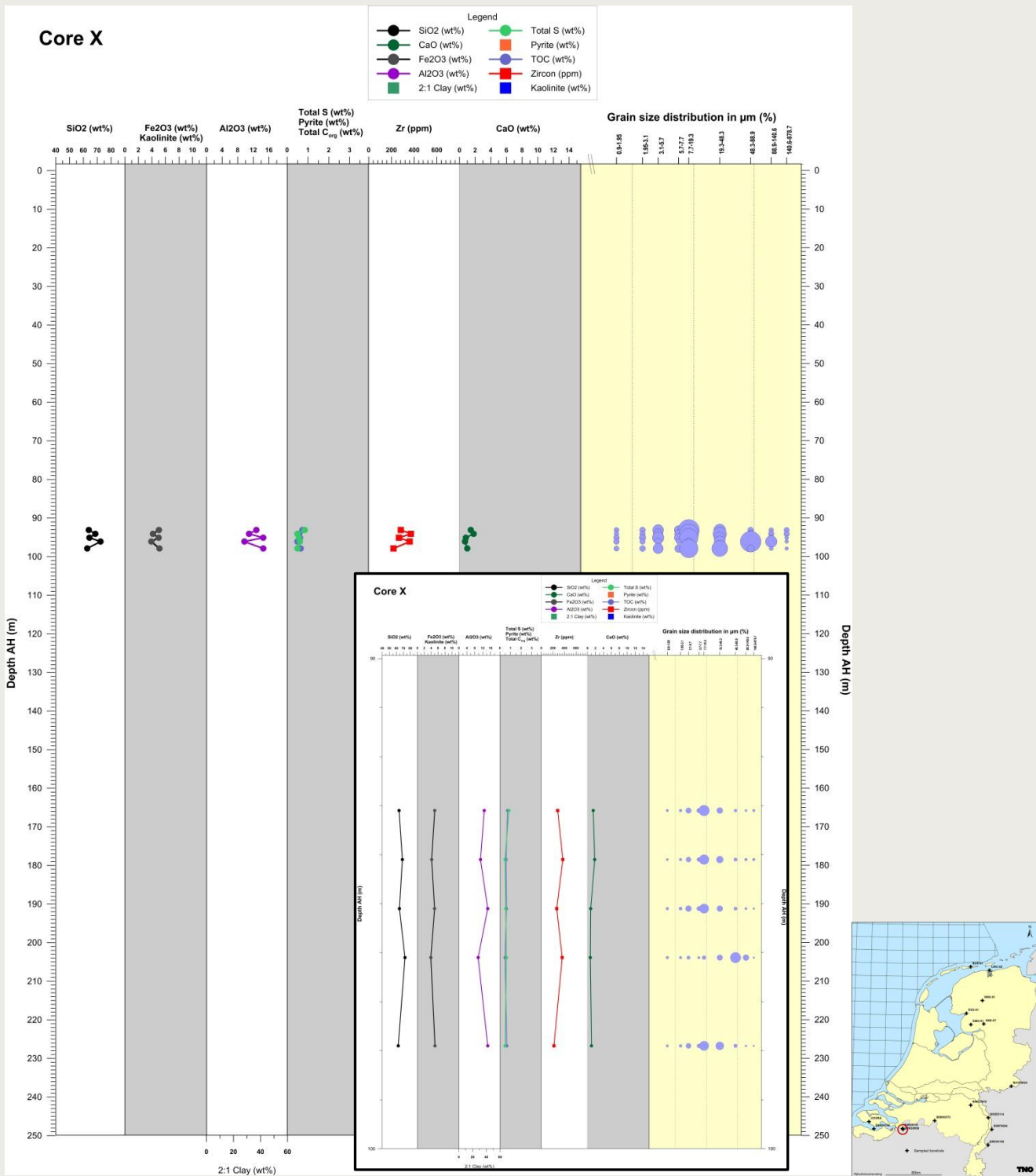


Figure 34. Depth profile of core X (left) and map with location (right). Since the samples are all on a small depth interval, the interval is stretched in the onset.

Relatively homogeneous composition, with slightly fluctuating Al content, which has a negative correlation with Si and Zr. Low Total S, organic C and carbonate content. The second sample from the bottom is siltier than the other samples.

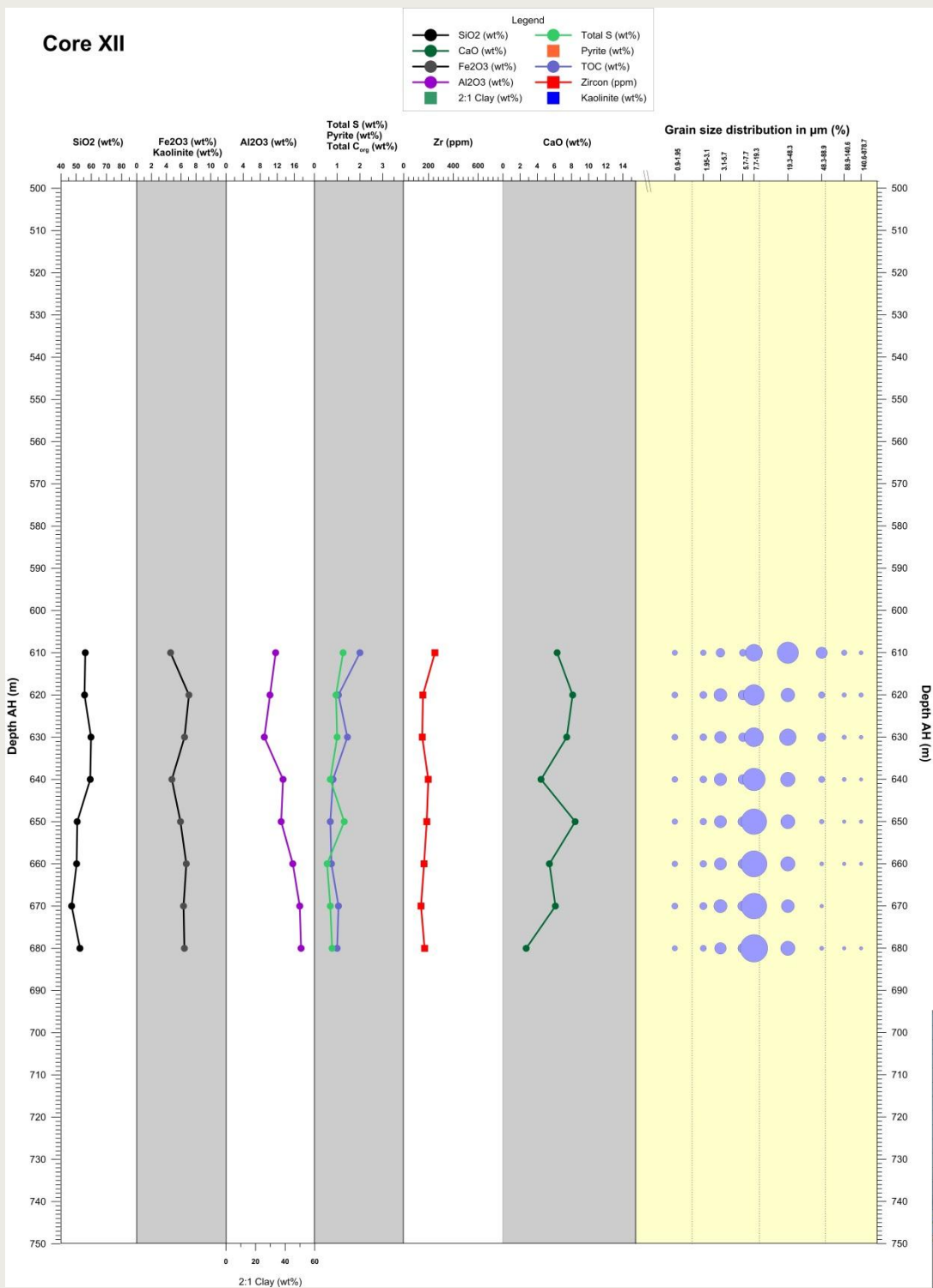


Figure 35. Depth profile of core XII (left) and map with location (right). Fluctuating composition with depth. The bottom part is more clay-rich than the top. The grain size distribution is relatively homogeneous, but the bottom is finer grained and better sorted. Total S, organic C and carbonate content are intermediate and they fluctuate without any correlation between the parameters.

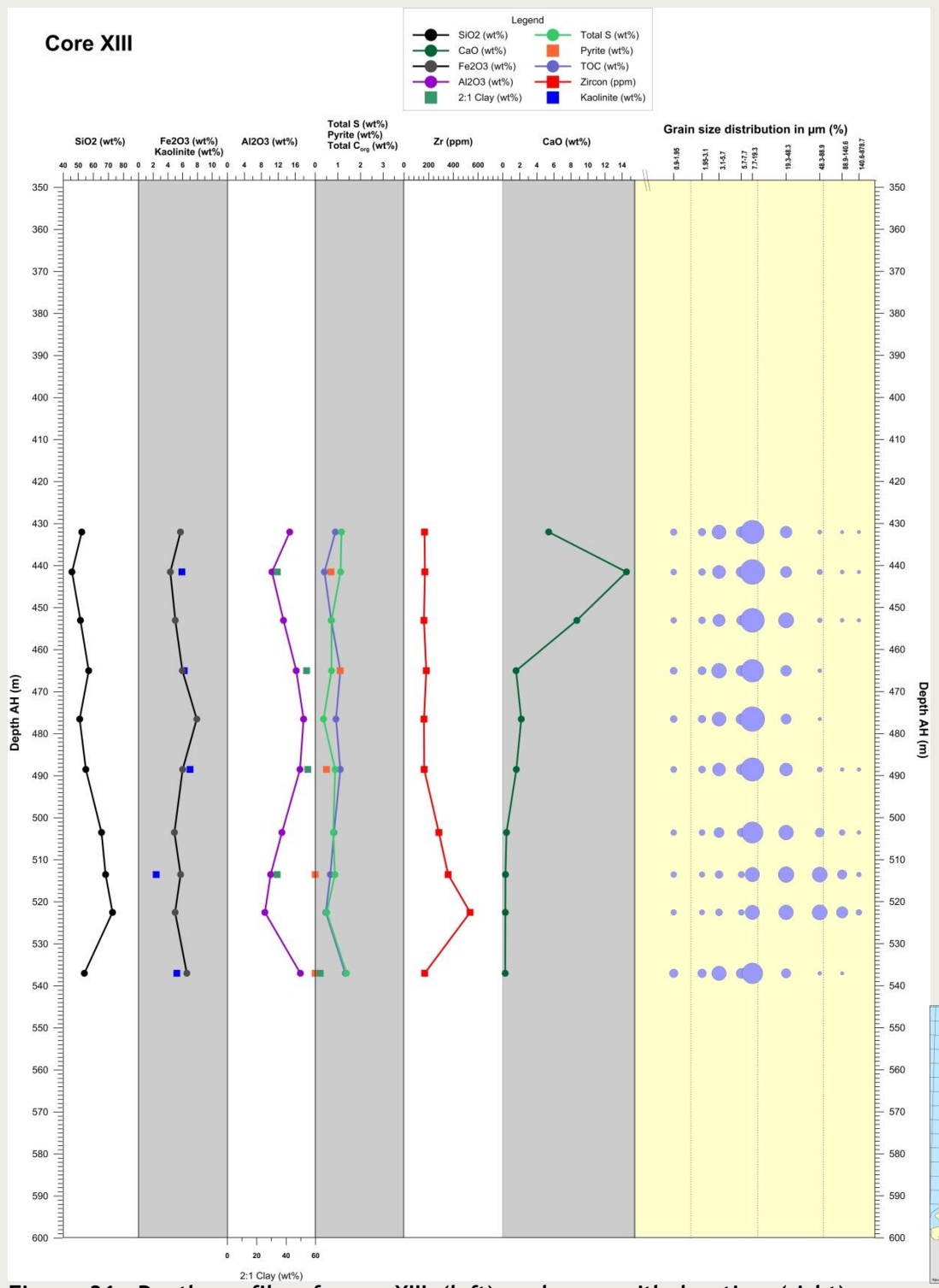


Figure 36. Depth profile of core XIII (left) and map with location (right). Gradually fluctuating SiO₂ with a Si-rich bottom (except for the lowest sample). Zircon and the grain size distribution correlate with the SiO₂ profile. Fe₂O₃, Al₂O₃, kaolinite and 2:1 clay negatively correlate with SiO₂. The upper part of the core is rich in CaO.

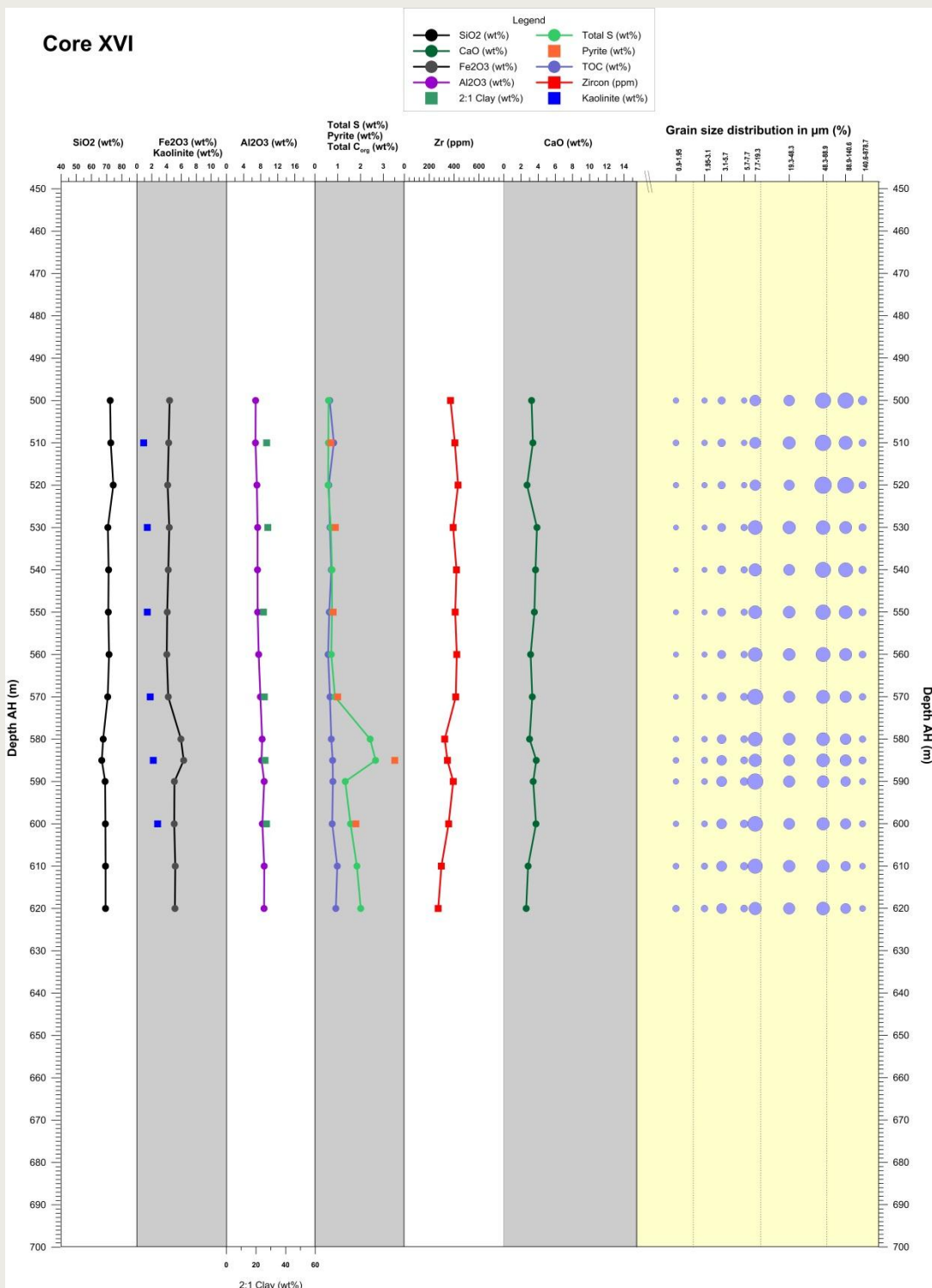


Figure 37. Depth profile of core XVI (fresh drilling, location is confidential). Relatively homogeneous composition. SiO₂ and Zr decrease slightly with depth, while Fe₂O₃, Al₂O₃ and total S increase slightly. Around 580 m a peak in Fe₂O₃ and total S is observed, which correlates with an increase in pyrite. The grain size becomes slightly lower with depth and is poorly sorted.

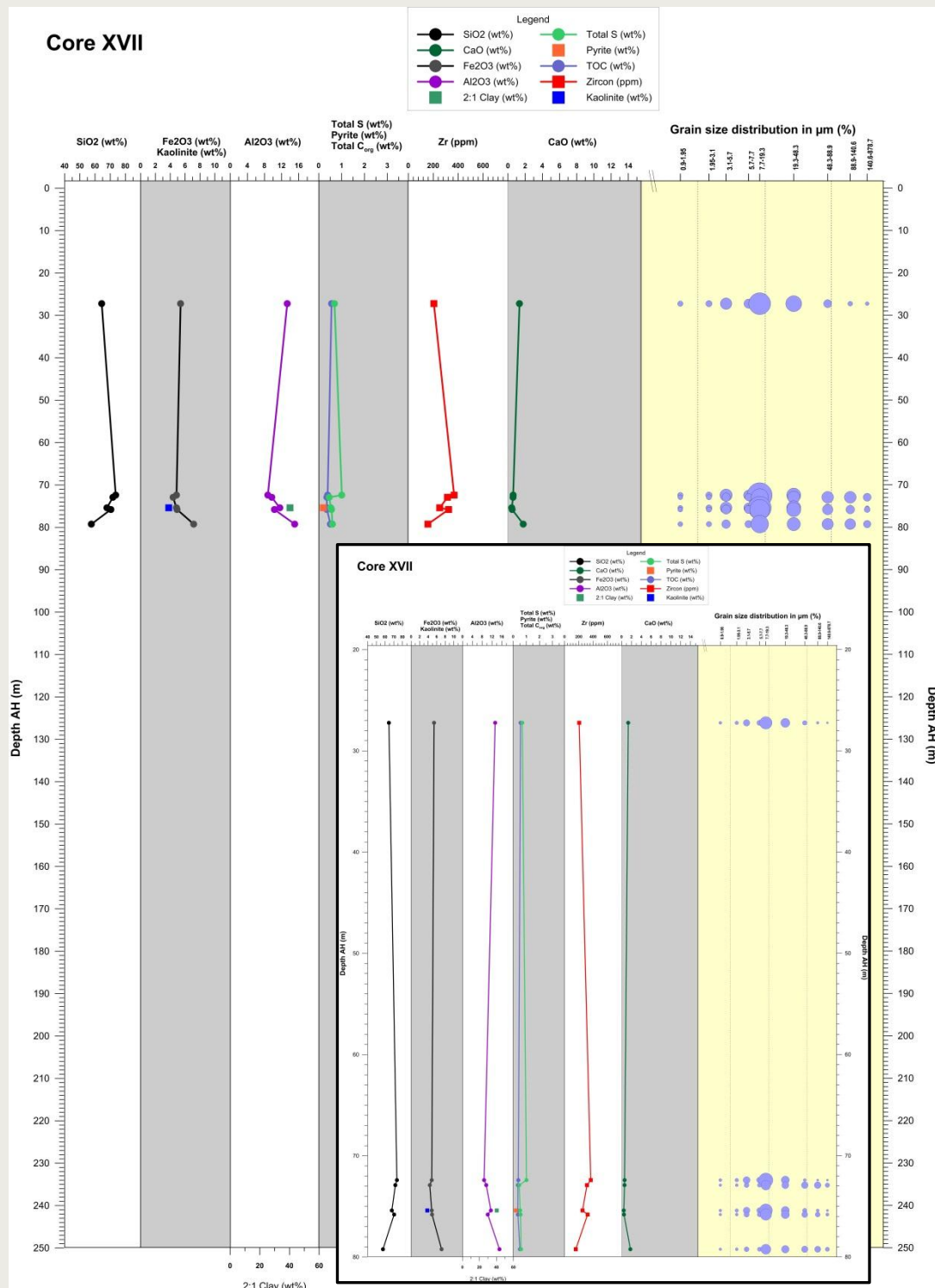


Figure 38. Depth profile of core XVII (COVRA core) (left) and map with location (right). Note that the shallowest sample represents the section of the core between 8.7 and 45.7 m (Table 8). The samples show a slightly fluctuating composition. The Si and Zr show a negative correlation with Fe and Al. Total S, organic C and Ca content are low.

Appendix F

Table 15. Correlation matrix showing values of $|R| > 0.6$ for the clay and sand fraction, the oxides, carbon and sulphur.

	Depth	Clay fraction	Sand fraction	SiO ₂	Al ₂ O ₃	Fe ₂ O ₃	CaO	MgO	Na ₂ O	K ₂ O	MnO	TiO ₂	P ₂ O ₅	Cr ₂ O ₃	SO ₃	V ₂ O ₅	Total C	Total S	Organic C	Inorganic C
Depth																				
Clay fraction																				
Sand fraction																				
SiO ₂			0.76																	
Al ₂ O ₃			-0.85	-0.81																
Fe ₂ O ₃				-0.70	0.65															
CaO																				
MgO			-0.83	-0.87	0.90	0.73														
Na ₂ O																				
K ₂ O			-0.62		0.72			0.70												
MnO																				
TiO ₂			-0.83	-0.69	0.92			0.82		0.69										
P ₂ O ₅						0.67									0.66					
Cr ₂ O ₃							0.67													
SO ₃																				
V ₂ O ₅		0.61	-0.73	-0.72	0.90	0.75		0.80				0.81		0.68						
Total C				-0.70			0.73													
Total S																				
Organic C			-0.61		0.62															
Inorganic C							0.94										0.79			

Table 16. Correlation matrix showing values of $|R| > 0.6$ for the oxides versus the trace elements.

	Clay fraction	Sand fraction	SiO ₂	Al ₂ O ₃	Fe ₂ O ₃	CaO	MgO	Na ₂ O	K ₂ O	MnO	TiO ₂	P ₂ O ₅	Cr ₂ O ₃	SO ₃	V ₂ O ₅	Total C	Total S	Organic C	Inorganic C
Ba									0.62										
Co			-0.69	-0.75	0.81	0.70		0.82		0.66	0.72				0.77				
Cs	0.67		-0.76	-0.69	0.87			0.76			0.78				0.82			0.65	
Ga			-0.85	-0.81	0.99	0.65		0.89		0.70	0.91			0.66	0.90			0.64	
Hf					0.62			-0.62											
Nb			-0.80	-0.71	0.93			0.81		0.68	0.95			0.62	0.82				
Rb	0.65		-0.81	-0.72	0.94			0.85		0.71	0.87			0.62	0.87		0.62		
Sr						0.89										0.62		0.78	
Ta			-0.76	-0.63	0.86			0.74		0.62	0.88				0.74				
Th			-0.83	-0.78	0.96	0.64		0.88		0.72	0.93			0.68	0.88		0.60		
U										0.88									
V	0.60		-0.72	-0.72	0.90	0.73		0.79			0.81			0.68		0.98			
Zr	0.66		0.63	-0.66				-0.66										-0.61	
Y			-0.76	-0.65	0.84			0.73		0.62	0.88				0.79				
La			-0.79	-0.78	0.95	0.67		0.86		0.70	0.90			0.68		0.91			
Ce			-0.69	-0.77	0.88	0.74		0.84		0.72	0.80			0.66		0.85			
Pr			-0.72	-0.73	0.90	0.67		0.80		0.68	0.85			0.67		0.88			
Nd			-0.67	-0.71	0.86	0.65		0.76		0.66	0.80			0.62		0.85			
Sm			-0.72	-0.71	0.89	0.66		0.79		0.66	0.84			0.67		0.88			
Eu			-0.75	-0.74	0.91	0.68		0.82		0.67	0.86			0.66		0.89			
Gd			-0.76	-0.72	0.90	0.63		0.80		0.66	0.87			0.65		0.88			
Tb			-0.81	-0.79	0.92	0.67		0.85		0.68	0.89			0.65		0.88			
Dy			-0.73	-0.63	0.85			0.75		0.65	0.88					0.81			
Ho			-0.79	-0.74	0.89			0.81		0.65	0.90			0.64		0.84			
Er			-0.78	-0.70	0.87			0.77		0.64	0.90			0.63		0.81			
Tm			-0.78	-0.69	0.85			0.77		0.66	0.91			0.63		0.78			
Yb			-0.68		0.79			0.67			0.88			0.60		0.76			
Lu			-0.74	-0.63	0.80			0.70		0.61	0.89			0.62		0.73			
Mo																			
Cu																			
Pb																			
Zn																			
Ni			-0.72	-0.79	0.76	0.70		0.77			0.70	0.64				0.68			
As																			

Table 17. Correlation matrix for the log values of the trace elements, showing values of $|R| > 0.6$.

	Ba	Co	Cs	Ga	Hf	Nb	Rb	Sr	Ta	Th	U	V	Zr	Y	La	Ce	Pr	Nd	Sm	Eu	Gd	Tb	Dy	Ho	Er	Tm	Yb	Lu	Mo	Cu	Pb	Zn	Ni	As														
Ba																																																
Co																																																
Cs	0.65																																															
Ga	0.80	0.89																																														
Hf																																																
Nb	0.70	0.83	0.93																																													
Rb	0.71	0.94	0.95		0.90																																											
Sr																																																
Ta	0.62	0.78	0.86		0.92	0.85																																										
Th	0.78	0.85	0.96		0.95	0.92		0.88																																								
U																																																
V	0.77	0.84	0.91		0.83	0.88		0.75	0.88																																							
Zr					0.98																																											
Y	0.64	0.80	0.86		0.92	0.86		0.84	0.90		0.81																																					
La	0.79	0.84	0.95		0.94	0.92		0.85	0.97		0.91	0.91																																				
Ce	0.81	0.70	0.87		0.83	0.82		0.74	0.90		0.85	0.81	0.94																																			
Pr	0.74	0.80	0.91		0.90	0.90		0.81	0.93		0.90	0.91	0.97	0.95																																		
Nd	0.72	0.75	0.87		0.86	0.85		0.76	0.89		0.86	0.88	0.94	0.93	0.97																																	
Sm	0.73	0.78	0.90		0.88	0.88		0.78	0.92		0.89	0.90	0.96	0.94	0.99	0.96																																
Eu	0.77	0.80	0.92		0.90	0.89		0.80	0.93		0.91	0.90	0.97	0.93	0.98	0.94	0.97																															
Gd	0.75	0.81	0.92		0.91	0.90		0.82	0.92		0.89	0.94	0.96	0.91	0.97	0.93	0.97	0.97																														
Tb	0.80	0.78	0.91		0.89	0.86		0.81	0.94		0.88	0.89	0.96	0.91	0.91	0.87	0.90	0.93	0.92																													
Dy	0.65	0.78	0.87		0.91	0.87		0.84	0.90		0.82	0.94	0.92	0.83	0.92	0.88	0.92	0.92	0.93	0.88																												
Ho	0.74	0.78	0.89		0.91	0.85		0.83	0.93		0.85	0.92	0.93	0.85	0.88	0.85	0.87	0.89	0.91	0.96	0.89																											
Er	0.68	0.76	0.86		0.90	0.83		0.83	0.91		0.82	0.92	0.92	0.82	0.86	0.82	0.85	0.87	0.88	0.94	0.90	0.95																										
Tm	0.70	0.72	0.84		0.89	0.81		0.84	0.90		0.77	0.90	0.90	0.82	0.84	0.81	0.83	0.84	0.86	0.94	0.87	0.95	0.95																									
Yb	0.74	0.80		0.89	0.80		0.82	0.85		0.77	0.93	0.86	0.76	0.84	0.81	0.83	0.83	0.87	0.85	0.90	0.90	0.91	0.90																									
Lu	0.60	0.69	0.79		0.87	0.77		0.82	0.86		0.73	0.88	0.84	0.75	0.79	0.76	0.78	0.79	0.80	0.88	0.85	0.91	0.93	0.94	0.89																							
Mo																																																
Cu																																																
Pb																																																
Zn																																																
Ni	0.85	0.61	0.75		0.64	0.64		0.73	0.68		0.72	0.73	0.65	0.63	0.64	0.71	0.67	0.77		0.70	0.66	0.68																										
As																																																

Appendix G

Table 18. Cluster means for the 6-cluster case and clay and sand fraction averages. Same as Table 2.

	Cluster					
	1	2	3	4	5	6
SiO ₂	70.9	87.7	86.8	53.0	69.6	57.8
Al ₂ O ₃	10.4	2.7	4.5	14.1	7.5	16.0
Fe ₂ O ₃	4.3	3.0	2.4	6.1	4.4	5.8
CaO	0.9	1.1	0.3	5.0	4.5	0.9
MgO	1.4	0.4	0.5	2.0	1.1	1.9
Na ₂ O	0.8	0.1	0.4	1.0	0.7	0.7
K ₂ O	2.7	1.0	1.8	2.8	2.3	3.1
MnO	0.02	0.01	0.01	0.04	0.02	0.02
TiO ₂	0.7	0.2	0.3	0.7	0.5	0.8
P ₂ O ₅	0.06	0.07	0.04	0.12	0.07	0.08
Cr ₂ O ₃	0.02	0.01	0.01	0.02	0.02	0.02
SO ₃	0.3	0.1	0.0	0.6	0.7	0.4
V ₂ O ₅	0.02	0.01	0.01	0.02	0.01	0.03
Organic C	0.6	0.4	0.2	1.0	0.6	1.3
Inorganic C	0.1	0.2	0.1	1.1	0.9	0.1
Ba	336	178	301	272	328	312
Rb	99	36	57	118	80	141
Sr	139	89	81	320	270	148
U	2.9	1.2	1.8	3.7	2.9	4.2
Zr	352	184	364	181	418	216
Mo	0.9	1.1	0.7	1.7	1.7	1.3
Pb	10.5	4.5	11.9	19.2	7.8	18.1
Zn	53	18	19	122	35	68
As	6.8	9.1	4.5	8.0	10.7	11.6
Clay fraction	7.0 (4-14)	5.8 (2-10)	3.9 (4)	8.2 (4-12)	6.8 (0-12)	11.8 (5-25)
Sand fraction	19.1 (3-45)	59.1 (38-89)	78.4 (76-82)	3.2 (0-13)	35.8 (0-91)	3.8 (0-30)
Nr of samples	35	3	3	36	36	36

Table 19. Cluster 1 of 6-cluster case.

	Sub-cluster			
	1	2	3	4
SiO ₂	70.3	65.4	73.3	73.2
Al ₂ O ₃	9.7	12.9	9.2	9.6
Fe ₂ O ₃	5.3	4.9	3.9	3.8
CaO	0.7	1.0	0.3	0.9
MgO	1.5	1.7	0.9	1.3
Na ₂ O	1.1	0.8	0.5	0.7
K ₂ O	2.6	3.0	2.1	2.7
MnO	0.0	0.0	0.0	0.0
TiO ₂	0.7	0.8	0.6	0.6
P ₂ O ₅	0.06	0.08	0.06	0.06
Cr ₂ O ₃	0.02	0.02	0.02	0.02
SO ₃	0.2	0.3	0.1	0.3
V ₂ O ₅	0.02	0.02	0.02	0.02
Organic C	0.4	0.7	1.6	0.5
Inorganic C	0.1	0.2	0.0	0.1
Ba	303	352	267	344
Rb	89	115	91	95
Sr	167	161	91	124
U	2.5	3.0	6.3	2.9
Zr	360	278	291	382
Mo	0.4	0.3	8.4	0.9
Pb	10.1	13.9	8.0	9.4
Zn	65	63	42	47
As	8.4	6.9	14.4	5.8
Nr of samples	6	8	1	20

Table 20. Cluster 4 of 6-cluster case

	Sub-cluster			
	1	2	3	4
SiO ₂	47.9	53.1	56.3	50.4
Al ₂ O ₃	14.6	15.6	11.7	12.0
Fe ₂ O ₃	5.7	6.6	5.7	5.0
CaO	8.2	3.4	5.3	9.2
MgO	2.3	2.2	1.8	1.7
Na ₂ O	0.8	1.1	1.0	0.9
K ₂ O	2.9	3.0	2.3	2.3
MnO	0.0	0.1	0.0	0.0
TiO ₂	0.7	0.8	0.7	0.6
P ₂ O ₅	0.09	0.14	0.12	0.10
Cr ₂ O ₃	0.02	0.02	0.02	0.02
SO ₃	0.7	0.5	0.8	0.9
V ₂ O ₅	0.02	0.03	0.02	0.02
Organic C	0.9	0.9	1.5	0.6
Inorganic C	1.8	0.8	1.1	2.2
Ba	255	298	231	261
Rb	130	129	93	106
Sr	410	268	301	521
U	3.8	3.6	4.3	3.1
Zr	149	180	200	175
Mo	0.7	0.8	4.7	0.7
Pb	19	23	14	16
Zn	117	117	153	84
As	5.3	8.3	9.6	5.9
nr of samples	4	19	9	4

Table 21. Cluster 5 of 6-cluster case

	Sub-cluster 1	2	3	4
SiO ₂	76.4	68.8	71.3	57.6
Al ₂ O ₃	7.4	4.8	7.8	10.9
Fe ₂ O ₃	3.5	3.5	4.8	4.3
CaO	0.7	8.6	3.0	7.6
MgO	0.8	0.8	1.1	1.7
Na ₂ O	0.4	0.7	0.8	0.6
K ₂ O	1.8	1.6	2.5	2.5
MnO	0.0	0.0	0.0	0.0
TiO ₂	0.5	0.4	0.5	0.6
P ₂ O ₅	0.06	0.06	0.07	0.07
Cr ₂ O ₃	0.02	0.01	0.02	0.01
SO ₃	0.2	0.9	0.6	0.8
V ₂ O ₅	0.02	0.01	0.01	0.02
Organic C	1.0	0.2	0.6	1.0
Inorganic C	0.0	1.5	0.7	1.6
Ba	265	287	354	283
Rb	83	53	81	118
Sr	107	463	215	333
U	5.0	2.2	2.7	3.8
Zr	310	612	401	229
Mo	6.5	0.6	1.6	2.2
Pb	6.3	5.0	7.9	12.6
Zn	35	28	38	37
As	12.2	8.6	11.7	7.5
Nr of samples	2	7	23	4

Table 22. Cluster 6 of 6-cluster case

	Sub-cluster 1	2	3	4
SiO ₂	59.6	63.7	55.9	54.7
Al ₂ O ₃	15.6	13.0	15.4	17.6
Fe ₂ O ₃	5.4	5.2	6.2	6.3
CaO	1.0	0.9	0.8	0.9
MgO	2.0	1.4	1.8	2.0
Na ₂ O	0.7	0.6	0.6	0.7
K ₂ O	3.1	2.6	3.0	3.2
MnO	0.0	0.0	0.0	0.0
TiO ₂	0.8	0.7	0.8	0.9
P ₂ O ₅	0.07	0.06	0.08	0.09
Cr ₂ O ₃	0.02	0.02	0.03	0.02
SO ₃	0.4	0.4	0.6	0.3
V ₂ O ₅	0.03	0.03	0.03	0.03
Organic C	0.9	1.7	2.0	1.4
Inorganic C	0.1	0.1	0.1	0.1
Ba	333	295	283	301
Rb	136	131	143	149
Sr	146	150	109	167
U	3.6	5.5	6.2	3.8
Zr	227	253	225	188
Mo	0.6	3.4	3.6	0.6
Pb	18	13	16	20
Zn	66	57	69	72
As	9.0	13.2	14.5	13.3
Nr of samples	10	2	5	19

Appendix H

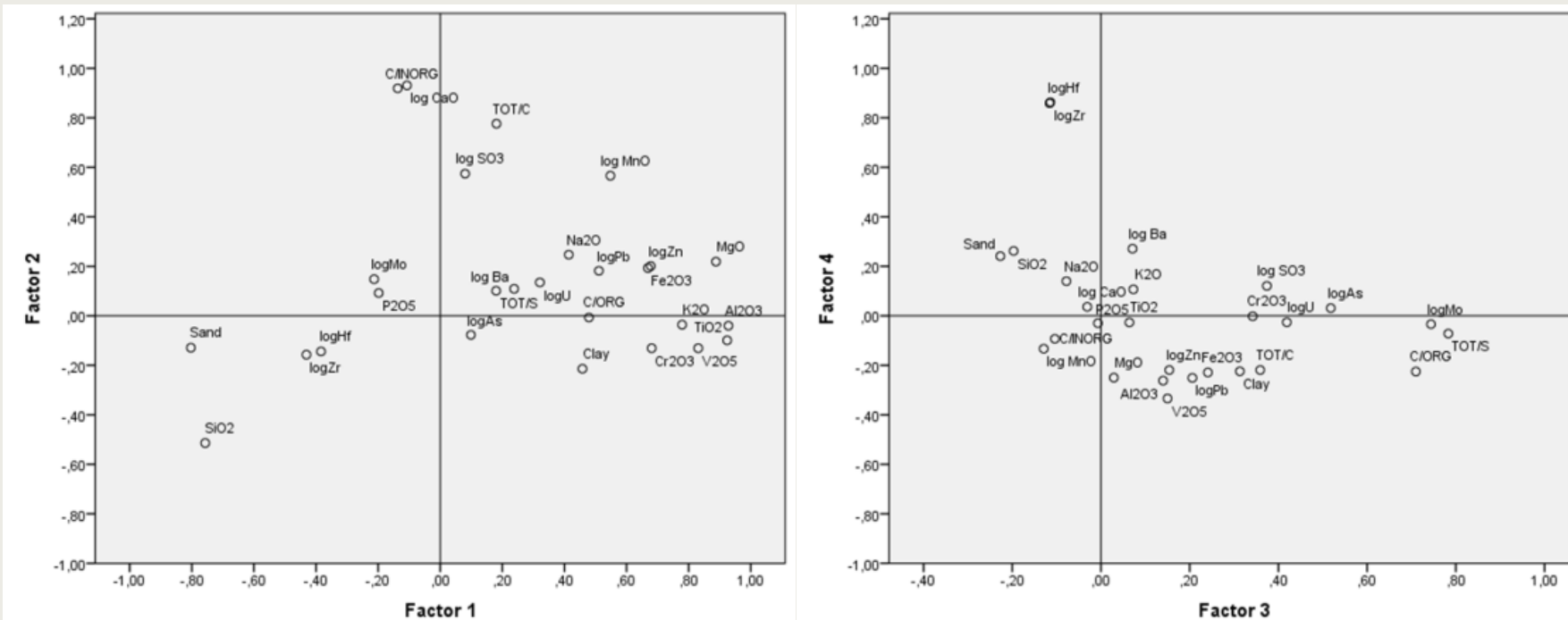


Figure 39. Factor plots for the 4-factor case. The closer the component is located near the factor axis, the better it is explained by that factor. For example Al₂O₃ lies almost on top of the x-axis in the left plot, near value 1, indicating that this component is for almost 100% explained by factor 1. In the right plot Al₂O₃ is close to the origin, indicating that it hardly explained by factor 3 and 4.

Table 23. Factor scores for each sample. The method used is ‘regression’ (default).

Sample	Factor 1	Factor 2	Factor 3	Factor 4	Sample	Factor 1	Factor 2	Factor 3	Factor 4	Sample	Factor 1	Factor 2	Factor 3	Factor 4
I 1	-1.0	0.6	-0.5	2.5	IV 1	-2.6	-0.5	-1.0	-0.5	VII 1	0.2	2.3	-0.7	-1.2
I 2	-1.2	3.0	-1.0	2.2	IV 2	-2.5	1.0	-0.3	-0.3	VII 2	1.0	-0.8	-0.2	0.1
I 3	-0.9	0.4	-0.9	2.3	IV 3	-0.4	-0.6	-0.8	0.4	VII 3	0.8	-0.4	2.4	-0.1
I 4	-1.1	0.7	-0.8	1.7	IV 4	-0.4	-1.1	0.1	0.5	VII 4	1.3	-1.0	-0.5	0.4
I 5	-0.7	2.3	-0.2	2.6	IV 5	-0.3	-0.4	1.6	0.3	VII 5	1.2	-0.8	0.6	0.1
I 6	-1.4	0.4	-1.0	-1.5	IV 6	-1.6	-1.0	1.6	-0.6	VII 6	-0.3	-0.9	-1.5	1.5
I 7	-0.9	-0.4	-0.5	1.3	IV 7	-2.6	-1.6	-1.0	-1.7	VII 7	-0.5	-1.0	-1.2	0.6
I 8	-0.5	0.0	0.4	1.9	IV 8	-0.5	2.1	-0.1	-1.2	VII 8	-0.5	-0.2	-0.8	0.9
I 9	-0.5	0.1	0.6	0.9	IV 9	-3.6	-1.5	0.0	-5.2	VIII 1	0.6	0.4	-0.2	-0.6
I 10	-0.9	-0.7	-0.3	0.7	IV 10	-1.5	1.6	0.7	1.2	VIII 2	0.7	0.7	-0.2	-0.6
I 11	-1.4	-1.0	1.3	-0.1	IV 11	-3.3	-1.6	-1.1	-4.9	VIII 3	1.1	1.1	-0.7	-0.5
I 12	-0.5	-0.8	-0.3	0.1						VIII 4	0.9	0.8	-0.2	-0.5
I 13	-0.5	1.1	1.4	-0.4						VIII 5	0.9	0.9	-1.0	-0.6
II 1	-0.6	0.7	-0.4	1.4	V 1	0.6	-0.5	0.1	-0.1	VIII 6	1.1	0.2	0.0	-0.5
II 2	-0.8	-0.6	-0.5	0.9	V 2	0.1	-0.4	-1.1	0.3	VIII 7	0.8	0.3	0.3	-0.4
II 3	-0.1	0.9	0.2	0.5	V 3	-0.1	-0.7	-0.8	0.8	VIII 8	1.0	0.5	0.0	-0.3
II 4	1.2	-0.8	1.2	-0.5	V 4	0.8	-0.4	-0.4	0.3	VIII 9	1.0	0.4	-0.1	-0.5
II 5	1.0	-0.8	0.9	-0.6	V 5	1.1	-0.2	-0.2	-0.2	VIII 10	0.9	0.2	0.6	-0.1
II 6	-1.0	-1.2	2.2	-0.2	V 6	1.5	-0.6	-0.4	-0.8	IX 1	0.6	-0.7	1.1	0.0
II 7	0.0	-0.7	2.8	-0.1	V 7	1.1	-0.6	0.8	-0.4	IX 2	0.8	-0.4	2.5	-0.1
II 8	1.0	-1.1	-0.7	-0.2	V 8	0.2	-0.8	1.6	-0.2	IX 3	1.3	0.0	0.0	-0.4
II 9	0.4	2.5	-0.8	-1.1	V 9	0.4	-0.6	-0.4	0.1	IX 4	1.2	-0.8	-0.5	-0.1
II 10	-1.2	-0.6	0.3	1.2	V 10	-1.4	-1.4	-1.2	0.4	IX 5	1.0	-0.7	1.7	-0.7
II 11	-2.3	-1.5	-0.9	-0.7	V 11	0.0	-0.1	-1.0	0.9	IX 6	1.1	-0.5	0.4	-0.6
					V 12	0.2	-0.7	-1.6	0.2	IX 7	1.0	0.3	-1.3	-0.4
III 1	-0.3	0.2	-0.2	0.4	VI 1	-0.7	-1.2	-0.4	0.2	IX 11	0.2	-0.9	-0.8	0.9
III 2	-0.1	0.0	-0.9	0.6	VI 2	-0.3	-0.9	-0.4	0.6	IX 12	0.3	-0.9	-1.3	0.4
III 3	1.1	-0.8	-0.1	0.0	VI 3	-0.5	1.7	-0.1	-0.6	X 1	0.4	-0.4	-0.4	0.2
III 4	1.3	-0.6	-0.1	0.3	VI 4	-0.3	-1.0	-0.2	-0.2	X 2	-0.1	-0.3	-0.5	0.8
III 5	1.1	-0.7	1.0	-0.1	VI 5	0.0	-0.6	-0.1	0.8	X 3	0.8	-0.8	-1.2	0.1
III 6	1.1	0.8	-0.4	-0.1	VI 6	-0.4	-0.8	0.3	0.1	X 4	-0.3	-0.8	-0.7	0.4
III 7	0.9	-0.7	0.5	0.0	VI 7	0.8	-0.9	-0.2	-0.4	X 5	0.8	-0.6	-1.2	-0.4
III 8	1.3	-0.8	0.1	-0.2	VI 8	0.4	-0.9	1.8	0.1					
III 9	1.2	-0.2	-0.6	-0.3	VI 9	0.6	-0.9	2.0	0.0					
III 10	0.0	-0.8	-1.0	0.5	VI 10	0.7	0.0	2.5	0.1					
III 11	-0.2	-0.4	-1.3	2.0	VI 11	0.9	-0.8	0.2	0.0					
					VI 12	0.5	-0.1	-0.1	-0.2					

Sample	Factor 1	Factor 2	Factor 3	Factor 4	Sample	Factor 1	Factor 2	Factor 3	Factor 4
XI 1A	0.4	0.9	2.0	0.2	XVI 1	-1.2	0.3	0.0	0.4
XI 2A	0.7	1.2	0.6	-0.2	XVI 2	-1.1	0.1	0.1	0.7
XI 3A	1.0	1.5	-0.4	-0.7	XVI 3	-1.1	0.1	-0.1	0.9
XII 1A	-0.3	1.6	1.9	0.3	XVI 4	-0.9	0.5	0.0	0.7
XII 2A	-0.6	1.9	1.0	-1.2	XVI 5	-0.9	0.4	0.0	0.9
XII 3A	-1.1	1.6	1.5	-1.6	XVI 6	-0.9	0.5	0.1	0.9
XII 4A	0.4	0.7	-1.1	-0.6	XVI 7	-0.9	0.3	0.1	0.9
XII 5A	0.2	2.0	-0.3	-0.5	XVI 8	-0.8	0.4	0.2	0.9
XII 6A	1.0	1.5	-1.3	-0.7	XVI 9	-1.0	0.5	1.7	0.5
XII 7A	1.0	1.4	-0.5	-1.1	XVI 10	-0.9	0.8	2.0	0.8
XII 8A	1.3	0.3	-0.7	-0.6	XVI 11	-0.6	0.5	0.7	0.9
XIII 1A	0.7	1.0	-0.3	-0.8	XVI 12	-0.9	0.6	1.0	0.5
XIII 2A	-0.4	3.3	-0.7	-0.9	XVI 13	-0.9	0.3	1.6	0.2
XIII 3A	0.3	1.8	-1.2	-1.2	XVI 14	-1.1	0.3	1.7	-0.1
XIII 4A	1.1	-0.2	-0.8	-0.7	XVII 1	0.4	-0.4	-1.0	-0.6
XIII 5A	1.7	0.3	-1.3	-0.8	XVII 2	0.7	-0.2	-1.2	-1.2
XIII 6A	1.1	-0.3	-0.5	-0.9	XVII 3	-0.5	-0.9	-0.1	0.5
XIII 7A	0.5	-1.0	-0.4	0.2	XVII 4	-0.4	-1.0	-1.0	0.0
XIII 8A	0.2	-1.1	0.1	0.8	XVII 5	0.2	-0.9	-1.2	-0.3
XIII 9A	0.2	-1.1	-0.4	1.7	XVII 6	0.0	-0.9	-0.8	0.3
XIII 10A	1.3	-1.1	0.8	-0.7					
XIV 1A	0.0	0.4	1.7	0.0					
XIV 2A	0.2	0.7	1.3	-0.1					
XIV 3A	0.0	0.6	2.0	-0.3					
XIV 4A	1.0	0.9	-0.5	-0.8					
XV 1A	-0.5	1.4	0.3	-0.6					
XV 2A	-0.4	2.2	-1.1	-1.4					

Appendix I

Table 24. Correlation matrix of mineralogy showing values of $|R| > 0.6$. * Number of values above detection limit is below 6.

	Clay fraction	Sand fraction	Qtz	Plag	K-f	Clin/Heul	Cal	Arag	Ank/ dol*	Sid*	Py	Ana	Syl*	Hal	Gyp	Jar*	Chl	2:1 clay	Kaol	Tot_clay
Depth																				
Clay fraction																				
Sand fraction																				
Qtz			0.90																	
Plag																				
K-f					0.79															
Clin/Heul																				
Cal																				
Arag																				
Ank/ dol																				
Sid																				
Py																				
Ana	0.70	-0.81	-0.75																	
Syl																				
Hal													0.85							
Gyp																				
Jar	0.71												0.67							
Chl		-0.68	-0.67										0.73							
2:1 clay	0.64	-0.89	-0.94										0.81			0.66				
Kaol	0.62	-0.78	-0.81										0.85			0.71	0.79			
Tot_clay	0.65	-0.90	-0.94										0.85			0.72	0.99	0.86		

Appendix J

Table 25. Correlation matrix of mineralogy and oxides showing values of $|R| > 0.6$. * number of values above detection limit is below 6.

	Clay fraction	Sand fraction	Qtz	Plag	K-f	Clin/Heul	Cal	Arag	Ank/dol*	Sid*	Py	Ana	Syl*	Hal	Gyp	Jar*	Chl	2:1 clay	Kaol	Tot clay
SiO ₂		0.87	0.95									-0.70					-0.62	-0.84	-0.79	-0.86
Al ₂ O ₃	0.67	-0.88	-0.86									0.90					0.74	0.89	0.88	0.92
Fe ₂ O ₃	0.67	-0.73	-0.78									0.69					0.78	0.72	0.79	
CaO							0.97													
MgO			-0.60	-0.64													0.61	0.61		
Na ₂ O			-0.60	-0.71									0.81	0.77			0.70	0.63	0.71	
K ₂ O																				
MnO																				
TiO ₂													0.64							
P ₂ O ₅								0.68												
Cr ₂ O ₃	0.83	-0.78	-0.75									0.89				0.64	0.63	0.82	0.82	0.85
SO ₃			-0.63				0.80													
SO ₃																				
V ₂ O ₅			-0.62	-0.70								0.60	0.60				0.77	0.77	0.75	
TOT_C									0.96											
TOT_S			0.87	0.95								-0.70					-0.62	-0.84	-0.79	-0.86
Organic C	0.67	-0.88	-0.86									0.90					0.74	0.89	0.88	0.92
Inorganic C	0.67	-0.73	-0.78									0.69					0.78	0.72	0.79	

Table 26. Correlation matrix of mineralogy and trace elements showing values of $|R| > 0.6$. * number of values above detection limit is below 6.

	Clay fractio	Sand fractio	Qtz	Plag	K-f	Clin/H eul	Cal	Arag	Ank/ dol*	Sid*	Py	Ana	Syl*	Hal	Gyp	Jar*	Chl	2:1 clay	Kaol	Tot clay
Sc	0.69	-0.89	-0.86									0.90					0.72	0.90	0.88	0.93
Ba													0.99	0.85						
Co		-0.80	-0.77									0.80					0.68	0.77	0.85	0.82
Cs	0.70	-0.86	-0.84									0.93					0.71	0.88	0.88	0.91
Ga	0.66	-0.89	-0.87									0.92					0.74	0.90	0.89	0.93
Hf				0.62	0.73															
Nb		-0.84	-0.79									0.87					0.71	0.79	0.82	0.82
Rb	0.67	-0.85	-0.84									0.88					0.68	0.88	0.82	0.90
Sr						0.86														
Ta		-0.79	-0.73									0.85					0.64	0.73	0.81	0.77
Th	0.64	-0.85	-0.84									0.88					0.74	0.84	0.86	0.88
U		-0.70	-0.73									0.62					0.62	0.73		0.73
V	0.82	-0.77	-0.74									0.92					0.67	0.61	0.81	0.84
W		-0.67	-0.70														0.65	0.70	0.68	0.72
Zr				0.63	0.76															
Y		-0.81	-0.73									0.81					0.64	0.71	0.75	0.74
La	0.64	-0.84	-0.82									0.86					0.69	0.82	0.85	0.86
Ce	0.62	-0.80	-0.83									0.79					0.69	0.81	0.83	0.84
Pr	0.63	-0.78	-0.77									0.81					0.65	0.76	0.80	0.79
Nd	0.61	-0.76	-0.76									0.73					0.61	0.71	0.76	0.75
Sm	0.66	-0.78	-0.76									0.81					0.66	0.75	0.80	0.79
Eu	0.67	-0.80	-0.78									0.83					0.67	0.77	0.85	0.81
Gd	0.67	-0.80	-0.76									0.84					0.68	0.75	0.85	0.80
Tb	0.69	-0.85	-0.83									0.85					0.69	0.83	0.86	0.86
Dy	0.60	-0.79	-0.74									0.81					0.67	0.72	0.78	0.76
Ho	0.65	-0.86	-0.80									0.87					0.70	0.80	0.82	0.83
Er	0.62	-0.83	-0.77									0.82					0.66	0.77	0.79	0.80
Tm	0.62	-0.83	-0.78									0.82					0.68	0.77	0.77	0.80
Yb		-0.77	-0.70									0.81					0.62	0.67	0.72	0.71
Lu		-0.80	-0.72									0.78					0.63	0.70	0.71	0.73
Mo																				
Cu	0.71	-0.80	-0.77									0.90					0.71	0.84	0.83	0.87
Pb	0.73	-0.86	-0.82									0.87					0.69	0.84	0.88	0.88
Zn		-0.80	-0.78									0.72					0.77	0.80	0.74	0.82
logAs		-0.89	-0.87									0.76					0.70	0.85	0.82	0.88

OPERA

Meer informatie:

Postadres
Postbus 202
4380 AE Vlissingen

T 0113-616 666
F 0113-616 650
E info@covra.nl

www.covra.nl